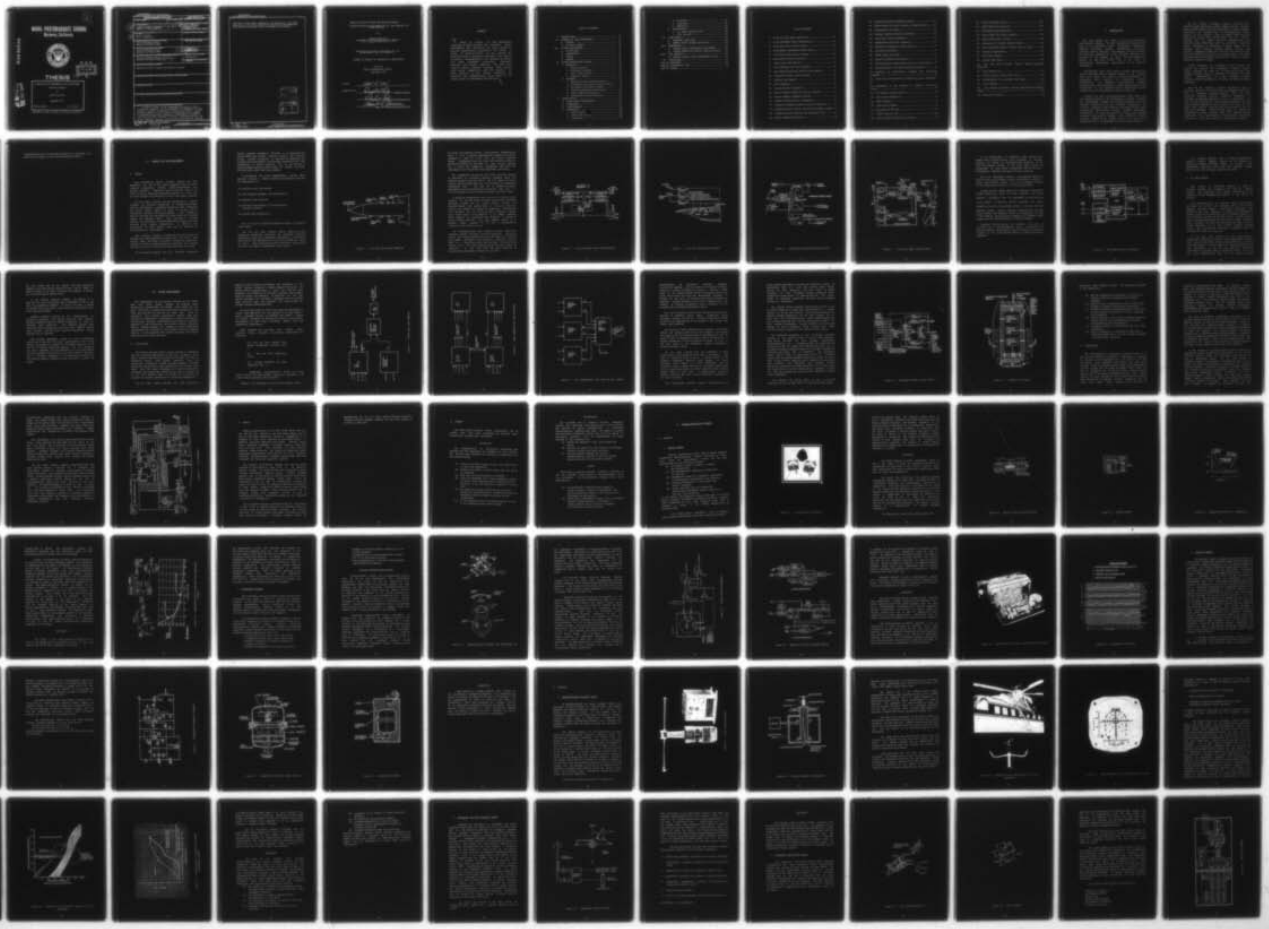
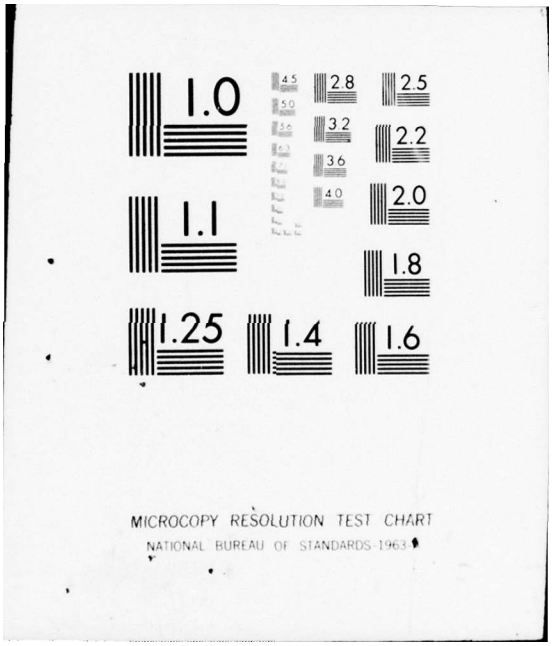
AD-A046 500 NAVAL POSTGRADUATE SCHOOL MONTEREY CALIF F/G 1/3
A STATE-OF-THE-ART ASSESSMENT OF AIR DATA SENSORS FOR NAVAL AIR--ETC(U)
SEP 77 R D NEIL

UNCLASSIFIED NL

1 OF 2
AD A046500




1.0
1.1
1.25
1.4
1.6
1.8
2.0
2.2
2.5
2.8
3.2
3.6
4.0
4.5
5.0
5.6
MICROCOPY RESOLUTION TEST CHART
NATIONAL BUREAU OF STANDARDS-1963-A

(2)
SC

NAVAL POSTGRADUATE SCHOOL
Monterey, California

AD A046500



DDC
RECEIVED
NOV 16 1977
B

THESIS

A STATE-OF-THE-ART ASSESSMENT OF AIR DATA SENSORS

FOR NAVAL AIRCRAFT

by

Robert Dale Neil

September 1977

Thesis Advisor: D. M. Layton

AD No.
DDC FILE COPY

Approved for public release; distribution unlimited.

Unclassified

SECURITY CLASSIFICATION OF THIS PAGE (When Data Entered)

REPORT DOCUMENTATION PAGE	READ INSTRUCTIONS BEFORE COMPLETING FORM
1. REPORT NUMBER	2. GOVT ACCESSION NO. / 3. RECIPIENT'S CATALOG NUMBER
4. TITLE (and Subtitle): A STATE-OF-THE-ART ASSESSMENT OF AIR DATA SENSORS FOR NAVAL AIRCRAFT	5. TYPE OF REPORT & PERIOD COVERED: Master's Thesis; September 1977
	6. PERFORMING ORG. REPORT NUMBER
7. AUTHOR(s): Robert Dale Neil	8. CONTRACT OR GRANT NUMBER(s)
9. PERFORMING ORGANIZATION NAME AND ADDRESS: Naval Postgraduate School, Monterey, California 93940	10. PROGRAM ELEMENT, PROJECT, TASK AREA & WORK UNIT NUMBERS
11. CONTROLLING OFFICE NAME AND ADDRESS: Naval Postgraduate School, Monterey, California 93940	12. REPORT DATE: September 1977 13. NUMBER OF PAGES: 176
14. MONITORING AGENCY NAME & ADDRESS (if different from Controlling Office): Naval Postgraduate School, Monterey, California 93940 (12) 176p.	15. SECURITY CLASS. (of this report): Unclassified 15a. DECLASSIFICATION/DOWNGRADING SCHEDULE

16. DISTRIBUTION STATEMENT (of this Report)

Approved for public release; distribution unlimited

17. DISTRIBUTION STATEMENT (of the abstract entered in Block 20, if different from Report)

18. SUPPLEMENTARY NOTES

19. KEY WORDS (Continue on reverse side if necessary and identify by block number)

20. ABSTRACT (Continue on reverse side if necessary and identify by block number)

A review of current air data measurement techniques in Naval aircraft was conducted. Future requirements were identified for three classes of aircraft: conventional, fly-by-wire, and V/STOL. A survey of state-of-the-art air data sensors was performed based on information obtained from current literature, correspondence, and personal interviews with major government contractors, government agencies, and private companies. The major areas covered include pressure, airspeed,

DD FORM 1 JAN 73 1473 (Page 1) EDITION OF 1 NOV 65 IS OBSOLETE S/N 0102-014-6601

Unclassified

SECURITY CLASSIFICATION OF THIS PAGE (When Data Entered)

251 450

AB

fiber optics, laser gyros, temperature, and fuel quantity. The basic operation of each system considered was presented and recommendations given based on its present stage of development and potential.

ACCESSION for
NTIS White Section
DDC Buff Section
UNANNOUNCED
JUSTIFICATION
BY
DISTRIBUTION/AVAILABILITY CODES
Dist. AVAIL. and/or SPECIAL
A

Approved for public release; distribution unlimited.

A STATE-OF-THE-ART ASSESSMENT OF AIR DATA SENSORS FOR NAVAL AIRCRAFT

by

Robert Dale Neil
Lieutenant, United States Navy Reserve
B.S., Niagara University, 1970

Submitted in partial fulfillment of the
requirements for the degree of

MASTER OF SCIENCE IN AERONAUTICAL ENGINEERING

from the
NAVAL POSTGRADUATE SCHOOL
September 1977

Author: Robert D. Neil

Approved by: Donald M. Layton
Thesis Advisor

Richard W. Bell
Chairman, Department of Aeronautics

Robert B. Brown
Dean Of Science And Engineering

ABSTRACT

A review of current air data measurement techniques in Naval aircraft was conducted. Future requirements were identified for three classes of aircraft: conventional, fly-by-wire, and V/STOL. A survey of state-of-the-art air data sensors was performed based on information obtained from current literature, correspondence, and personal interviews with major government contractors, government agencies, and private companies. The major areas covered include pressure, airspeed, fiber optics, laser gyros, temperature, and fuel quantity. The basic operation of each system considered was presented and recommendations given based on its present stage of development and potential.

TABLE OF CONTENTS

I. INTRODUCTION..... 10

II. CURRENT AIR DATA MEASUREMENT..... 15

A. FIGHTER..... 15

B. AIR DATA SYSTEMS..... 25

III. FUTURE REQUIREMENTS..... 29

A. FLY-BY-WIRE..... 29

B. CONVENTIONAL..... 38

C. V/STOL..... 44

D. SUMMARY..... 46

IV. CURRENT/PROSPECTIVE SENSORS..... 48

A. PRESSURE..... 48

1. Digital Quartz..... 48

2. Vibrating Diaphram..... 54

3. Solid State Silicon..... 58

4. Resonant Capsule..... 67

B. AIRSPEED..... 75

1. Omnidirectional Airspeed System..... 75

2. Orthogonal Low Range Airspeed System..... 88

3. Ultrasonic Wind Vector Sensor..... 91

4. Optical Convolution Velocimeter..... 98

5. Laser Doppler Velocimeter..... 104

6. Airspeed By Vortex Detection..... 109

V. FIBER OPTICS..... 115

A. FIBER OPTICS FUNDAMENTALS..... 115

B. ADVANTAGES..... 117

C. DISADVANTAGES..... 122

D. COMPONENTS..... 124

1. Light Sources..... 124

2. Fiber Optic Cables..... 126

3. Connectors..... 127

4. Detectors..... 131
5. Couplings..... 132
6. Modulation..... 134
E. APPLICATIONS..... 135
1. A-7 ALOFT Demonstration..... 136
2. P-3C Aircraft..... 139
VI. LASER GYROS..... 141
A. HONEYWELL LASER GYRO..... 143
B. SPERRY FLIGHT SYSTEMS LASER GYRO..... 144
VII. TEMPERATURE..... 147
A. TURBINE BLADE TEMPERATURE MEASUREMENTS..... 149
B. TURBINE ENGINE HOT SECTION DISPLAY CONCEPT... 154
VIII. FUEL QUANTITY..... 159
A. ELECTRO OPTICAL FLUID MEASUREMENT SYSTEM..... 161
IX. CONCLUSIONS..... 170
LIST OF REFERENCES..... 172
INITIAL DISTRIBUTION LIST..... 176
LIST OF FIGURES..... 7

LIST OF FIGURES

1. F-14A Air Data Probe Locations..... 17
2. F-14A AICS/CADC Probe Configuration..... 19
3. F-14A Air Inlet Control System..... 20
4. Auto/Rudder Interconnect/Flaps Slats..... 21
5. F-14A Wing Sweep Control System..... 22
6. Wing Sweep Failure Monitoring..... 24
7. Simple Fail Safe Monitor..... 31
8. Dual Redundant Air Data Computers..... 32
9. Fail Operational/Fail Safe Air Data System..... 33
10. Integrated Sensor System Concept..... 36
11. Complete ISS System..... 37
12. IPCS Schematic..... 43
13. Paroscientific Transducer..... 49
14. Quartz Crystal Resonator Mounting System..... 51
15. Torque Balance Suspension System..... 52
16. Pressure Deviations vs. Temperature..... 53
17. Vibrating Diaphram Pressure Sensing Transducer..... 55
18. Transducer Drive Circuit And Data Conversion Scheme. 57
19. Diamond Lattice Structure And Transducer Cup..... 60
20. Sensor Bridge Electronics..... 62

21. Analog and Digital Pressure Sensors..... 63

22. HG280 Digital Air Data Computer Pressure Sensor..... 65

23. Accelerated Life Tests..... 66

24. Resonant Capsule Pressure Transducer..... 68

25. Oscillator Circuit Schematic..... 69

26. Temperature Controller Schematic..... 71

27. Transducer Mechanical Design Details..... 72

28. Installed Transducer..... 73

29. LORAS System Prototype..... 76

30. Typical Standpipe Installation..... 77

31. Above-The-Rotor Installation On An S-61 Helicopter.. 79

32. Omnidirectional Low Range Airspeed Indicator..... 80

33. Variation Of Pitot-Static Airspeed With Calibrated Airspeed..... 83

34. Variation Of Pitot-Static Airspeed In Light Turbulence. 84

35. Comparison Of The Systems In Climbing Accelerated Flight..... 85

36. Orthogonal Airspeed System..... 89

37. Wind Vector Definition..... 92

38. UWVS Geometry..... 93

39. UWVS Block Diagram..... 95

40. Principle Of The OCV..... 99

41. Single Detector OCV.....100

42. Laser Doppler Velocimeter Schematic.....107

43. Proof-Of-Concept Setup.....108

44. Bluff Body Vortex Pattern.....110

45. Ultrasonic Beam Modulation.....111

46. Army Flight Test Center Results.....113

47. Single Fiber Optic Strand.....116

48. Properties Of Typical Optical Fibers.....120

49. Top: Loose-Tube Splice, Bottom: Plug and Jack.....129

50. Coupling Comparisons.....133

51. TBP Block Diagram.....151

52. Typical Test Data.....153

53. Top: HSD Block Diagram, Bottom: Typical Over-Temp Event.156

54. Eldec Model 9-311.....157

55. Electro Optical Fluid Level Probe.....162

56. Mechanization For Irregular Tank Shape.....163

57. Plate Support.....164

58. Top: Optical Interface, Bottom: Densimeter/Contaminant Probe.....166

59. Multi-Tank System.....168

I. INTRODUCTION

The last decade has ushered in an era of tremendous technological advances. The most significant advances have been in the following areas: electronics, propulsion, composite materials, lasers, aerodynamics, integrated circuits, digital computers, multiplexing, and fiber optics. The increased capabilities these advances afforded were attained at the expense of higher cost and complexity. Nowhere is this more evident than in the field of aeronautical engineering, particularly in the military environment.

Skyrocketing costs have made it readily apparent that today's engineers must be equally zealous in (a) reducing life cycle costs, (b) gaining enhanced performance, (c) decreasing pilot workload, (d) increasing aircraft availability, (e) improving survivability/ reducing vulnerability. The achievement of these goals requires full utilization of the enhanced computer capabilities through integration of the multifarious aircraft functions.

Perhaps the most challenging design tasks result from the renewed emphasis on the development of V/STOL aircraft. The tremendously complex flow fields associated with these aircraft, coupled with the low airspeeds accompanying the critical transition from hovering to forward flight, render conventional pitot-static airspeed systems inadequate. Furthermore, if these aircraft are to attain their maximum potential, they must be equipped with extremely accurate airspeed systems which become critical if night or IFR operations are to be performed from "Sea Control Ships."

The CCV (control configured vehicle) aircraft which recently became operational employ complex control systems. These systems require accurate measurement of displacements, velocities, and accelerations in six-dimensional space (motion of the aircraft center of gravity (cg) along the flight path; pitch, roll, and yaw about the cg). Control surfaces are not always deflected symmetrically, and therefore these deflections must be monitored. Advanced engine technology on supersonic aircraft makes use of variable throat heights, variable bypass ratios, and variable compressor bleeds plus variable flow rates in both main and afterburner sections of the power plant. All these variables must be carefully orchestrated to obtain a stable, efficient propulsion system.

Energy shortages and increasing prices provide the impetus for improved fuel management. Optimal control theory provides the best way of utilizing aircraft fuel through schedules which are functions of altitude and mach number. Implementation of these schedules requires extensive onboard measurement and control of numerous engine parameters.

The need for reliable, accurate navigation data is becoming crucial, both in military and commercial aircraft. With the available airspace becoming more and more congested, extremely accurate navigation information is necessary if adequate separation is to be maintained. In the military environment, the increased capability of enemy radar systems requires our strike aircraft to fly "on the deck" over hostile territory for long periods of time and over great distances. These aircraft must be capable of accomplishing these missions under all possible weather conditions. This "all-weather", low-altitude requirement constitutes the ultimate test for a navigational system.

Having successfully eluded enemy defenses, the aircraft must still deliver its weapon on target with minimum risk to the crew. An advanced system that would enable the pilot to perform evasive maneuvers while delivering the weapon would greatly increase the chance of survival. This can be done only with a system that has the necessary sensors and the sophisticated computer capability to compute the delivery solution.

With aircraft inventories shrinking due to budget cuts, accidental loss, and end of service life, any time lost to unscheduled maintenance is significant. In an effort to hold this down time to a minimum, the Navy is placing more emphasis on improving aircraft availability. One way to improve this situation is to incorporate a system that continually checks for imminent failure of aircraft components.

Many such monitoring systems are in use today, but in many cases they are subject to false indications. These false alarms cause anxiety in the pilot and possibly a mission abort if the warning concerns fire, low-oil pressure, or some other emergency requiring immediate action. Reliable sensors are the heart of any warning system, and improvements are necessary in this area.

The need for accurate, inexpensive, and reliable sensors permeates every facet of aviation. The areas mentioned above were designed to give the reader an appreciation for the scope of the problem and the part sensors play in the solution.

This paper is the result of research done to support NAVAIRSYSCOM AIRTASK A03A360A/186B/7P54-582-000. The major objectives of this study are to compile data on current Navy aircraft sensor configurations by aircraft types (i.e.

Fighter, ASW, Attack) and extrapolate requirements to the last two decades of the 20th Century utilizing available technology and new concepts. Specifically, the study seeks to:

1) Project operational requirements for aircraft sensors to the last two decades of the 20th Century .

2) Examine state-of-the-art sensors and sensor systems that are not being employed on current aircraft, and make recommendations concerning the utilization of these devices and systems to meet future requirements.

3) Investigate promising new aircraft sensor concepts and evaluate the feasibility/practicality of their use on Naval aircraft.

4) Evaluate the feasibility of establishing a Built-In-Test capability for each sensor/sensor system compatible with current and proposed Air Data Systems.

5) Search for inherently digital transducers that are compatible with current and proposed Air Data Systems.

A two-part program to accomplish these goals was undertaken. First, a search for pertinent information was initiated in current literature, including periodicals , journals, and papers presented at various symposiums and conferences. Data concerning potentially viable concepts discovered in this search were expanded through correspondence or personal interviews with the authors. Second, major government contractors, government agencies, and private companies were contacted for technical data concerning present and future sensor/sensor systems. The

recommendations and conclusions presented in this paper are based on the results of the program described above.

II. CURRENT AIR DATA MEASUREMENT

A. FIGHTER

High performance fighter aircraft require air data parameters for use by most major subsystems such as flight controls, propulsion, cockpit indicators/displays and weapons delivery. Advanced fighter aircraft, such as the F-14, utilize a dedicated subsystem approach, in which the air data hardware is dedicated to one or more major systems.

The F-14 Tomcat requires air data parameters in several airframe and avionics subsystems to satisfactorily meet mission requirements. Displayed parameters used throughout the flight regime consist of angle of attack, rate of climb/dive, altitude, and Mach/airspeed. Other parameters such as altitude rate and angle of attack error are utilized during the approach phase. Pilot workload is reduced through Altitude-Hold and Mach-Hold which require altitude and Mach error signals respectively. In addition, the derivatives of these signals may also be required for stabilization of these modes.

When variable geometry systems such as wing sweep and maneuvering flap/slat/glove are used, as in the F-14, they require Mach ,altitude, and angle of attack as parameters. Optimum air flow is also achieved by providing the correct air weight flow as a function of Mach and angle of attack.

The inherently unstable loop of an inertial Navigation

system requires barometric altitude as a correction for accelerometer bias errors, velocity errors, and position errors. Backup navigation is achieved by resolving true airspeed into North/South and East/West velocities and then integrating to obtain distance. Air to air and air to ground weapons systems require angle of attack, altitude, altitude rate, Mach, and true airspeed.

To accomplish the above requirements, current Naval aircraft utilize a design approach incorporating features and constraints to:

(1) Provide a Fail Safe Design

(2) Have Separate Hardware for Survivability

(3) Minimize Pilot Workload

(4) Provide a High Degree of Maintainability and Built-In-Test

(5) Provide High Reliability.

The F-14 uses a dedicated subsystem design to implement these goals.

The F-14 Air Inlet Control System (AICS) fail safe design was achieved by providing two identical dedicated subsystems which were completely independent of each other. The location and configuration of the F-14 probes are shown in Fig 1. Each pitot-static probe contains a single pitot tube with two sets of independent static ports.

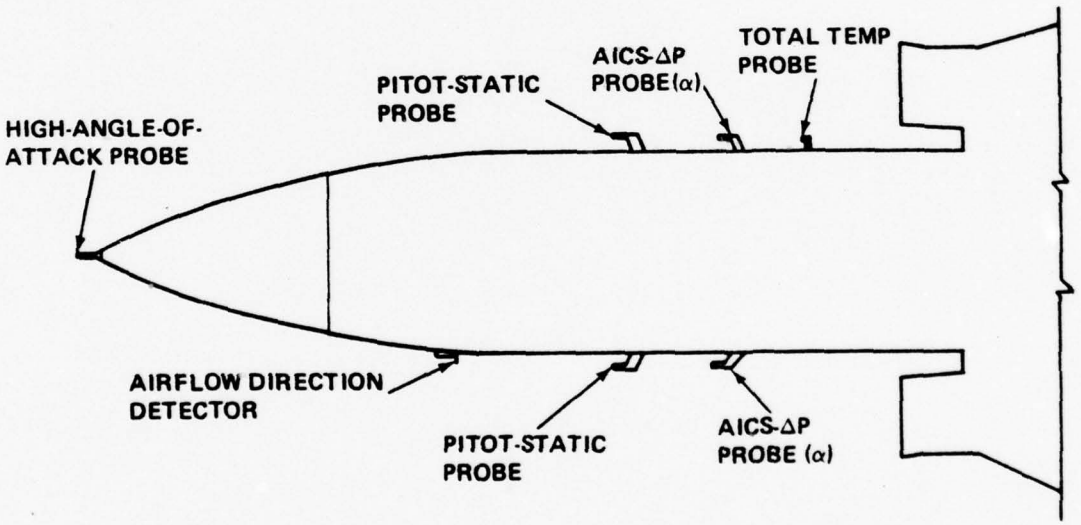


Figure 1 - F-14A AIR DATA PROBE LOCATIONS

The probe and pneumatic system interconnects schematically shown in Fig. 2 provide independently sensed pitot-static pressures to each air inlet total and static pressure sensor. Independent left and right side Delta-P probes and associated sensors are provided for each control system. Fig. 2 shows two completely independent dedicated AICS programmers, and associated electrohydraulic actuators.

The probability of survival for flight critical systems is maximized by providing separate hardware which are remotely located from each other. The F-14 engine air inlet control system accomplishes this by providing two completely independent AICS . The dual set of pneumatic probes, programmers and electrohydraulic actuators, (see Fig. 3), for each system are also remotely located from each other.

A subsystem incorporated into the F-14 to minimize pilot workload is the High Angle of Attack System which provides reference signals for the flight control system and Flap/Slat/Glove Vane System (Fig. 4). For small angles of attack, roll command is achieved by commanding differential tail movement. As the angle of attack increases, lateral stick inputs result in the phasing in of rudder movement while phasing out horizontal tail movement. At angles of attack greater than 20° , the roll comands result in a maximum rudder position of 19° with a corresponding horizontal tail position of 2°.

The Flap/Slat/Glove Vane System features completely automatic control with pilot overide capability. Automatic extend and retract signals are based on angle of attack and Mach number. Included in the system is a position limiter which is a function of Mach and altitude. The Wing Sweep System, Fig.5, is a dual channel system with four modes of operation. In the auto mode the wing position is automatically programmed between 20° and 68°.

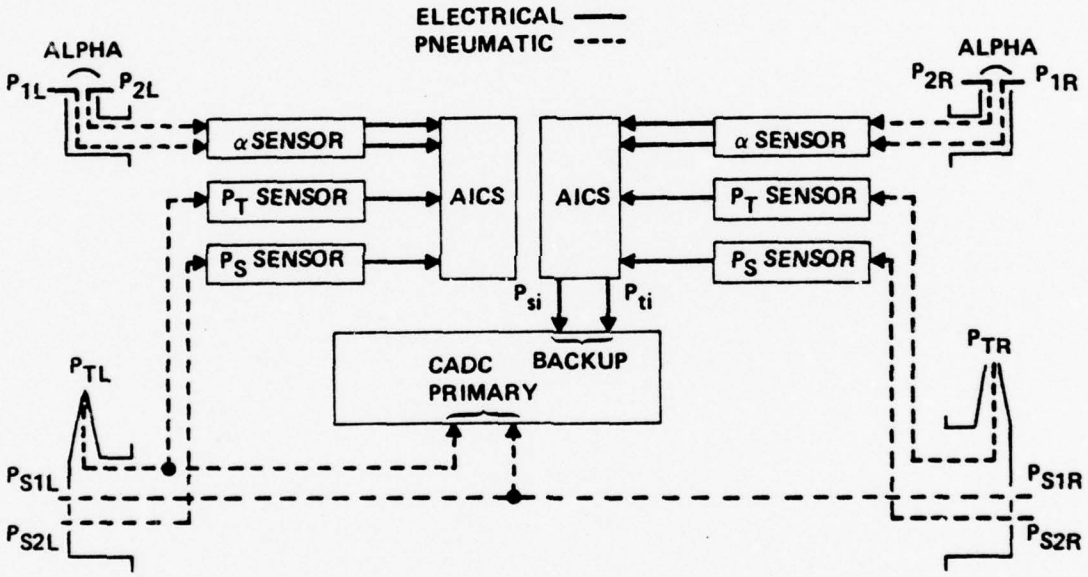


Figure 2 - F-14A AICS/CADC PROBE CONFIGURATION

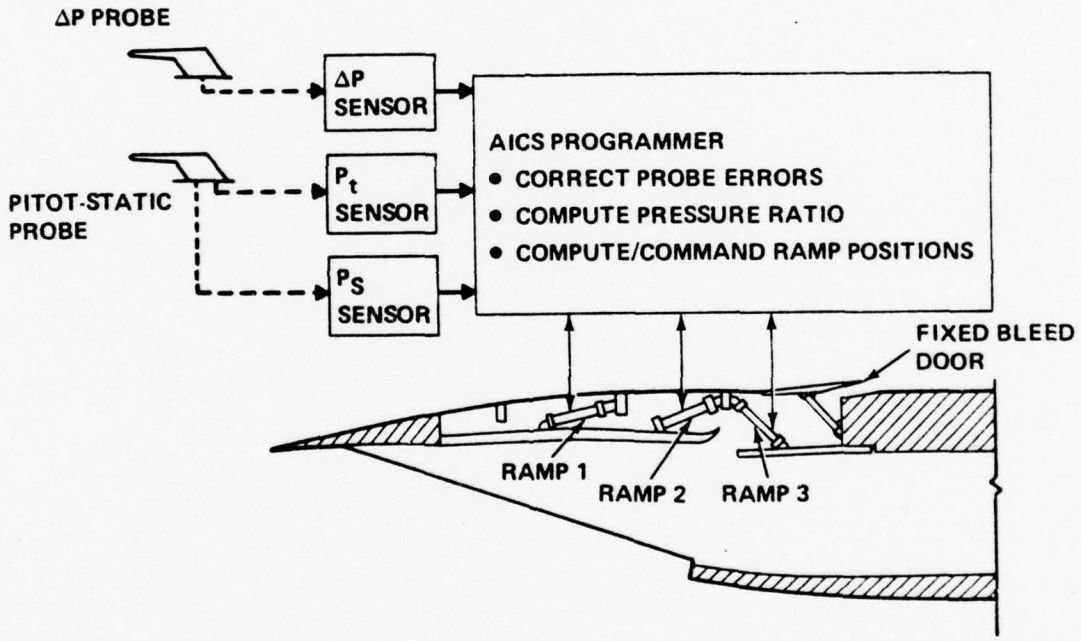


Figure 3 - F-14A AIR INLET CONTROL SYSTEM

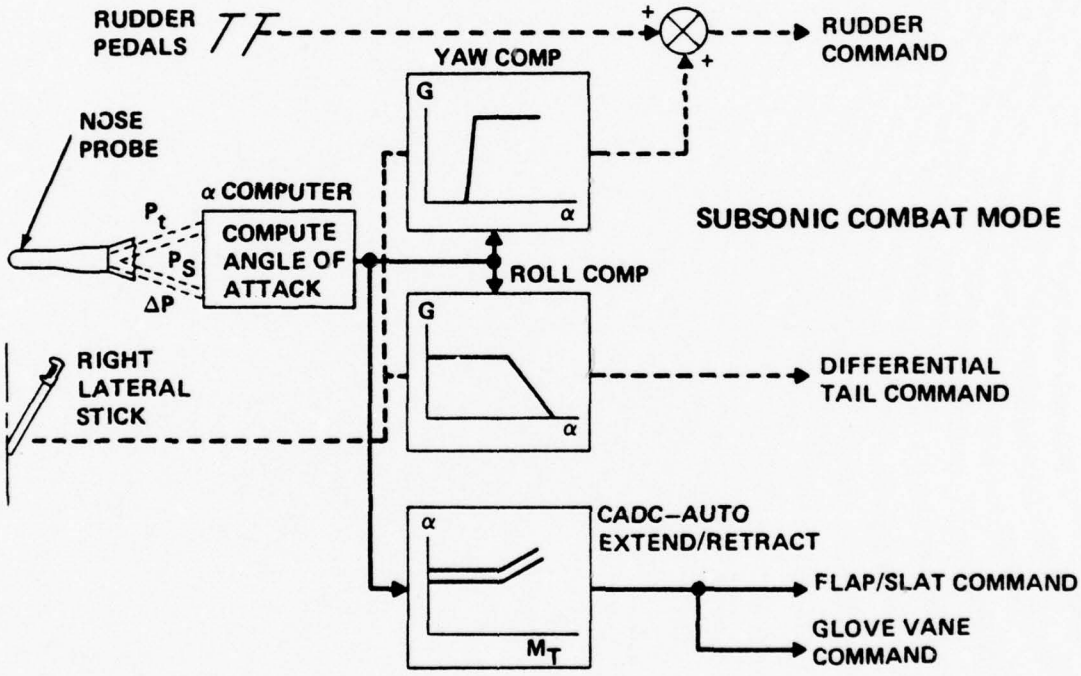


Figure 4 - AUTO/RUDDER INTERCONNECT/FLAPS SLATS

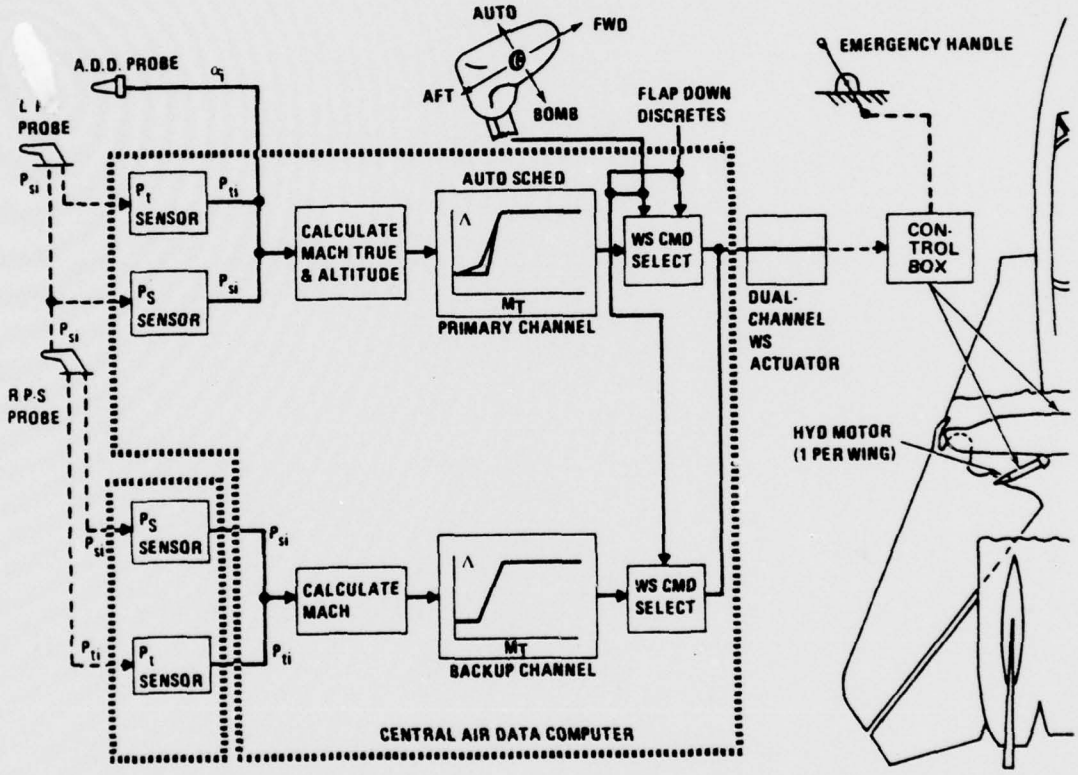


Figure 5 - F-14A WING SWEEP CONTROL SYSTEM

It is undesireable to configure major systems in a manner where a single failure will propagate to multiple systems, and result in increased pilot workload. In the F-14, the primary channel of the Wing Sweep System is independent of other major subsystems, such as the AICS. Consequently, subsystem failures are self contained.

The F-14 subsystems contain a considerable amount of built-in-test and in-flight failure monitoring to achieve a highly maintainable system. Fig. 6 is a schematic drawing of the failure monitoring for the Wing Sweep System.

Primary channel checks consist of comparing a calculated impact pressure, Q_0, from the total pressure and static pressure transducers with an independent Q_0 obtained from the Q_0 sensor. In addition, digital processor and output command self-tests are performed within the Control Air Data Computer, (CADC). Further, position feedbacks from the wing sweep actuator and hydraulic motors are compared by the CADC to the command. Backup channel commands and feedback signal comparisons are also performed in a similar manner.

Whenever a system failure is detected, the pilot is notified via a caution/advisory panel. In addition, the failed parameter is determined from the Tactical Information Display by the Naval Flight Officer or ground maintenance personnel.

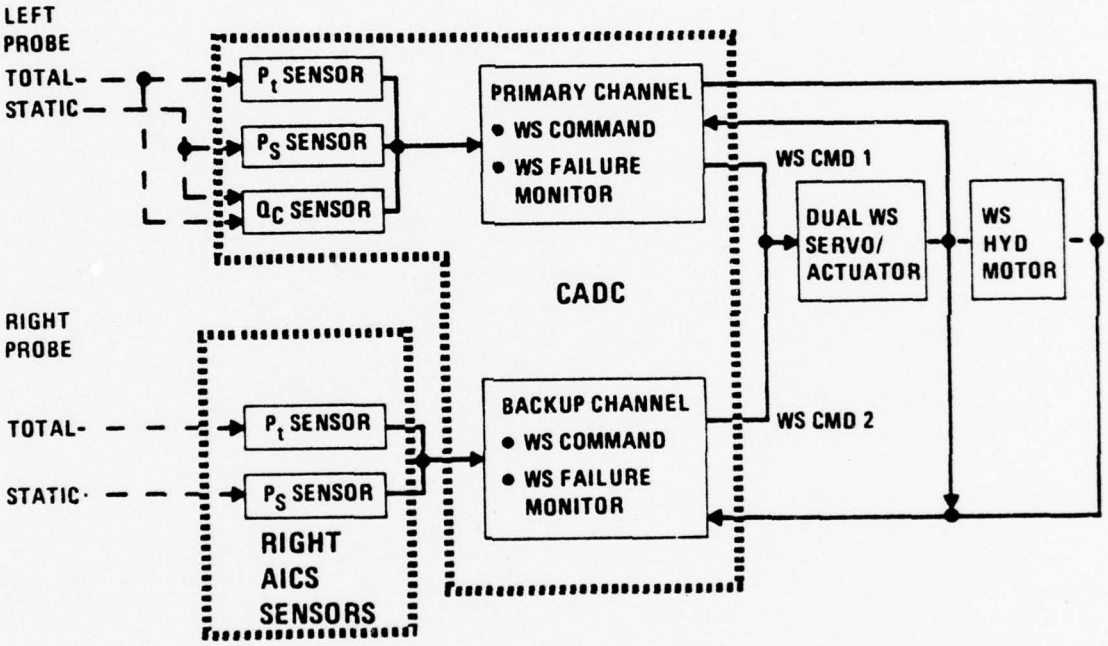


Figure 6 - WING SWEEP FAILURE MONITORING

It is readily apparent that a highly sophisticated fighter aircraft depends heavily on its sensors to accurately measure pressure, angle of attack, total temperature, position, flow rate, and failures through built-in-test and in-flight failure monitoring.

B. AIR DATA SYSTEMS

This subject is technically outside the realm of aircraft sensors, and therefore will only be covered lightly. The sensor/air data system integration is an important one and fundamentally impacts on the choice of sensors.

The controversy over the optimum system partitioning continues and neither the dedicated ADC or the central computer approach enjoys a significant advantage. The dedicated Air Data Computer is superior in performance, dynamic response, and software, with the safety inherent in the dedicated system its strongest point. Vehicle wiring, weight, and program management are areas of rough equality. Some engineers feel that the dedicated ADC seems to have a slight advantage, but as more central computer systems evolve along with better techniques to implement them, the pendulum may swing the other way.

In the past, when central air data computers were mechanized exclusively in analog, electromechanical fashion, they were by their very nature totally dedicated to the air data application. With the advent of digital technology and its application to the air data function, increasing consideration has been given to incorporating at least the air data computational task into the vehicle central

processor. While many avionics computational functions have already undergone the centralization process, there has been resistence in the air data case due to the following:

1.) Air data functions are by their nature flight-critical which precludes the use of a single central processor.

2.) The solid-state digital air data sensors , input interface, and output interface make the processor itself a relatively small percentage of the DADC hardware.

3.) Flight tested DADC algorithms and associated software are sufficiently stable to use PROM/ ROM memory techniques.

The choice of a dedicated air data computer or a central processor with remote sensors rests on the parameters mentioned earlier, that is, performance, dynamic response, weight, vehicle wiring, and software/program management.

Most digital air data pressure sensors currently in use require an analog-to-digital converter and a digital processor tc linearize the sensor. The sensor module usually contains a memory that stores the constants required for this linearization. This pressure output is not corrected for temperature or pressure non-linearities, and therefore must be routed to a digital processor, along with the temperature sensor output, in order to obtain a linear pressure signal. The dedicated air data computer combines this two-step procedure into a single dedicated air data

computer. Elimination of the pressure assembly processor requires buffering of the uncorrected signals, additional wiring and shielding, plus some means of formatting the signals. This adds up to increased weight and volume.

Regarding dynamic response, the maximum data "staleness" for the central processor approach could be as high as 7 times that of the dedicated approach (see ref. 2). If the pitot-static system dynamics were included, the staleness times would increase. Obviously, priority of systems data processing is an important factor in the dynamic response of the air data system.

The central computer approach seems to have an advantage in weight since presumably the sensors, without the analog circuitry, would weigh less. However, these signals must still be processed somewhere, and even if the input/output unit of the central computer is a versitale one, unique signals such as altitude reporting would still be required. Thus the argument that the central computer offers the least weight is debatable.

The amount of wiring to and from an air data computer is a function of systems requirements and the number of systems using air data. The B-1 CADC, for example, has 54 dc analog outputs, 40 of which interface with the Automatic Flight Control System. Since each output requires 2 wires, this is a total of 108 wires for the analog output alone. The tradeoff on vehicle wiring between the central computer versus the dedicated air data computer is meaningless if the systems still have a heavy analog interface such as the AFCS. More information would be required such as location of system units to determine wire run lengths.

The software management of the dedicated air data computer is relatively simple since the air data functions

are well known and do not change. The only correction needed is for pitot-static position error, and if PROMs or ROMs are used, it is easy to program new memories to correct for the pitot-static system error.

In the central computer concept, the memory is a volatile one, and the program must be managed in such a way that the program is modular. If this is not done, a change to correct for pitot-static error involves large costs and a total software change.

Another software problem is the apportionment of available processor time during critical work periods. Certain parameters must be updated frequently in order to maintain safe operation. The software manager must determine which systems can live with fewer updates during this critical time and still function effectively. Timing margins will be critical.

The program management aspect of the two approaches differ due to the fact that more responsibility for total system performance is assumed by the system supplier in the case of the Central Processor approach. For the dedicated air data approach, the responsibility for the multi-system interface problem rests with the air data computer supplier. From a monetary standpoint, it is generally conceded that the central computer approach allows for better control of funds.

III. FUTURE REQUIREMENTS

The requirements for new aircraft sensors can be broken down into three unique classes by aircraft type: fly-by-wire, conventional, and V/STOL. Even though the Air Force will have an operational fly-by-wire aircraft by late 1978, the Navy may not have one for some time. Thus the sensor/air data system requirements arising from this concept can correctly be classified as a future requirement. Conventicnal aircraft requirements stem from the increased emphasis on gust alleviation, multi-mode controls, Automatic Carrier Landing Systems, etc. Perhaps the most challenging requirements for reliable air data emanate from the combined effects cf slow speed and the complex turbulent flow fields associated with V/STOL aircraft.

A. FLY-BY-WIRE

Fly-by-wire aircraft pose a unique problem in redundancy and cost effective application of air data equipment since these aircraft feature full electronic control link with no mechanical backup. This radical departure from the traditional "emergency backup" systems requires a reliable electronic system that is fail operational or at worst fail safe. Thus the major challenge is to provide sufficient redundancy and operational monitoring so that a failure in an air data channel does not result in the loss cf the aircraft or serious degradation cf operational capability.

The air data system provides the link between the

sensing of the aircraft environment and operation of the flight control surfaces to achieve dynamic stability. The flight control computer must be given the critical gain schedules as a function of altitude, airspeed, Mach number, angle of attack, and sideslip. In addition, the air data system provides the necessary scheduling for the leading edge, trailing edge, and maneuver flap positioning for optimum aircraft maneuverability.

The critical nature of these jobs requires redundancy to insure safe operation, but the question is to what degree . Given a redundant system, the designer must devise a method of rapidly assessing the operational status of the system. Furthermore, he must weigh redundancy against cost and operational requirements.

Three systems are practical with todays' highly reliable, stable, accurate, solid-state sensors(Ref. 3). They are,

(1.) One air data channel with sensor performance monitors, Fig. 7.

(2.) Dual air data computers, Fig.8.

(3.) Triply redundant air data computers, Fig. 9.

Redundancy considerations affect the pitot static system, air data system, monitoring equipment, and flight control computer and actuators.

Ideally , the redundant air data system should employ

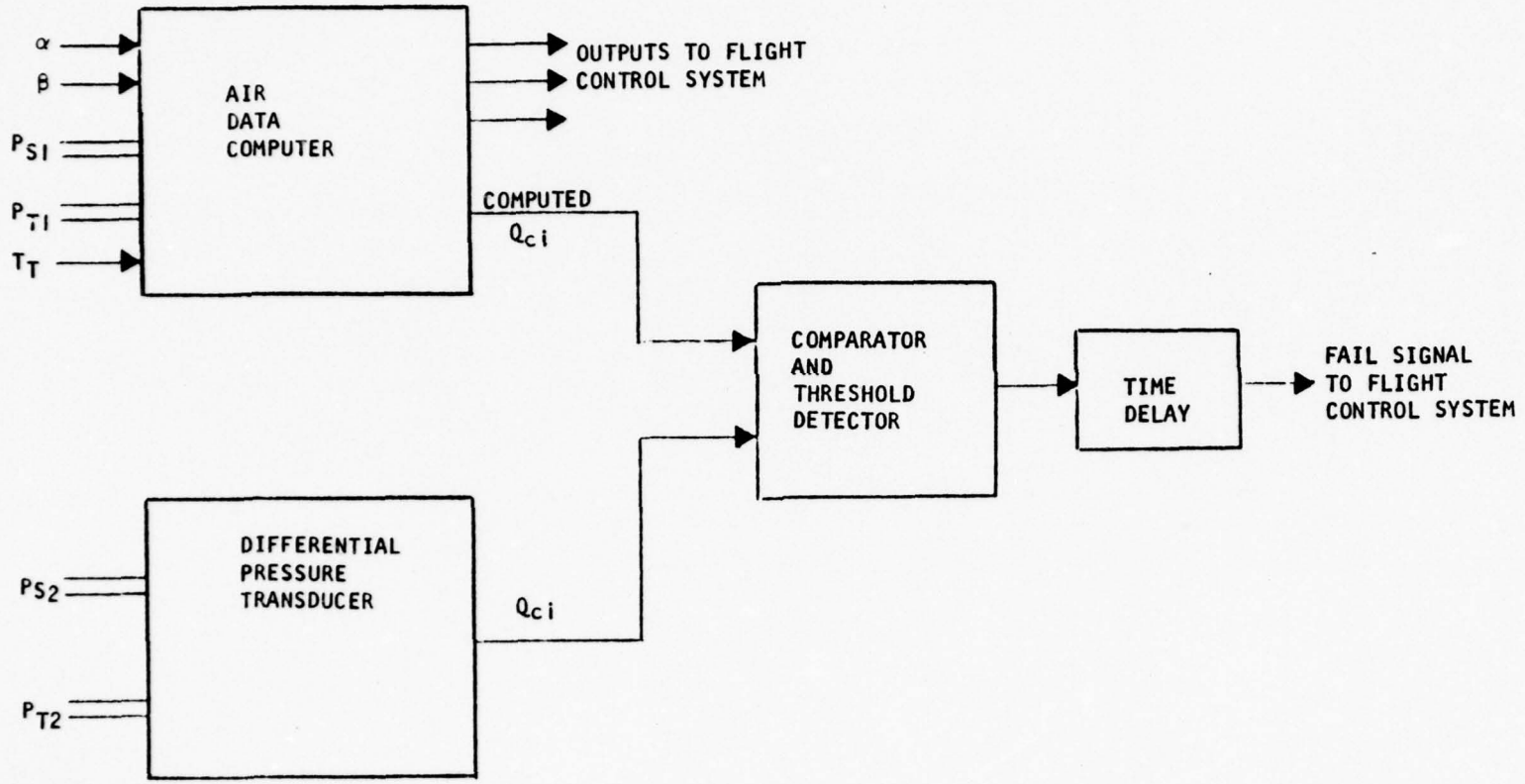


Figure 7 - SIMPLE FAIL SAFE MONITOR

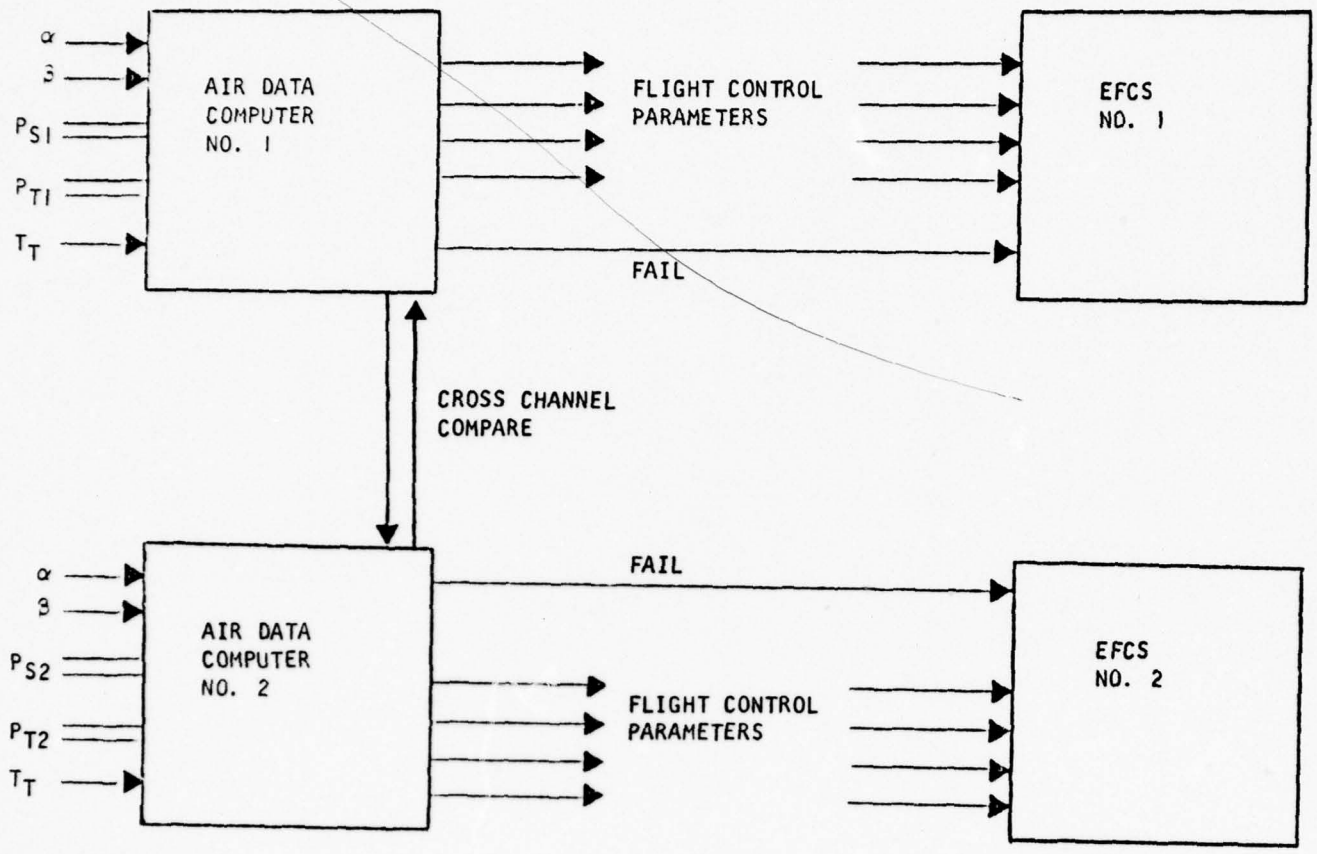


Figure 8 - DUAL REDUNDANT AIR DATA COMPUTERS

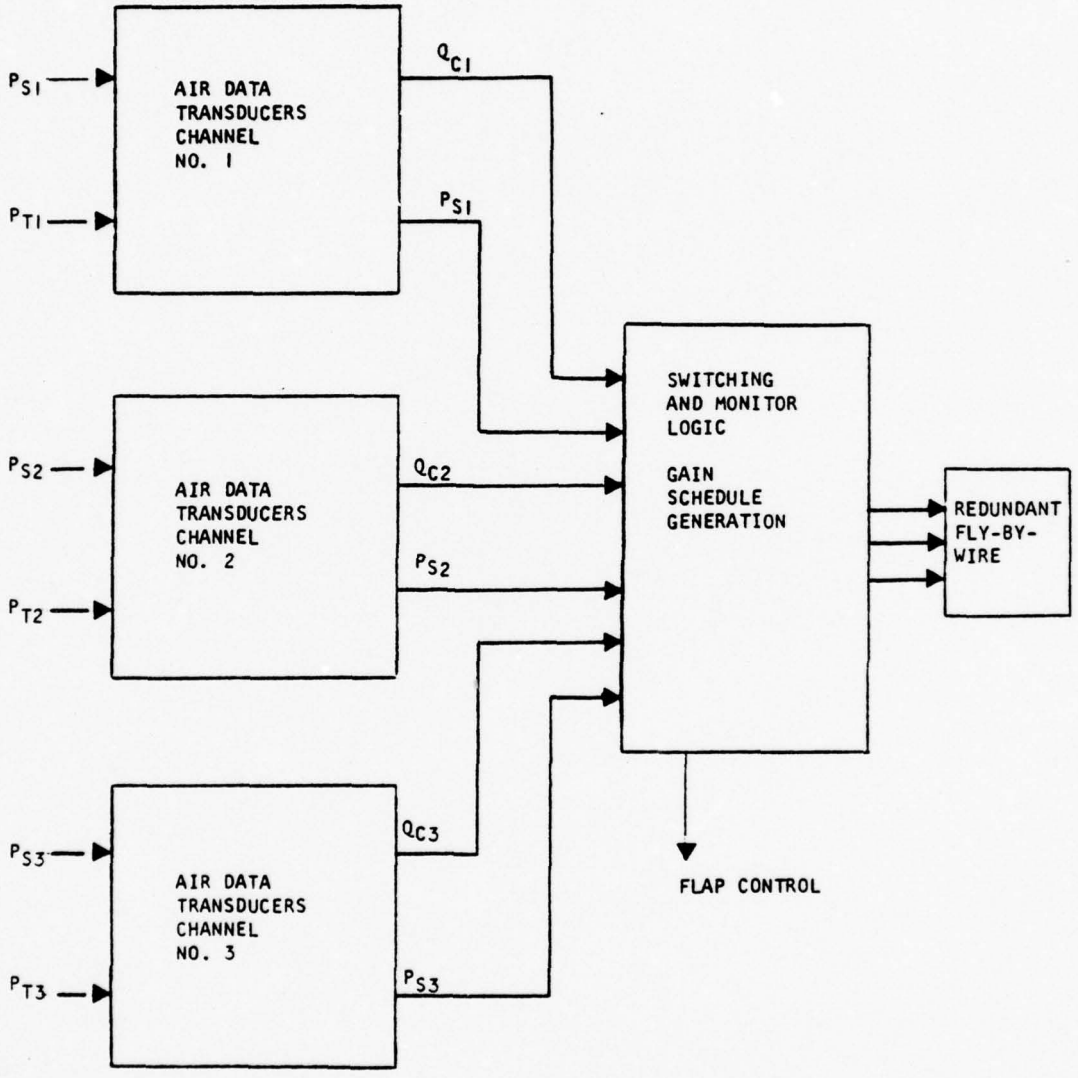


Figure 9 - FAIL OPERATIONAL /FAIL SAFE AIR DATA SYSTEM

pneumatically and physically isolated, redundant pitot-static systems. With the advent of "digital" pressure sensors, it should be possible to obtain a digital signal right at the sensor module thereby minimizing tubing runs which create havoc with lags and maintenance problems. A minimum of two sets of isolated pitot-static systems are required. Systems employing three sets of sensors face the problem of finding acceptable probe locations on the airframe plus increased maintenance costs.

The use of multiple pitot-static systems introduces the problem of different static source corrections which increases monitor trip levels. Judicial selection of probe locations and compensation in the design of the probes can reduce these problems.

The single air data computer with transducer monitoring offers the simplest form of fail safe system. Even though the computer can be self-monitored to approximately 98% by built-in-test, an undetected failure cannot be tolerated. A typical scheme for a fail safe system is shown in Fig. 7. The time delay on the comparator output is designed to minimize nuisance trips.

An air data system with two computers is fail operational in some modes and fail safe in all modes. This type of system is shown in Fig.8. A single failure of the pressure transducer, monitor, power supply, or input circuitry would result in a fail operational mode of operation, while a single failure of the output device would be fail operational since the failed computer flight control system would be shut down. A computational circuitry failure could be fail safe or fail operational depending on the actual failure.

High performance aircraft require the detection of a

cross channel miscompare and resultant shutdown in about 50 miliseconds (Ref. 3.). With the current trend toward digital air data computers, this will place an added restraint on data staleness between computers which necessitates some method of synchronization. The direct result is increased complexity and cost, with a possible decrease in reliability.

The typical triply redundant system shown in Fig. 9 has the added advantage of being fail operational for a single failure of any air data channel. This greatly enhances the mission success probability, but has been avoided due to high cost and increased weight. These disadvantages have been largely overcome with the new generation of small , low cost pressure transducers. Current aircraft are also using backup air data transducers which provide only those critical outputs required by the flight control system.

The redundancy necessary in the fly-by-wire aircraft extends to the sensors as well as the air data computers. This means multiple air data probes, transducers, accellerometers, etc. A research study for fighter/attack aircraft for the late 1980's has indicated the need for an integrated sensory subsystem which will increase operational readiness and reduce cost of ownership. The Integrated Sensor System (ISS) is illustrated in Fig. 10. Redundant sensor data and system feedback signals are linked to two or more flight control computers via a reliable and survivable data transfer. The computers will perform failure detection, isolation and signal selection of the sensor data for calculation of control system output commands. Backup air data and navigational parameters are provided for other using subsystems.

The complete ISS system shown in Fig. 11 is being developed by GAC for NADC under the Advanced Skewed Sensor

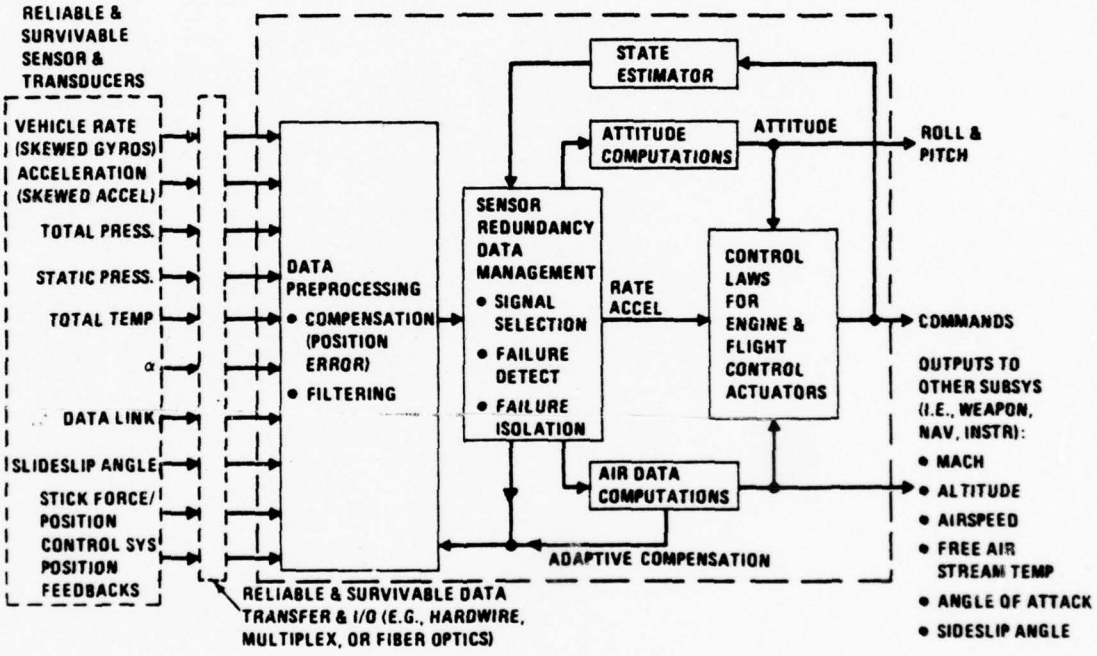


Figure 10 - INTEGRATED SENSOR SYSTEM CONCEPT

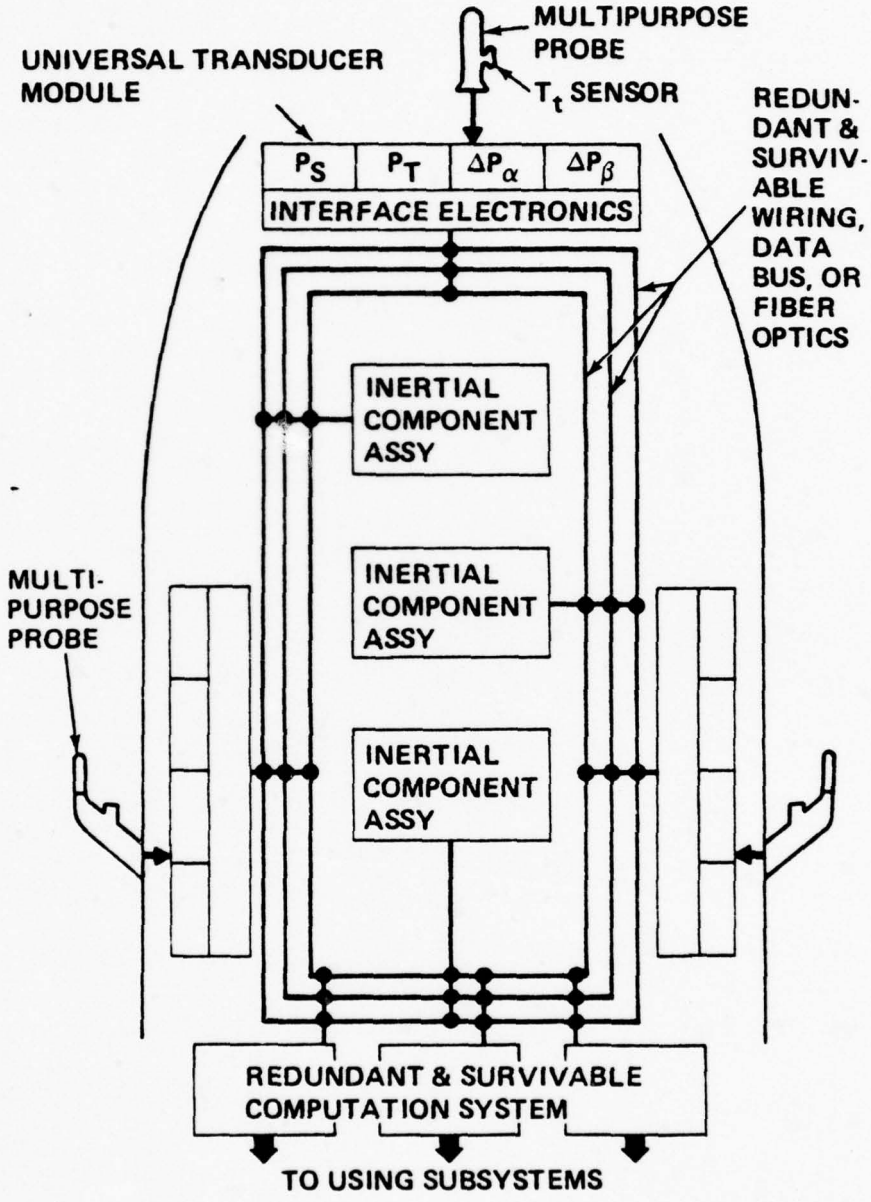


Figure 11 - COMPLETE ISS SYSTEM

Electronic Triad (ASSET) Contract. The advantages inherent to this design are:

(a) The fail operational requirement for single and multiple failures is achieved with minimum hardware.
(b) Built-in-test is optimized in that no additional hardware is required for failure monitoring.
(c) Automatic hardware reconfiguration can take place to meet mission requirements without increasing pilot workload.
(d) Reduced pneumatic tubing runs eliminate pneumatic system lags as well as enhancing the aircraft maintainability and survivability.
(e) A common interface is obtained for use with other subsystems.
(f) Cost of ownership is considerably lower than a dedicated system due to the use of common hardware and rapid fault isolation.

B. CONVENTIONAL

The developments in conventional aircraft design in the past 20 years have been incredible. Computational analysis is playing an ever expanding role in an effort to cut down the costly, time consuming wind tunnel and full scale testing. These new techniques have given the aerodynamicist a better insight into the realm of dynamic loads which has led to increased use of flexible wings. Modern aircraft such as the B-1 encounter formidible defenses that require flight for long periods at low altitudes and high speeds. This combination of flexible aircraft components and low level high speed flight exposes these aircraft to

potentially catastrophic gust loads. In addition, rising costs are reducing aircraft procurement and the aircraft in the inventory must serve out their full service life (or longer) if we are to maintain an effective combat force. Advances in flight control technology have led to the emergence of a new aircraft design concept, the Control Configured Vehicle (CCV). Two CCV concepts which show particular promise for fighter aircraft performance improvements are Maneuver Load Control (MLC) and Relaxed Static Stability (RSS).

The basic performance improvement objectives to be achieved through the use of MLC and RSS are not the same for fighter aircraft as they are for bomber/transport aircraft. The objective for bomber/transport aircraft is to improve cruise efficiency as measured by such performance parameters as range and payload. For fighter aircraft, the design objective is to improve maneuvering performance as measured by such performance parameters as specific excess power (P_s) and maximum load factor. While the RSS design concepts are essentially the same for both fighter and bomber/transport aircraft, the MLC design concepts are quite different.

A MLC system is one which employs control surfaces and maneuvering devices automatically positioned by an active feedback control system to redistribute the loading on a wing in maneuvering flight. For the large bomber or transport vehicle, the aircraft is designed so that at one g flight the wing lift distribution associated with minimum drag is obtained. This type of aircraft is almost always at one g flight so there is no particular reason to minimize drag during maneuvering flight. Therefore, MLC for a bomber/transport is used to reduce the wing root bending moments during maneuvering flight and thereby alleviating structural fatigue of the wings. This reduction in wing root bending is obtained by shifting the wing lift

distribution inboard through the proper deflection of trailing edge flaps and possibly other wing control surfaces such as outboard spoilers.

In contrast, the fighter aircraft must maintain an efficient wing lift distribution in maneuvering flight. Therefore, a fighter MLC system employs aerodymanic devices such as leading edge slats for redistributing the wing load in maneuvers in order to achieve benefits in maneuvering performance through drag reduction and delayed buffet onset.

For a conventionally designed aircraft, static stability and acceptable handling characteristics must be obtained through aerodynamic design and judicious location of the c.g. In maneuvering subsonic flight and in supersonic flight this usually results in significant tail down loads to provide the required moment balance for the aircraft. However, if a high authority feedback control system is used to provide artificial stability then the unaugmented aircraft's longitudinal static stability can be relaxed. Relaxing the aircraft's static stability by shifting the c.g. aft results in a significant reduction in down loads or even an up-loaded tail. The wing loads are now reduced since the tail loads are aiding instead of opposing the wing's lift, so the aircraft's drag is reduced and its maneuvering capability is enhanced. Relaxing longitudinal static stability with horizontal canards can also be used to provide similar drag reductions. The lift from the canards is ahead of the c.g., so if properly designed an up-loaded tail will also result. Shifting the c.g. aft and using horizontal canards are RSS concepts since they tend to make the aircraft statically unstable.

a research program conducted from 1971 to 1973 by McDonnell Douglas Aircraft Company for the Air Force Flight Dynamics Lab explored the compatibility of MLC and RSS

applied to military aircraft (Ref. 7). The study sought to determine whether desireable handling qualities and adequate stability margins could be attained when MLC and RSS were introduced to an F-4E aircraft with a fly-by-wire control system. Five MLC devices were used in the analytical aeodynamic performance studies:

(1) Operable canards
(2) Leading edge slats
(3) Leading edge flaps
(4) Trailing edge flaps
(5) Flaperons (drooped ailerons)

All possible combinations of these MLC devices were considered in the configuration selection phase of this program. Canards moved the control-fixed neutral point forward as much as 13.5% mean aerodynamic chord (MAC) subsonically and 9.5% supersonically.

The aerodynamic and control system analytical studies established that significant maneuvering performance improvements are attainable for the F-4 fighter aircraft through the application of MLC and RSS aircraft design concepts. It has also been shown that MLC and RSS are compatible design concepts in the sense that performance benefits attainable through the use of both MLC and RSS are greater than can be attained through the use of MLC or RSS individually.

Gust load alleviation is a term given to a system that senses loads on various aircraft components and actuates the controls in such a manner to reduce the magnitude of the vertical load factor.

An analysis done by NASA Langley Research Center (Ref. 8) applied stochastic control theory to the gust alleviation problem for a STOL aircraft . Elevator and flaps were used to reduce the root-mean-square value of the normal

accelerations associated with the aircraft response to gusts. The results showed that normal acceleration could be reduced by 92 percent when the intensity of the measurement noise had a very low value. However, the filter gains were large and large control deflections were required. Normal acceleration was reduced by 63.2 percent for moderate gain values.

The advantages of in flight engine monitoring are well known. Great progress has been made in this field in the last few years, and the benefits from new sensors should make it possible to equip all Naval aircraft with these systems. Advanced sensors and a digital computer/control system provide more accurate and stable control resulting in extended engine life, greater fuel economy, and reduced maintenance costs.

The Air Force Systems Command, Wright-Patterson AFB, Ohio awarded Boeing a contract for a research and development program to evaluate the benefits of inflight engine monitoring. The Integrated Propulsion Control System (IPCS) program employed digital quartz pressure sensors and a digital electronic control system on one set of hydromechanical engine and inlet controls on an F-111 aircraft. The system schematic is shown in Fig. 12 (Ref. 10). The contract was awarded in March 1973 and the flight test phase was completed in March 1976. The conclusions were that more precise control of a propulsion system is desireable and possible, but depends on the availability of precise measurements made with accurate, reliable, compatible sensors.

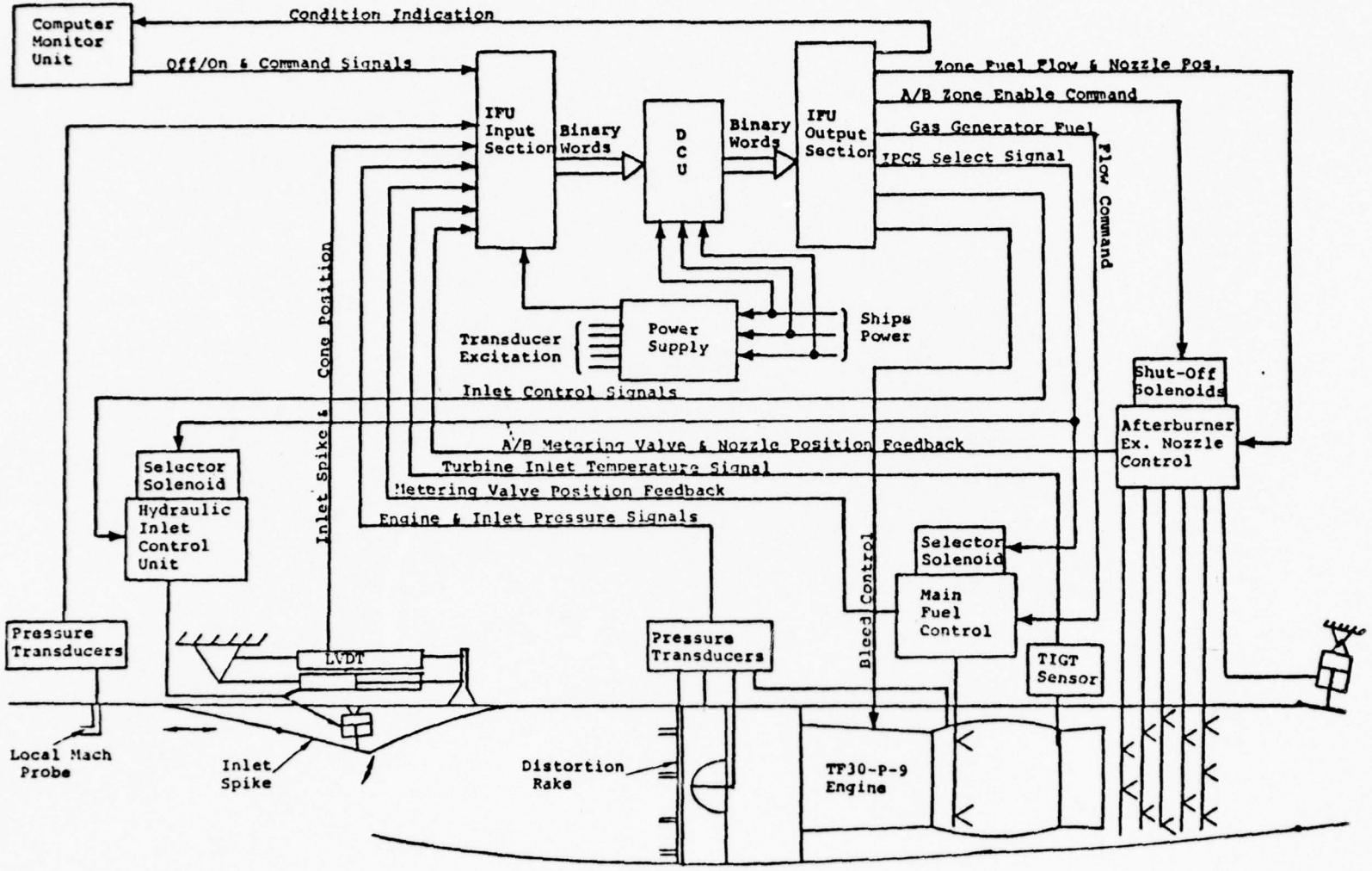


Figure 12 - IPCS SCHEMATIC

C. V/STOL

V/STOL aircraft such as the x-22, AV-8A, AV-8B, XFV-12A, and VAK-191 all operate in the slow speed regime, and all tend to have poor directional stability accompanied by a tendency to roll with sideslip in slow speed flight. In addition, they have turbulent flow fields , serious ground effect problems (suckdown and ground erosion), power loss due to hot gas re-ingestion problems, and poor vertical response characteristics. The single most demanding sensor requirement generated by these aircraft is for an accurate, reliable, omnidirectional airspeed system which functions throughout the hover and transition regions.

The present pitot-static systems may lag the actual airspeed by 15-30 knots or more (Ref. 5). In addition, present systems are unidirectional and consequently cannot tolerate significant sideslip angles. Current airspeed systems give no indication of lateral velocity which makes hover control impossible without visual cues. Since the astronomical rise in cost of conventional carriers has forced the Navy to shift its emphasis toward the development of "Sea Control Ships" with V/STOL aircraft, these visual cues will largely be absent. Thus, the need exists for an airspeed system that displays lateral as well as longitudinal velocity. Candidate systems will be discussed in sections B-1 through B-6.

While Automatic Carrier Landing Systems are approaching a high level of sophistication for conventional aircraft, the same cannot be said for V/STOL aircraft. All weather operation of these aircraft from small platforms will make such a system a necessity. A velocity command system was

demonstrated by the U.S Navy Hovering Vehicle Versatile Automatic Control (HOVVAC) Program, but much work remains to be done in this area.

D. SUMMARY

The future Naval aircraft sensor requirements may be broken down into three categories by aircraft type: fly-by-wire, conventional, and V/STOL.

Fly-By-Wire

The implementation of fly-by-wire technology has precipitated the requirement for redundant air data systems. The designer must consider the following in choosing an air data system design:

(1) Does the aircraft mission warrant fail operational or fail safe capability.
(2) Based on the above, to what degree must the system be redundant.
(3) What are the cost/reliability tradeoffs.
(4) Given the necsssity for a triply redundant system, are there three suitable sensor locations on the aircraft, or can the sensors be housed in a single unit.
(5) For physically remote locations can the error correction, synchronization, staleness problems be overcome without seriously degrading system performance.
(6) Do the cost/reliability tradeoffs warrant the use of an integrated sensor system design.

Conventional

The increased use of flexible aircraft components coupled with sustained high speed flight at low altitudes has resulted in greater susceptibility to structural failure/fatigue inducing gust loads. The desire to achieve more efficient aerodynamic control has led to the design of multi-mode controls. Thus the requirements for Naval aircraft in this category are:

(1) Design and implement a gust load alleviation system.

(2) Continue to improve the efficiency of aerodynamic controls through multi-mode controls.

(3) Utilize advanced sensors and digital computer/control systems to provide inflight engine monitoring for all Naval aircraft.

V/STOL

This class of aircraft presents difficult problems in the low airspeed flight region of takeoff/landing, hover, and transition. The requirements stemming from these problems are:

(1) An operational airspeed system capable of giving accurate, reliable, longitudinal, and lateral velocities from 0 to 200 knots must be developed and implemented.

(2) Operational requirements dictate that an Automatic Carrier Landing System be developed for V/STOL aircraft which functions throughout the hover and transition region.

IV. CURRENT/PROSPECTIVE SENSORS

A. PRESSURE

1. Digital Quartz

Several manufacturers offer digital quartz pressure transducers (Paroscientific, Garrett Electronics, Setra, etc.) which are particularly suited for air data applications for the following reasons:

(1) The digital output is simple to process and characterize.

(2) The uncompensated temperature coefficient is very low.

(3) Compensation makes the transducer insensitive to orientation, acceleration, and vibration.

(4) Pressure resolution of .003 percent full scale is possible.

(5) Quartz crystals have low temperature sensitivity, remarkable elastic properties, and long term stability.

On the surface, the properties listed above make the digital quartz pressure transducer extremely attractive. However, these transducers do have some drawbacks which will be examined in regard to the sensor manufactured by Paroscientific.

The Paroscientific transducer , Fig. 13, employs a quartz-crystal oscillating beam whose resonant frequency

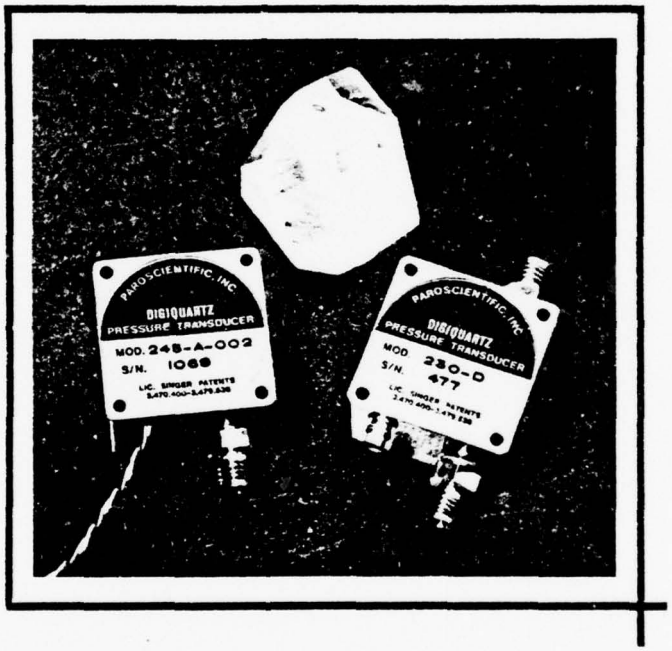


Figure 13 - PAROSCIENTIFIC TRANSDUCER

varies with applied loads. The mounting system shown in Fig.14 effectively decouples the fixed-fixed beam from the force producing structure. The resonant frequency of the vibrating beam is determined by its dimensions, composition, and stress load. The entire resonator is fabricated from one piece of quartz to minimize energy loss due to joints. The beam is driven at its resonant frequency through piezoelectric excitation. The theoretical mean-time-before failure is over 100,000 hours (Ref. 9). Although the quartz-crystal resonator can operate at normal ambient pressures and temperatures, its performance is significantly improved in a vacuum.

DISCUSSION

The torque balance or seesaw arrangement shown in Fig.15 was chosen to make the transducer insensitive to acceleration or orientation in the earth's gravity field. This system does not work in operational applications other than for bench top measurements.

The short term stability of the absolute pressure transducers appears to be quite good. The major factors in intermediate stability are environmental effects such as temperature. Long term stability is dependent on the aging of the quartz crystal resonator, stability of the absolute pressure reference, and mechanical relaxation effects. The effects of temperature on two models, the 2200-A and the 230-A, are shown in Fig. 16. There are significant deviations for both models over the temperature range shown. This is not satisfactory performance. The overall accuracy appears to be approximately .05 percent excluding temperature.

The mathematical model which characterizes the

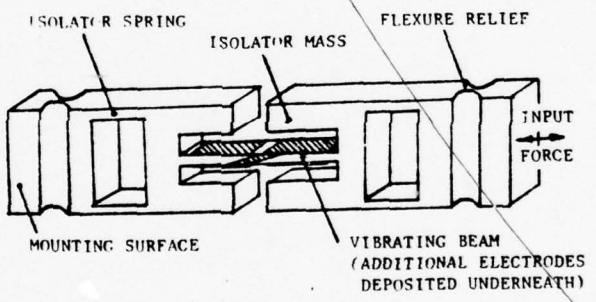


Figure 14 - QUARTZ CRYSTAL MOUNTING SYSTEM

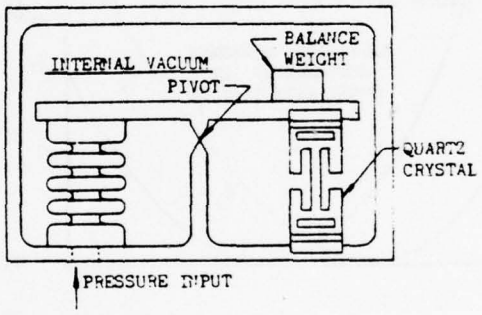


Figure 15 - TORQUE BALANCE

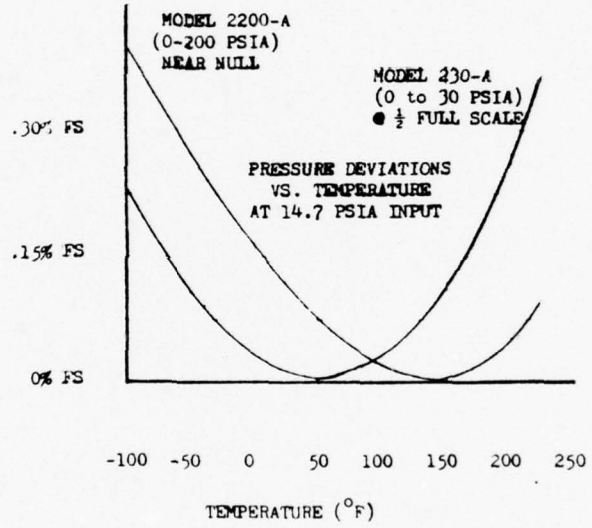


Figure 16 - PRESSURE DEVIATIONS VS TEMPERATURE

outputs of the DIGIQUARTZ Pressure Transducers is:

$$\text{Pressure} = A\left(1 - \frac{t_o}{t}\right) - B\left(1 - \frac{t_o}{t}\right)^2$$

t =period of output

t_o =period output at zero pressure input

A,B =curve fit coefficients

The transducers available require external signal conditioning which is accomplished through a micro-processor or programmable calculator, which makes the latter more suitable for bench top applications.

To summarize, the digital quartz pressure transducer is an attractive candidate for air data applications but requires further testing and refinement. The major drawbacks are:

(1) The force balance system employed does not perform well under an operational environment.
(2) The temperature effects are unsatisfactory.
(3) The sensor is not linear.
(4) The Paroscientific sensor requires external signal conditioning.

2. Vibrating Diaphram

The Sperry Vibrating Diaphram Pressure Transducer is shown in Fig. 17 (Ref. 11). The diaphram separates the vacuum reference chamber located just under the cover from the internal pressure chamber. A magnet is attached to the center of the diaphram and is coupled with a driving coil. A dummy coil, having the same elecrtical character as the drive coil, is mounted in the base along with a temperature sensing resistor. The diaphram stiffens as it is deflected under pressure load and its resonance varies with this load and needs only to be excited to measure a pressure

VIBRATING DIAPHRAGM PRESSURE SENSING TRANSDUCER

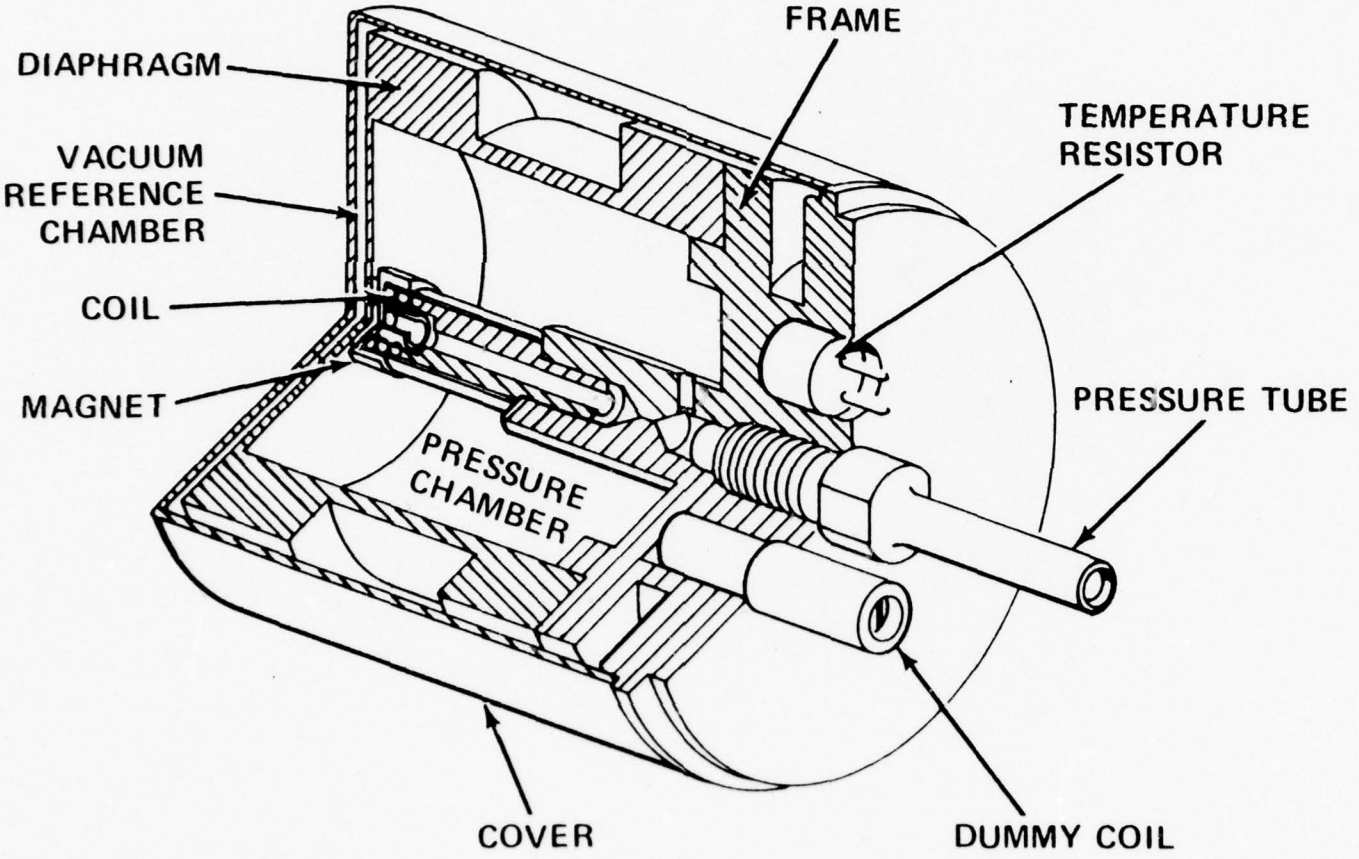


Figure 17 - VIBRATING DIAPHRAM PRESSURE SENSING TRANSDUCER

proportional to output. The interfacing between the mechanical resonance and the electronic drive is made electromechanically through the coil and magnet.

Figure 18 illustrates the basic circuit elements of the sensor drive and data conversion scheme. The transducer is represented by the magnet and fragment of the diaphram at the left side of the figure. An electrically balanced bridge containing resistors, drive coil, and dummy coil inductors provides the driving energy and feedback signals required for the closed loop oscillator. At the mechanical resonant frequency, an equivalent resistance representing the diaphram is added to the lower right hand segment of the bridge. This added resistance drives the bridge out of balance providing a signal at the output corners of the bridge which is amplified and fed back to provide the driving signal. This signal has a very narrow band pass frequency due to the high Q of the diaphram. The left portion of the circuit to the input of the squaring amplifier is essentially an electromechanical oscillator with the resonant diaphram as the tuning element. In digital applications the frequency is divided down and used to gate a high resolution counter. This provides a count output proportional to the pressure applied to the diaphram. Temperature compensation and calibration is provided electrically at the output amplifier stage. The transducer can also be used for analog applications by converting frequency to DC voltage.

DISCUSSION

The graph in the lower portion of Figure 18 is a plot of the sensor period vs pressure for the 32 inch (Ps sensor) and the 90 inch (supersonic Pt sensor).

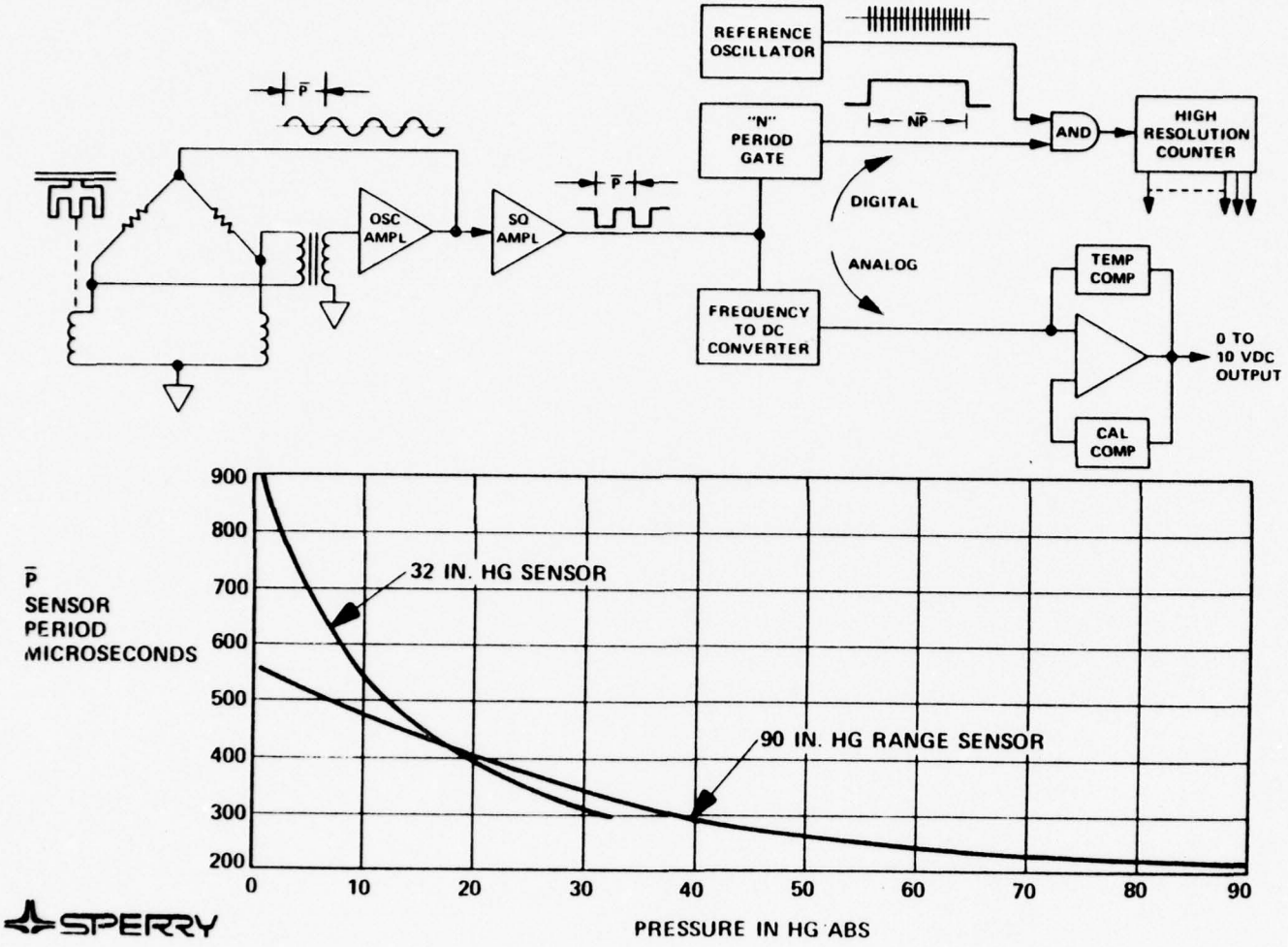


Figure 18 - TRANSDUCER DRIVE CIRCUIT AND DATA CONVERSION SCHEME

The manufacturer states that although the response is non-linear with pressure (Fig. 18), the frequency of the 32in Hg sensor, which would be used for altimeter functions, is nearly linear with altitude. The sensor is temperature compensated, but improvements in accuracy could probably be achieved if the transducer and local circuitry are held at constant temperature. The manufacturer employs numerous process controls and multiple screening to produce acceptable transducers. Thus the basic questions to be answered concern cost, resolution, and temperature compensation. These transducers are currently in use on the F-15 and F-16. Operational results should be evaluated for the Navy's choice of a digital pressure transducer.

3. Solid-State Silicon

The solid-state silicon pressure sensor manufactured by Honeywell Inc. marks a change in solid-state pressure sensors. In the past they have been used only for absolute pressure measurements. Current technology allows the silicon piezoresistive pressure sensor to be used differentially to provide more accurate pressure measurement of low airspeed, angle of attack, and sideslip.

The solid-state silicon pressure transducer uses the anisotropic properties of silicon to transduce strain into a measureable electrical signal. Silicon containing peizoresistive strain gage elements possess the following desireable characteristics which make it very attractive for pressure sensing applications (Ref. 12):

- A sensitivity that can be up to two orders of magnitude higher than a wire strain gage.
- Infinite resolution of applied pressure to resistive variation.
- Absence of measurable hysteresis-type errors

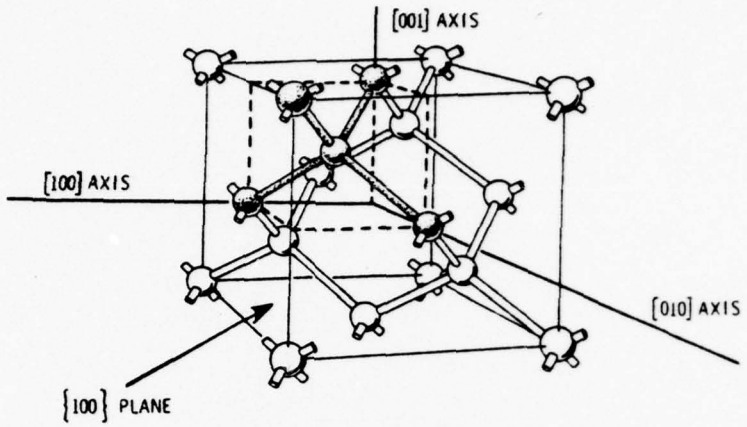
because of the near perfect elasticity of the silicon material.

- Insensitivity to large acceleration loading due to its extremely low mass.
- Mass producibility at low cost using standard semi-conductor processing.

SILICON PIEZORESISTANCE THEORY

Single-crystal silicon has a diamond cubic lattice (Fig. 19) and is both mechanically and electrically anisotropic. The result is that the resistivity of a semiconductor element within the silicon crystal not only changes, but that the fractional resistance change is a function, relative to the crystal axes, of applied stress. In addition, the mobility of the current carriers is a function of the location of the piezoresistors with respect to the crystal lattice structure of the silicon. Careful alignment of the resistive elements at a location which is a specific distance from the constraint area of the diaphram (lower portion of Fig. 19) produces a maximum change and opposite sign in piezoresistance in each element.

Processing piezoresistive strain transducers is simpler than that required for integrated bipolar or MOS circuits since the circuitry is less complex and a major portion of the manufacturing process is accomplished using standard integrated circuit wafer processing. The silicon strain transducer is a combination of a thin-member diaphram, containing two piezoresistors, and an integral edge or constraint. The constraint region of the chip is mounted onto a supporting member (or back plate) that is in turn mounted onto the transducer housing. Other construction techniques eliminate thermal hysteresis-type errors, and mechanical shock.



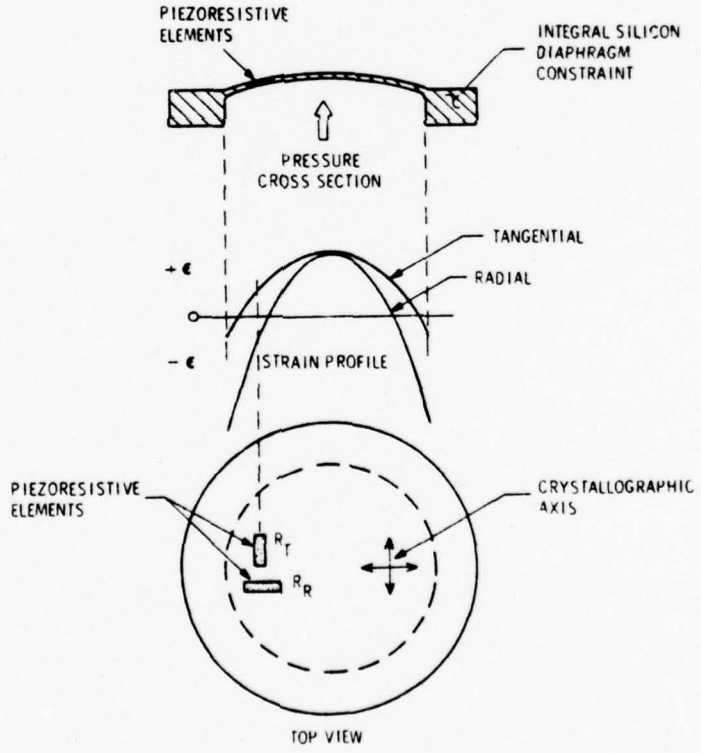


Figure 19 - DIAMOND LATTICE STRUCTURE AND TRANSDUCER CUP

The temperature dependence of piezoresistance is inherent and unavoidable. The problem is diminished by the fact that the temperature coefficient of each piezoresistor is nearly identical, and the half-bridge circuit provides the capability for measuring the temperature of the piezoresistors to effect a correction. This type transducer exhibits pressure nonlinearity which is independent of temperature, and is usually less than 0.5 percent full scale.

The pressure sensor exhibits excellent dynamic response due to the small size, minimum mass, and high natural frequency of the silicon piezoresistive diaphram and backplate. The weight of the silicon chip and stem is less than 0.4 grams, and the natural frequency of the diaphram is greater than 100 kHz (Ref. 12).

Honeywell's method of exciting the resistors is the current-excited half-bridge configuration shown in Fig. 20, which is common to both analog and digital output signal sensors. Common moding is the means for removing the large R(T) (TCR) of the piezoresistors and converting only the piezoresistance R(P) into an electrical signal representing applied pressure. Amplifier U4 will not respond to equal changes in the outputs of U1 and U2. Amplifier U3, however, responds to an equal change in the piezoresistors but not an equal and opposite change (i.e. pressure change). The circuitry used following the bridge electronics of Fig. 20 for the digital application is shown in Fig. 21. This converts the signals from U3 and U4 to 17-bit binary words. The time pulse , or binary digital signal contains the temperature dependent and pressure nonlinearity errors which must be removed in the central processor. The PROM constants are unique to each transducer and all sensors with identical part numbers may be interchanged without calibration.

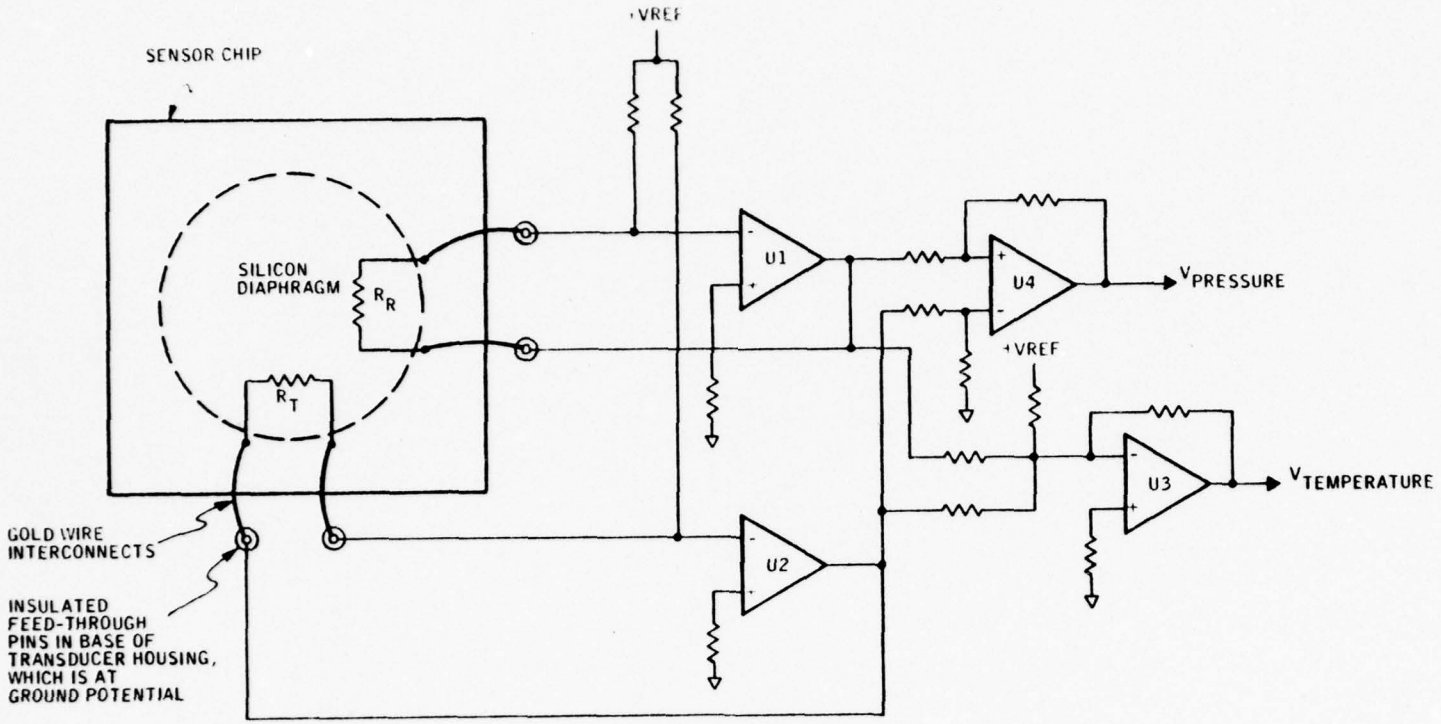
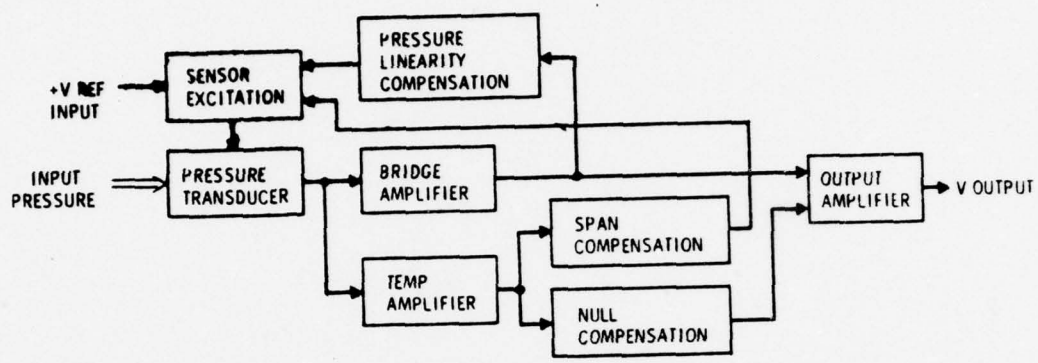
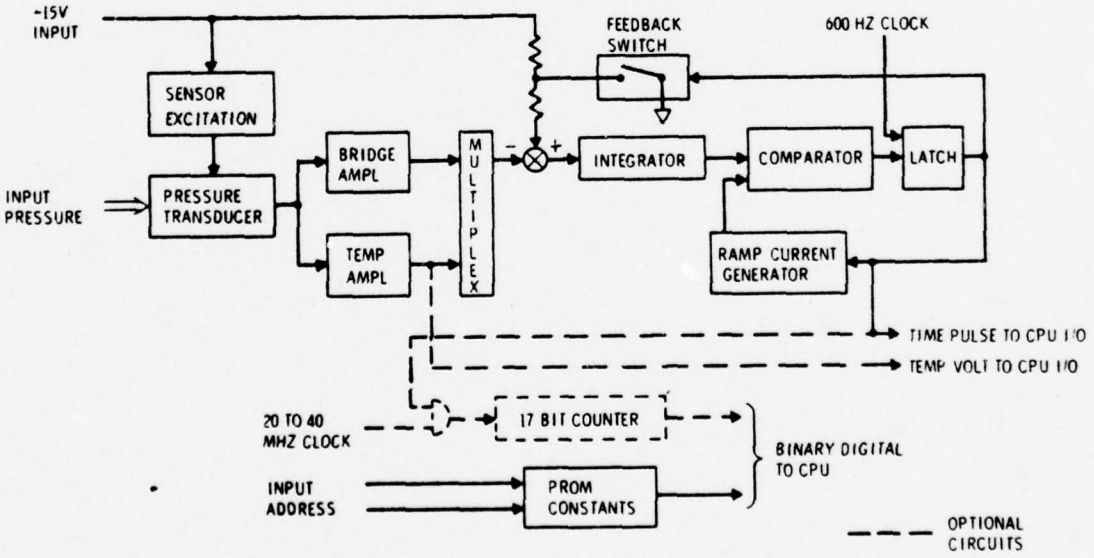


Figure 20 - SENSOR BRIDGE ELECTRONICS



a. ANALOG MECHANIZATION



b. DIGITAL MECHANIZATION

Figure 21 - ANALOG AND DIGITAL PRESSURE SENSORS

A maximum of 20 constants are required to provide ± 0.005 percent full scale over a temperature range of -54° to +71°C. The accuracy of the constants stored in the PROM is easily achieved by including an extra constant that forces the sum of the required constants to zero if they are correct. Figure 22 shows an example of the complete digital pressure sensor which have accumulated over 9.7 million hours of operation and demonstrated a reliability of 58,800 operating hours MTBF (Ref. 12).

Honeywell produces silicon piezoresistive sensors with accuracies ranging between ±0.03 and 1.0 percent full scale. The results of Honeywell's accelerated life tests on the silicon transducers is shown in Fig. 23.

DISCUSSION

The silicon piezoresistive pressure sensor provides high performance, minimum weight and size package, plus a weight advantage over other sensor concepts when the need for a dual-redundant transducer and a high BIT capability becomes a requirement. This sensor can output analog or digital signals and may be used in dedicated air data computers or in remote applications. Additional size and weight reductions are possible with hybrid and LSI circuits.

This piezoresistive transducer requires a lot of electronics if high accuracy is desired. Thus, these transducers are very well suited for low cost high output moderate accuracy pressure transducers and accelerometers. High accuracy is attainable at the expense of additional external circuitry. For the moderate accuracy application, this circuitry could be minimized by reducing the number of bits slightly without compromising too much accuracy.

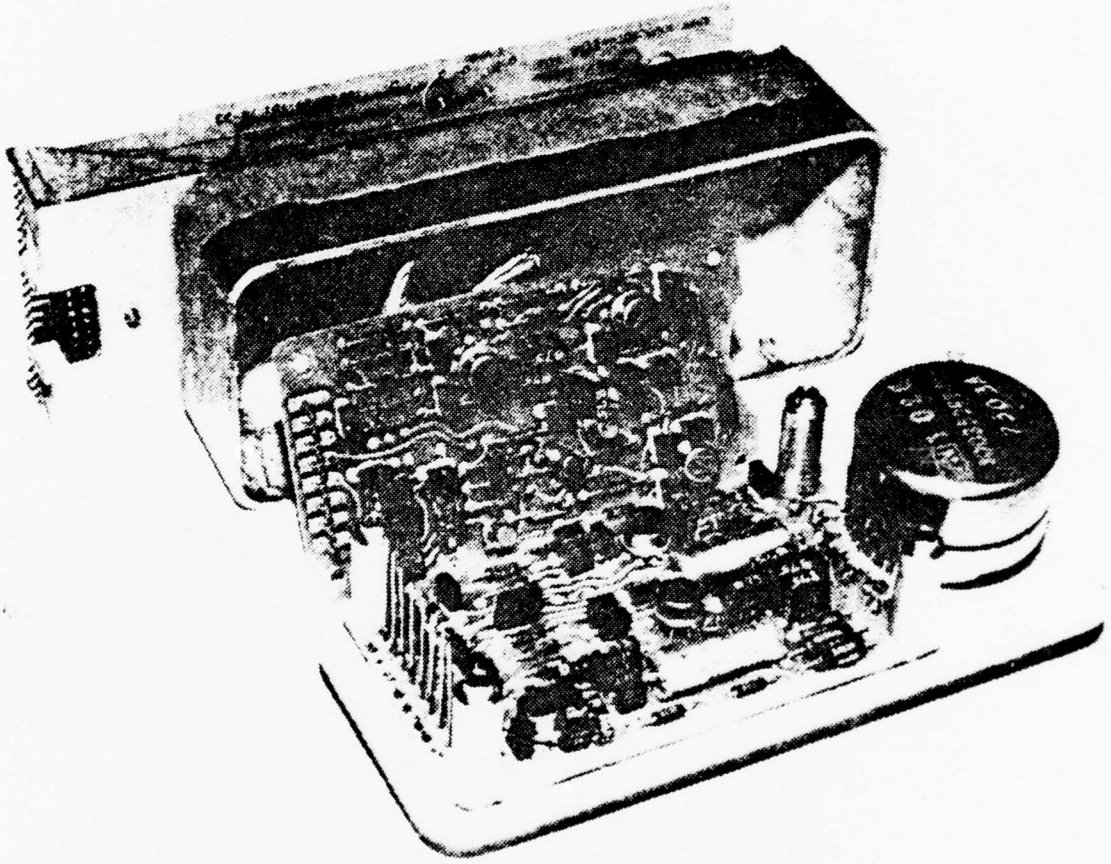


Figure 22 - HG280 DIGITAL AIR DATA COMPUTER PRESSURE SENSOR

OPERATING ENVIRONMENT

- CONTINUOUS AMBIENT TEMPERATURE CYCLING, -40°F TO 131°F
- CONTINUOUS PRESSURE CYCLING
- VIBRATION ±2.0g (10 MINUTES EVERY HOUR)
- 7000 TOTAL OPERATING HOURS

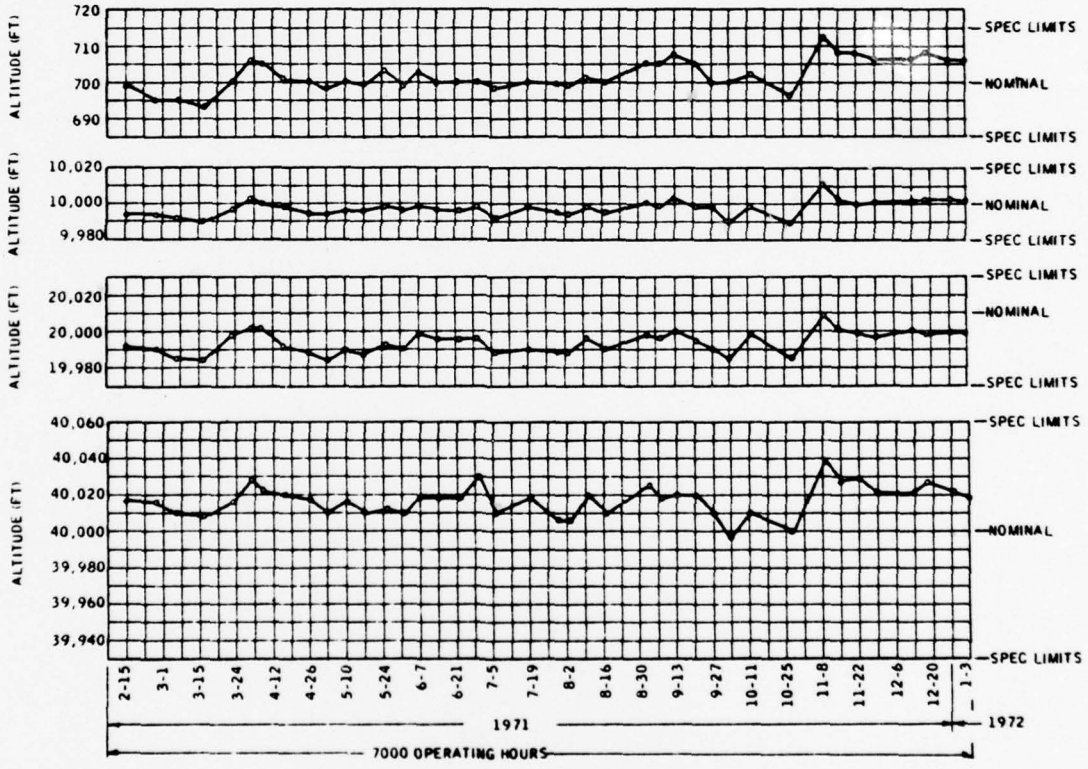


Figure 23 - ACCELERATED LIFE TESTS

4. Resonant Capsule

The Kollsman resonant capsule pressure transducer is essentially an electronic oscillator whose tuning element is a vibrating capsule formed by a pair of pressure-sensitive diaphrams. The resonant capsule is magnetically coupled to the electronic circuits of the oscillator . A magnetic circuit, consisting of a ferromagnetic outer ring, a pair of Alnico V permanent magnets, and an air gap, is mounted on each diaphram. Figure 24 shows two generations of these transducers (Ref. 13). The permanent magnets establish a constant flux density in the air gap, and this magnetic flux cuts a number of stationary coil conductors located in the air gap. The coil is fastened to a "Trestle" spanning the capsule and the attached magnetic circuit. When the capsule vibrates relative to the coil, voltage appears in the coil as it cuts the flux field of the magnet pair air gap. On the "pick-up" side of the capsule, the voltage is amplified and a current is produced in the "drive" coil positioned on the other side of the capsule. This current produces a force on the drive magnets through the interaction with the flux lines, which accelerates the diaphram assembly. Through mechanical coupling in the capsule, the driven side causes the pick-up side to move, and the system goes into self-oscillation, when suitable gain is provided by the amplifier. The drive and pick-up magnetic assemblies are mounted in such a way that the fields are orthogonal, so that a direct signal path through the capsule cannot exist without diaphram motion.

A schematic diagram of the circuit is shown in Fig. 25. It consists of an oscillator loop and a an automatic gain control loop. The oscillator circuit is designed to

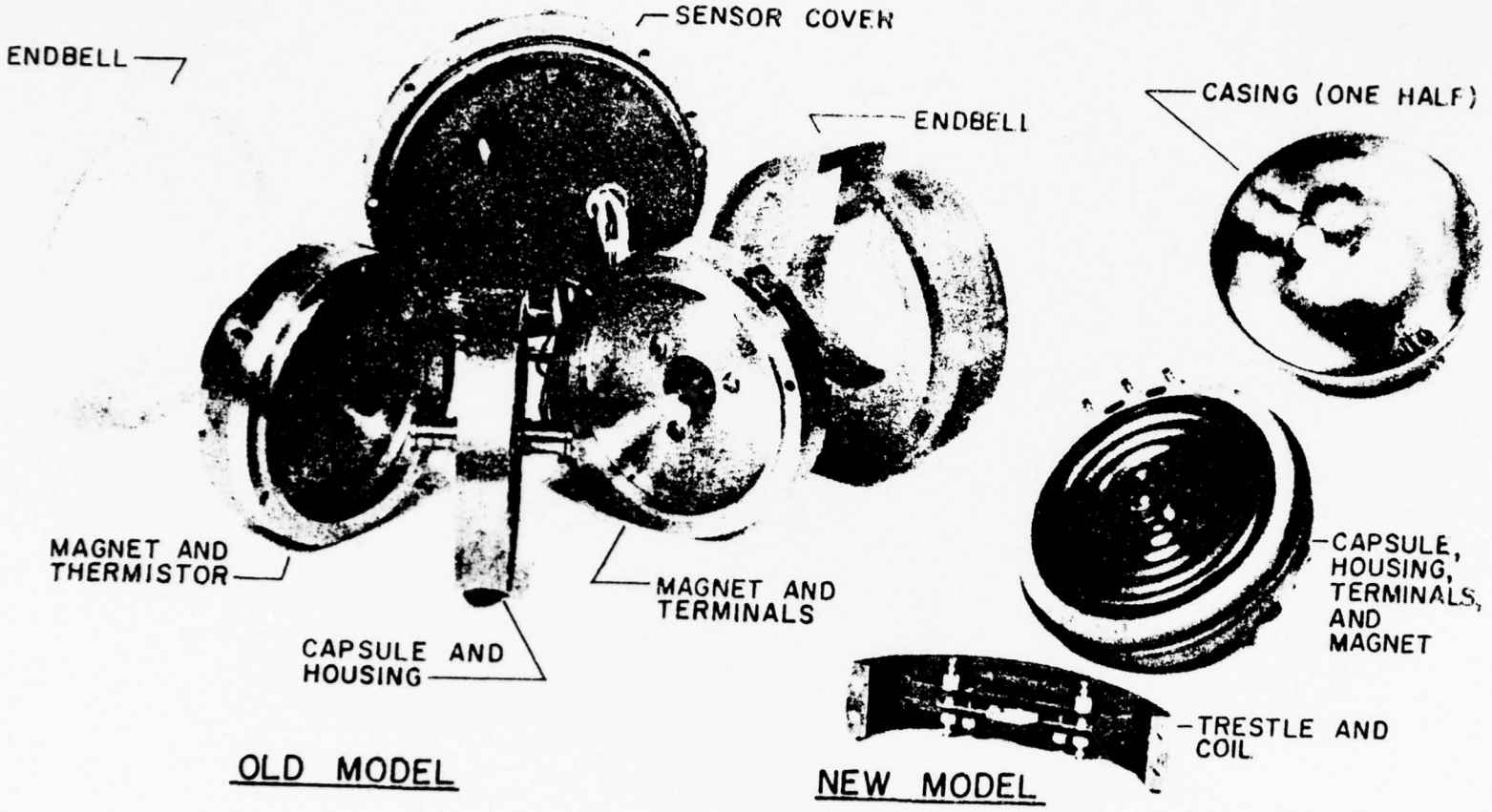


Figure 24 - RESONANT CAPSULE PRESSURE TRANSDUCER

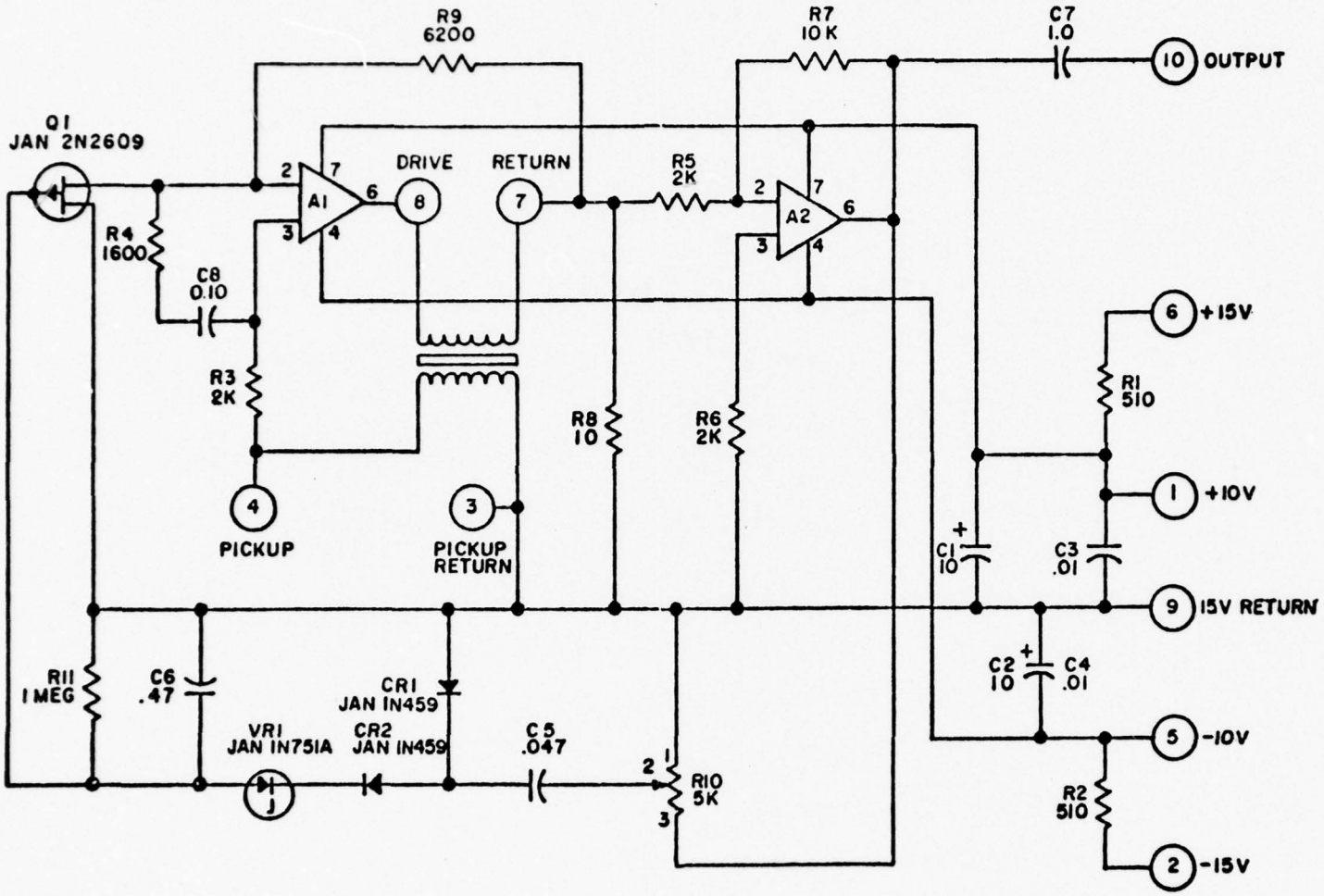


Figure 25 - OSCILLATOR CIRCUIT SCHEMATIC

provide a peak drive current of 11 milliamperes, and at sea level pressures, the capsule has a Q of about 750 (Ref. 13). The thermal controller schematic is shown in Fig. 26. The heater control thermistor is located in the sensor in thermal contact with the housing in order to maintain the sensor boundary at a constant 65°C.

The most advanced RCPT drive design is shown in Fig. 27 in which an electron beam welded aneroid capsule is secured within an aluminum housing by a rubber-like mold. It has two trestles, one for the oscillator board, and one for the temperature controller board. Figure 28 shows a typical unit installed in its insulated case.

The manufacturer states that the basic accuracy against a primary standard is at the 1σ level is:

± 0.001" for 0.25" Hg < p < 30" Hg

± 0.001 P/30" for 30" Hg < p < 110" Hg

Digital pressure transducers with 16 or 18 bit binary output are available.

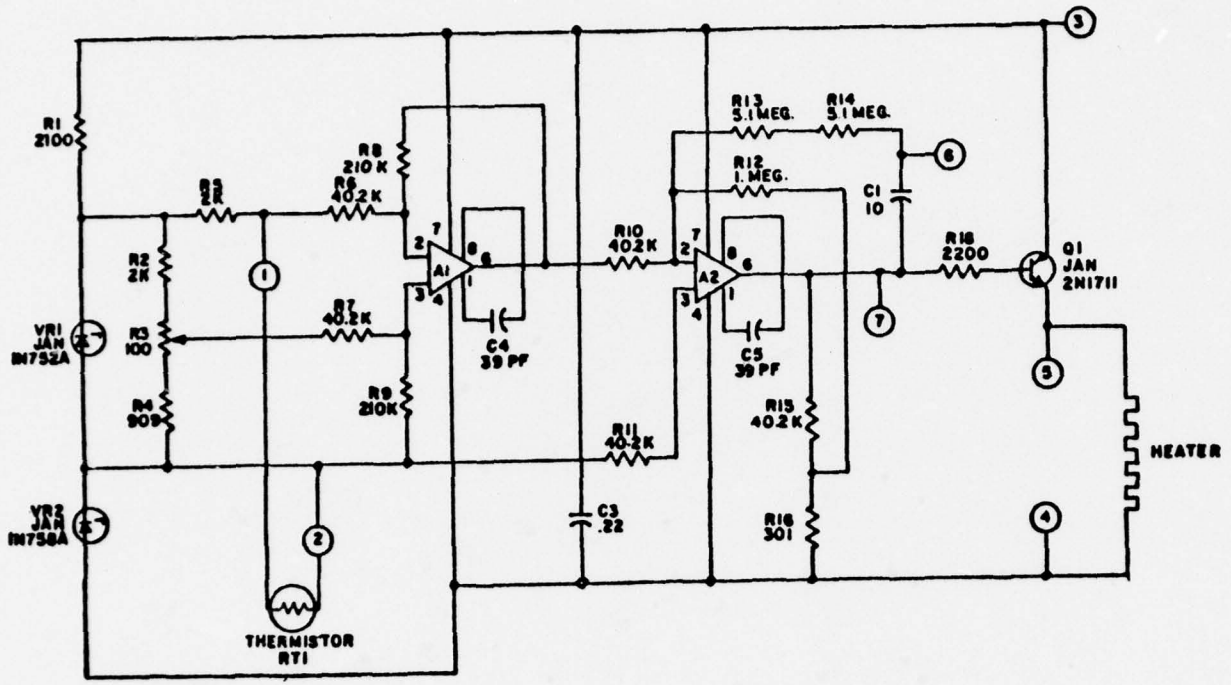


Figure 26 - TEMPERATURE CONTROLLER SCHEMATIC

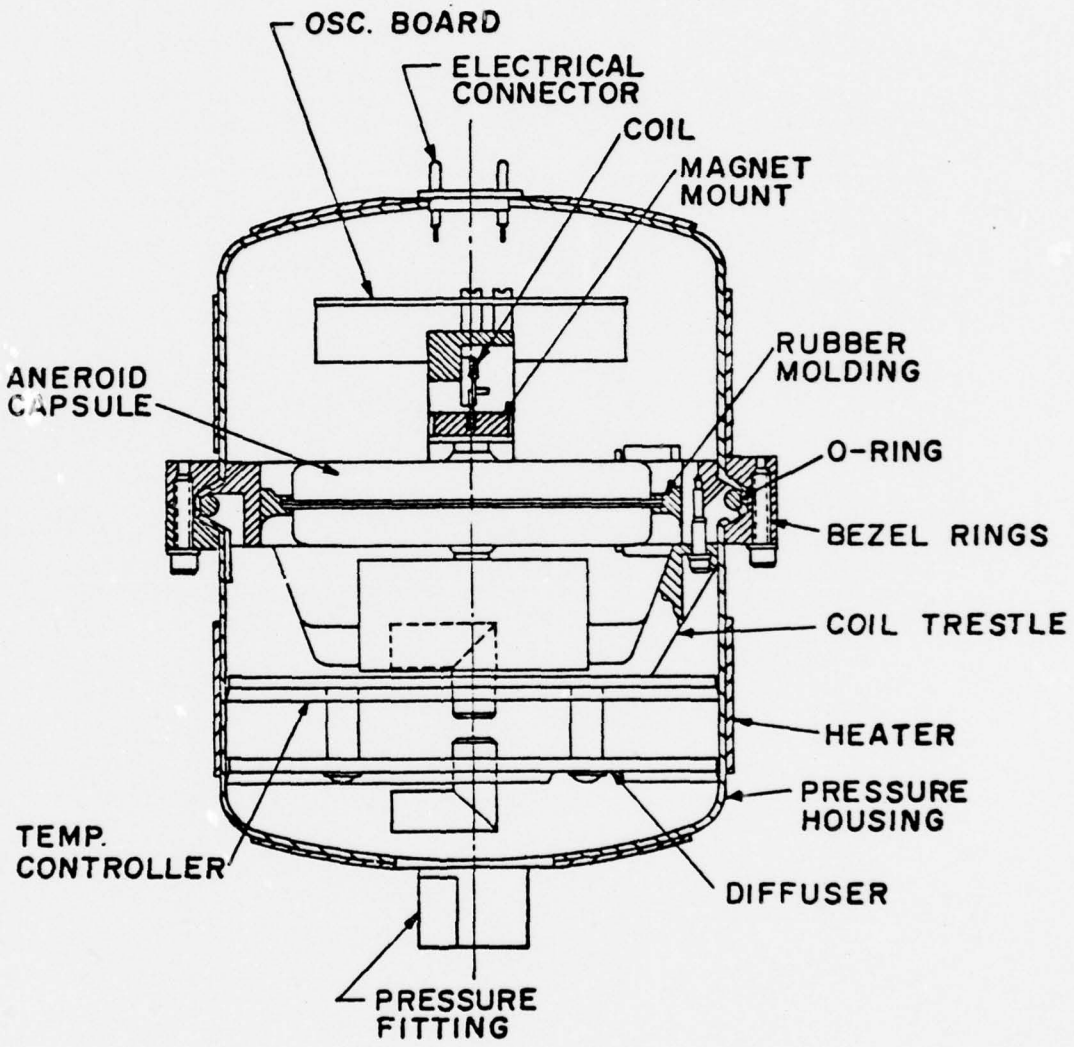


Figure 27 - TRANSDUCER MECHANICAL DESIGN DETAILS

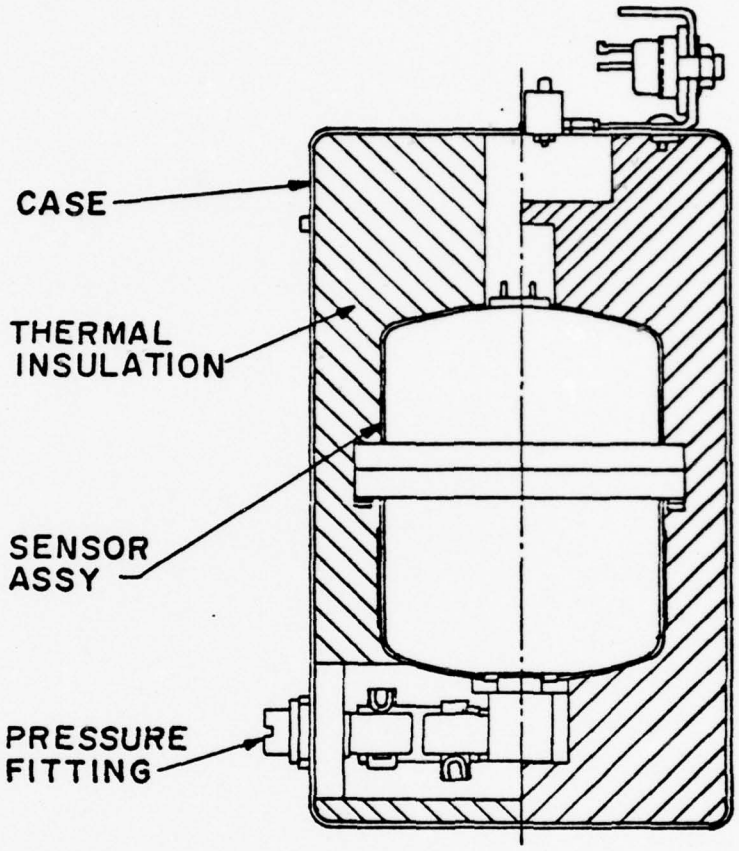


Figure 28 - INSTALLED TRANSDUCER

DISCUSSION

This sensor has a common property with several of the transducers discussed previously. It is nonlinear and curves of pressure vs period would have to be obtained from the manufacturer in order to ascertain the degree of nonlinearity. Since this transducer is a resonant device, it is sensitive to external vibration and shock. Thus the success of this transducer in a given application depends upon the ability to isolate the unit. Overall, the present device seems most suited for bench top measurement.

B. AIRSPEED

1. Omnidirectional Airspeed System

An omnidirectional low range airspeed system was developed by Pacer Systems, Inc. called LORAS. This system measures and displays relative airspeed or relative wind through 360 degrees azimuth. It can measure true or calibrated airspeed in any flight path direction; forward, rearward, right, left, or quartering. In addition, the system is capable of measuring absolute zero airspeed and responds quicker than any modern aircraft can accelerate or decelerate.

The system consists of the sensor unit, air data converter, omnidirectional airspeed indicator (OAI), and non-rotating standpipe mounting. The sensor (Fig. 29) weighs 2.25 pounds, stands 9 inches high, and has a rotating arm 12 inches in diameter. The mounting base is designed to fit into a 3 inch OD tube (.064 wall). The arms rotate at 12 Hz, driven by a constant speed motor in the lower portion of the sensor body. A typical standpipe installation is shown in Fig.30. The arms are constructed of stainless steel, and the sensor body is corrosive resistant aluminum. The LORAS model 1000-T is designed to operate at speeds up to 250 knots, but can withstand supersonic flight loads when turned off. The shrouds at each end of the sensor arm were designed to provide environmental protection against rain, snow, and freezing rain. Production models will have a heater for de-ice capability.

The air data converter weighs 2.9 pounds and

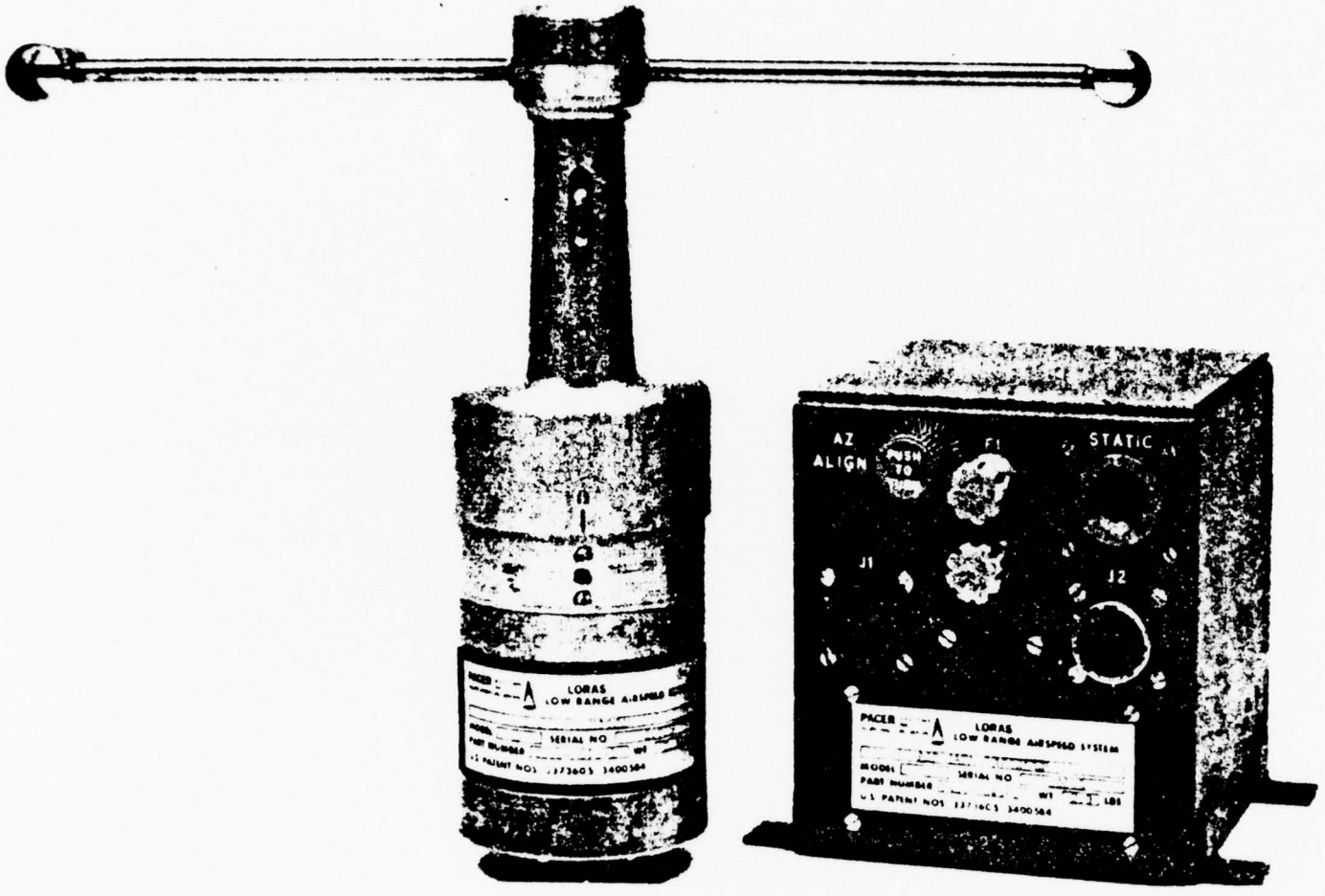


Figure 29 - LORAS SYSTEM PROTOTYPE

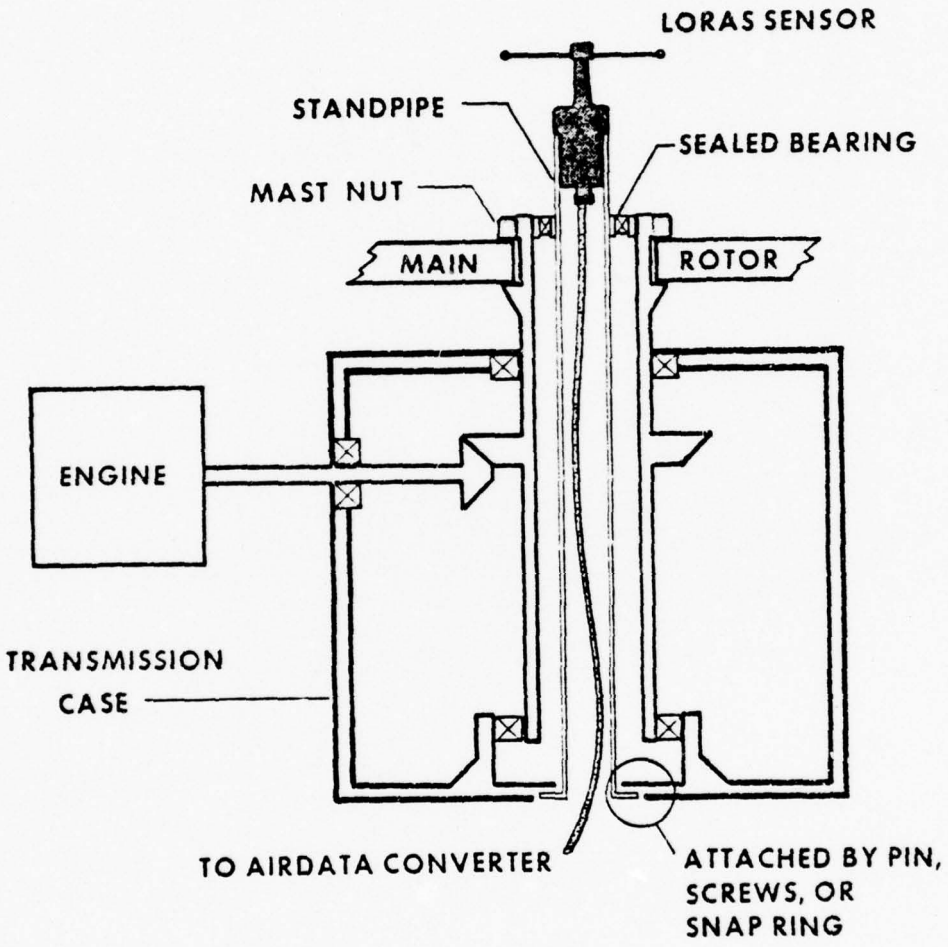


Figure 30 - TYPICAL STANDPIPE INSTALLATION

measures 5.25 inches high, 4.63 inches wide, and 6.12 inches deep. Power requirements are: DC, 28VDC +4V 20 Watts; AC, 115VAC +10%, 400Hz, Single Phase, 60VA.

The system has a dc analog output signal proportional to flight path airspeed as well as the forward (rearward) and sideward (left or right) components. An additional output is a dc signal proportional to density altitude. The equipment has been designed to output two sets of signals, one set to drive the necessary displays, and one set to service other aircraft subsystems (i.e. stability augmentation system, navigation system, etc.).

The Navy's main contingent of low speed aircraft are helicopters, and extensive testing was done with the system installed on these aircraft. Several sensor locations were tested with the optimum configuration shown in Fig. 31 (Ref. 15). This has proven to be a feasible location for all helicopters.

The LORAS sensor has been mounted in the rotor mast location on the OH-58, the Bell 212, AH-1G, UH-1H, and the UH-1N. The weight penalty for an operational mast installation should be less than 4 pounds and requires no unusual maintenance proceedures.

LORAS does more for the pilot than measure low airspeeds. The display shown in Fig. 32 allows the pilot to control the helicopter under even the most demanding flight conditions. Current systems do not give the pilot a ready or accurate indication of the margin of controllability remaining during dynamic omnidirectional flight maneuvers.

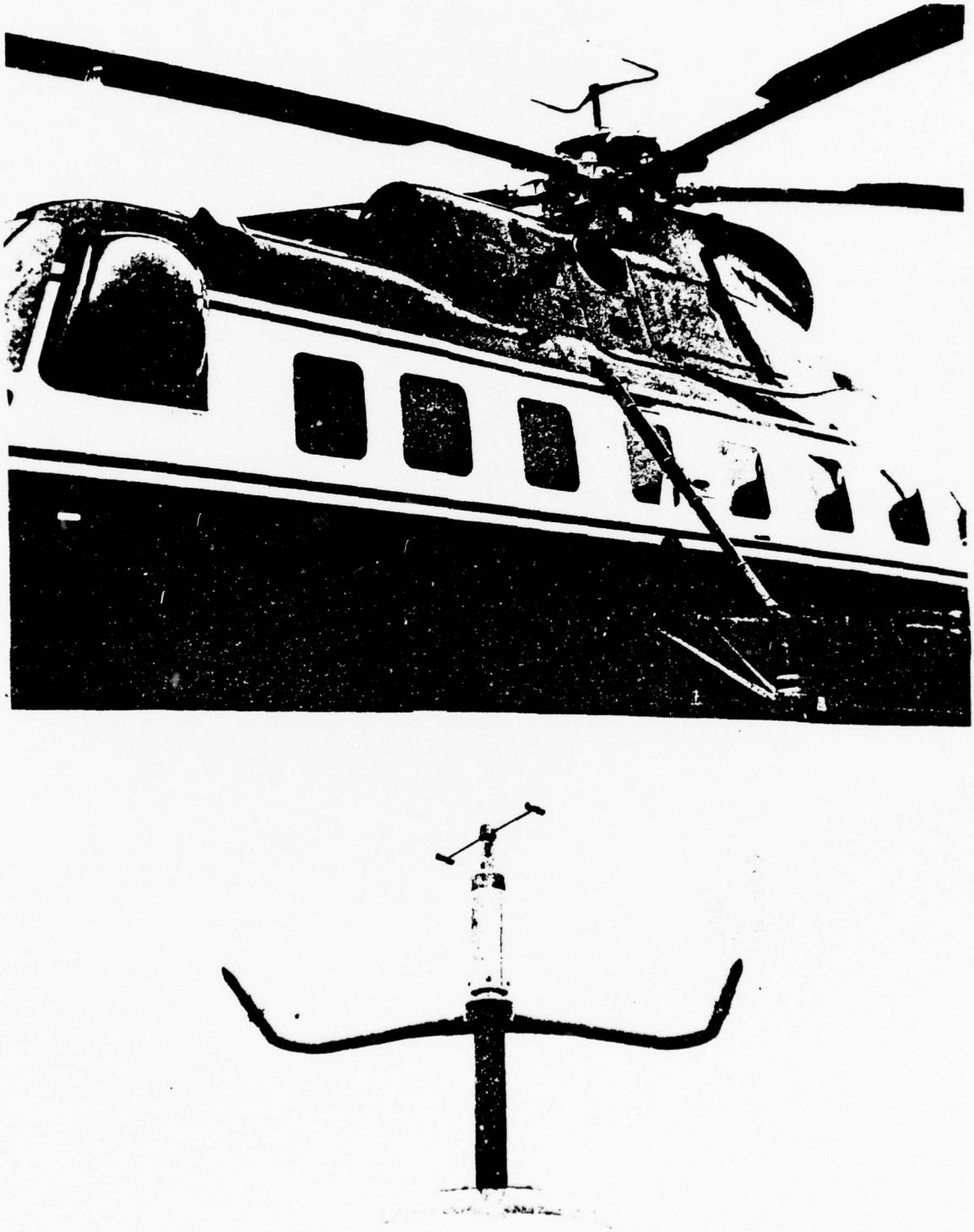


Figure 31 - ABOVE-THE-ROTOR INSTALLATION ON AN S-61 HELICOPTER

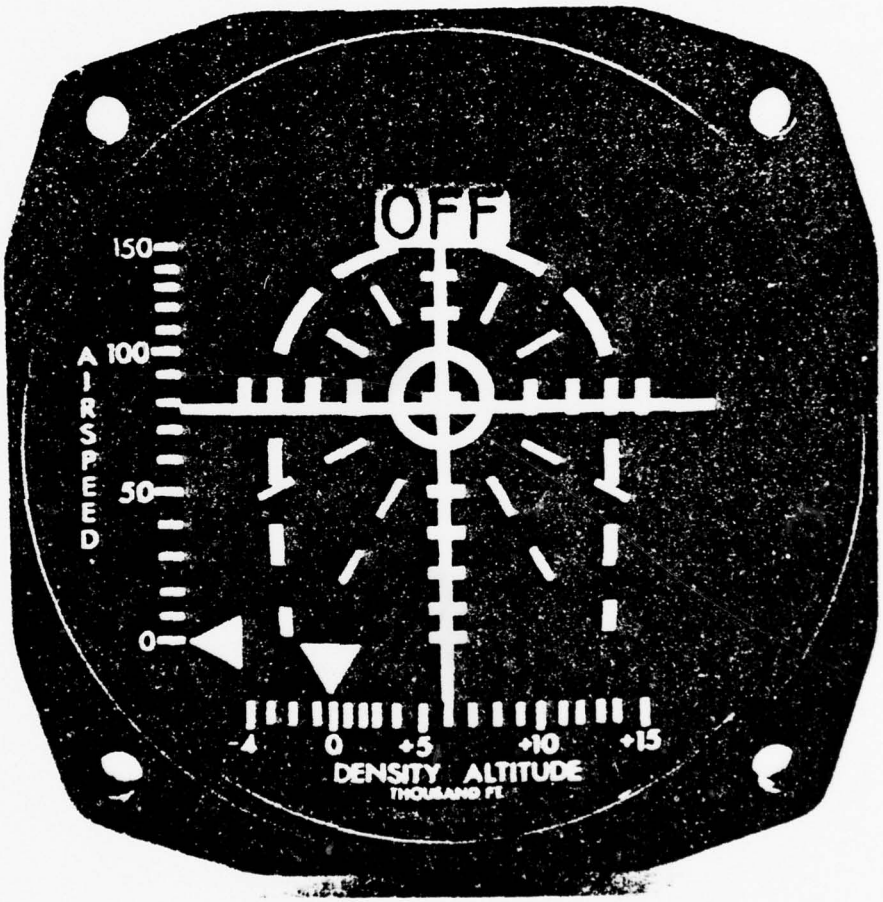


Figure 32 - OMNIDIRECTIONAL LOW RANGE AIRSPEED INDICATOR

The LORAS system is capable of giving the pilot this information in order to avoid inadvertent loss of control resulting in:

Collision with the ground or obstruction.

Pilot disorientation or vertigo.

Airframe or power train damage due to an overly aggressive recovery control technique.

A display similar to that shown in Figure 32 gives the pilot a quick and easy reference for the maneuver margin remaining.

The flight loads on the airframe, control system, rotor, and power train are all functions of flight path angle, flight path speed, normal acceleration, side force, gross weight, power demanded, and pilot control activity. Slow speed flight necessitates the use of high power and heavy pilot control activity. The highest flight loads in the slow speed regime are associated with cross wind and down wind conditions, where the pilot workload is greatly increased. Due to this heavy workload, the pilot is incapable of accurately assessing when the aircraft has departed the approved flight envelope and the severity of the departure. Thus the observed or estimated flight loads which are used to document the loads experienced by the airframe for calculating component life are inadequate. LORAS has the capability to define the safe flight envelope, depicted by the dashed horseshoe in Fig. 32. Implementation of this system will significantly improve component life estimates by more accurately depicting the actual loads experienced in flight. In addition, it would reduce the number of materiel failures in flight since maintenance personnel would know when a part is approaching the fatigue

limit.

The LORAS system received an extended operational flight test performed by the 1st Helicopter Squadron at Andrews Air Force Base. The objective was to evaluate the contribution of the system to safety and mission effectiveness. The LORAS-II system provided by Pacer Systems, Inc. was installed on a non-rotating standpipe above the rotor of a UH-1N helicopter, by squadron personnel during routine maintenance. The LORAS indicator was mounted directly below the pitot-static indicator for quick reference and comparison. The system logged 76 flights and 121 flight hours during the 6 month test (Ref. 14). Four flights (7 hours) were flown at night, and 2 flights were flown for system alignmet and checkout. Temperatures ranged from 40°F to 100°F and speeds of -25 to +130 knots. Sideward flight was limited to 35 knots . Most flights were conducted below 2000 feet pressure altitude , both in and out of ground effect. The aircraft received no special maintenance and was available for any squadron commitment. It was allowed to sit outside in the rain and high winds, and was washed regularly with no special precautions taken to protect the sensor. Pilots were required to perform maneuvers twice, once using LORAS and once using the pitot-static system. Parameters such as pitch attitude and airspeed variations were recorded as well as pilot opinions. It should be noted that LORAS output True airspeed which differed from the pitot-static Calibrated airspeed by only a few knots due to the low altitudes flown.

Nc failures were experienced by the LORAS system during the evaluation. The two systems exhibited general agreement for speeds above 60 knots (Fig. 33). This figure and Fig. 34 show the pitot-static system error in calm air and light turbulence. Figure 35 compares the two systems during a climbing acceleration to 50 knot level flight.

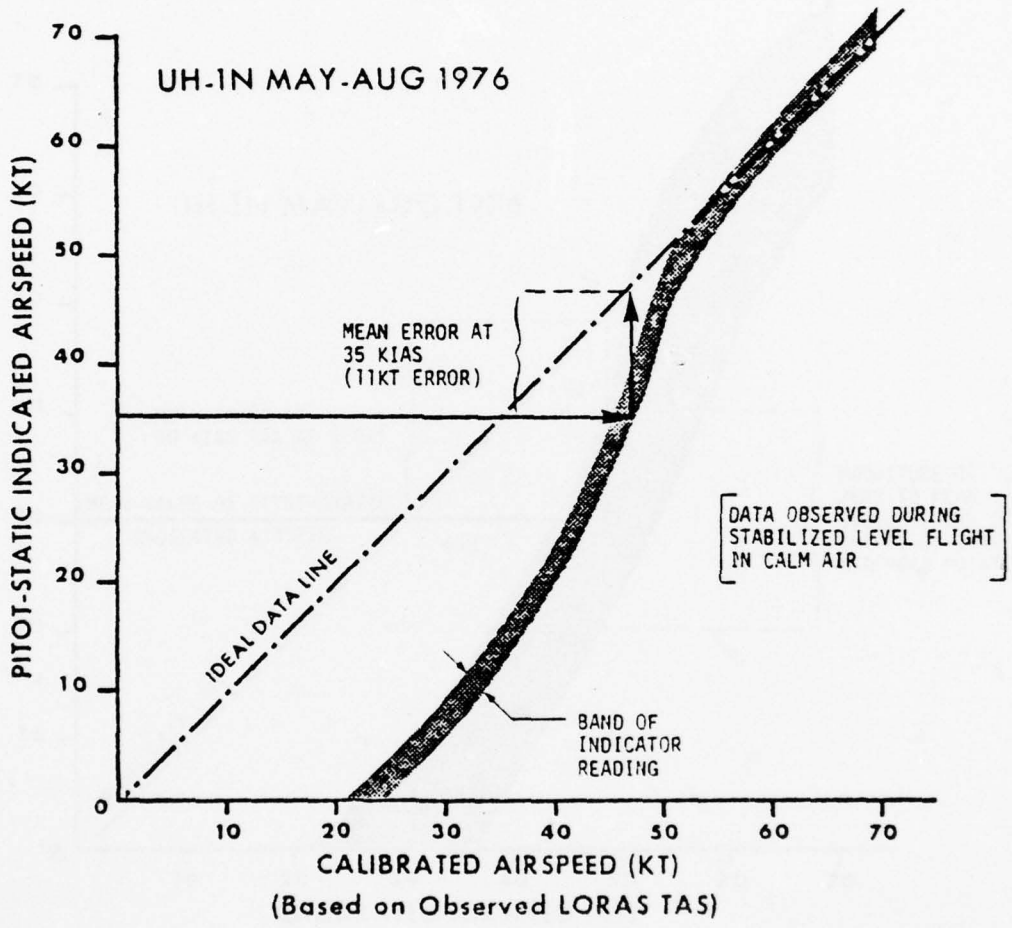


Figure 33 - VARIATION OF PITOT-STATIC AIRSPEED WITH CALIBRATED AIRSPEED

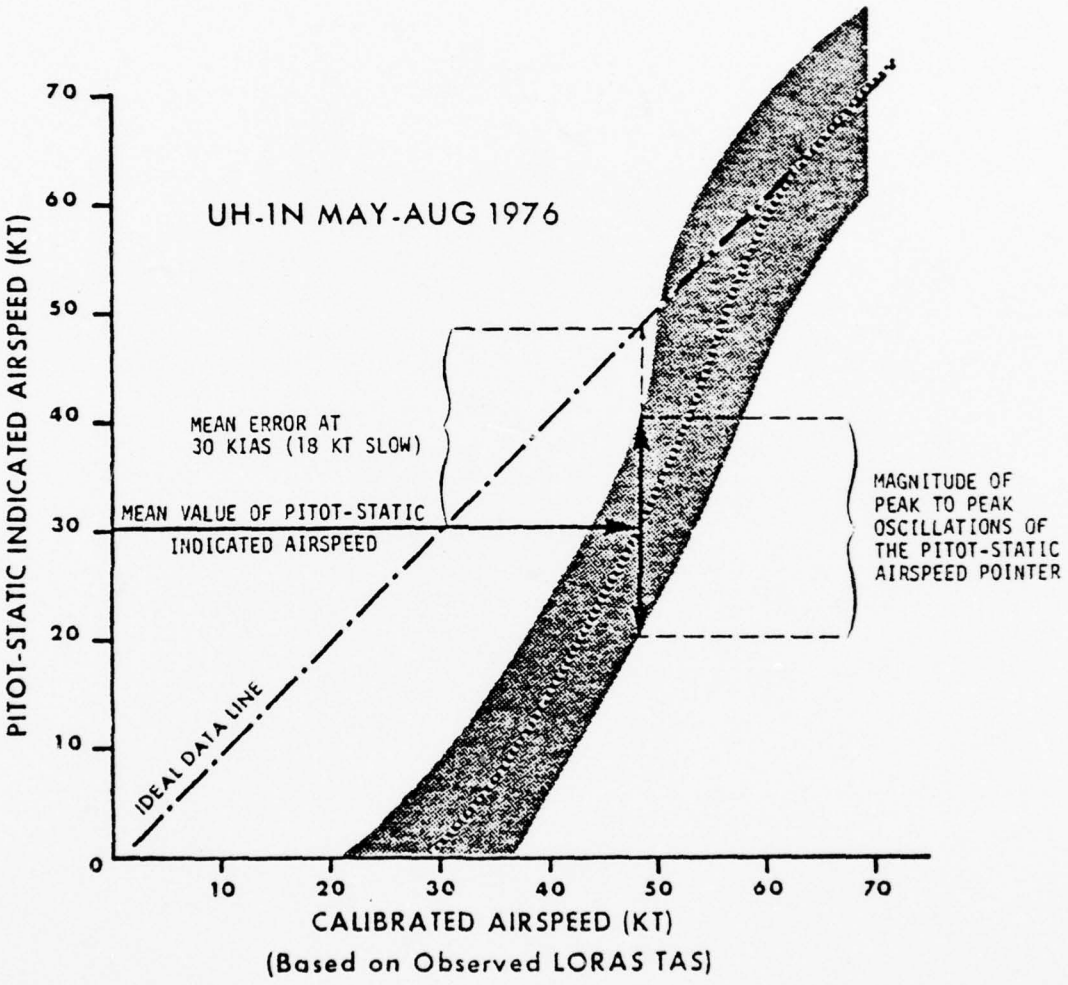


Figure 34 - VARIATION OF PITOT-STATIC AIRSPEED IN LIGHT TURBULENCE

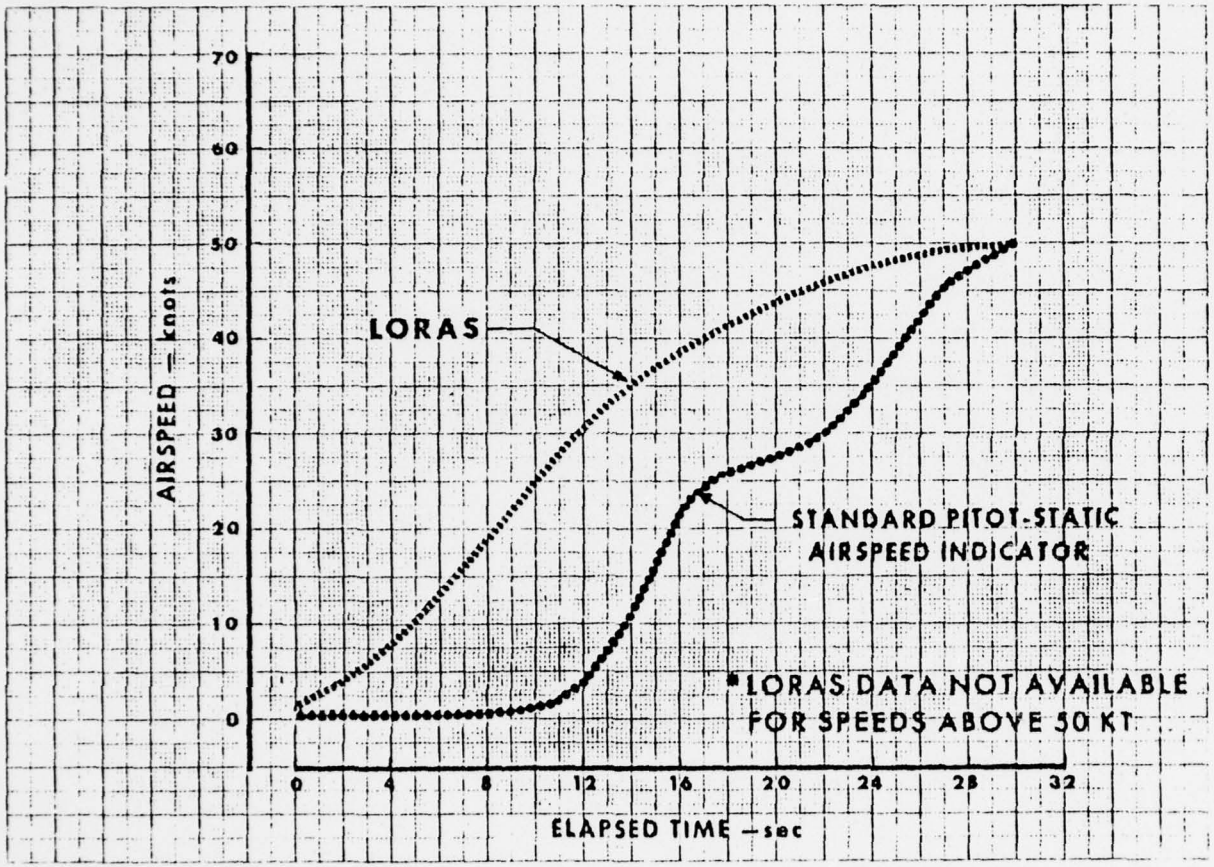


Figure 35 - COMPARISON OF THE SYSTEMS IN CLIMBING ACCELERATED FLIGHT

In climbing flight, LORAS seems to be very accurate, but seems to indicate low in descents. Evaluation of slow speed climbs and descents failed to find any condition where LORAS failed to provide what appeared to be an appropriate response to command airspeed changes.

The 1st Helicopter Squadron concluded that the pitot-static system currently in use is inadequate in the slow speed regime and that LORAS was an operationally suitable unit capable of significantly enhancing mission effectiveness and operational safety by providing accurate pilot cues in the slow airspeed regime, enhancing the pilot's ability to safely control the aircraft.

DISCUSSION

The need for an accurate and reliable omnidirectional low range airspeed system is well documented. LORAS has proven to be just such a system. The location of the sensor on the rotor mast above the rotor has been shown to be feasible requiring no unusual maintenance. This installation carries a very low weight penalty. The permissible flight envelope can be easily depicted on the LORAS display, or a power available vs power required may be presented. Thus, the LORAS system has the following advantages over conventional pitot-static systems:

(1) The capability to display the permissible flight envelope, power required vs power available, rotor engagement envelope.
(2) The capability to display omnidirectional airspeed from 0 to 250 knots.
(3) The capability to prevent or identify conditions which overload the airframe.
(4) Increased accuracy for component life cycle estimates.

(5) A decrease in the number of inflight materiel failures.

(6) No significant environmental effects.

(7) Decreased probability of vertigo-induced accidents due to imperceptible sideward or rearward velocities.

(8) Increased precision under IFR conditions.

Future helicopter designs should include provisions for mounting LORAS or a similar system on the rotor mast. V/STOL aircraft also require an omnidirectional airspeed system and the feasibility of using LORAS should be investigated.

2. Orthogonal Low Range Airspeed Sensor

Rosemount has developed an orthogonal low range airspeed sensor which will operate in the 0 to 50 knot range (Ref. 16). The system is comprised of a pneumatic airspeed sensor, pressure transducer, and dual pointer indicator. The airspeed sensor, which is a pressure type flow sensor employs a hemisphere-cylinder combination with a the pressure sensing ports located on the cylindrical portion of the unit. The sensor has four internal chambers with a symmetrical orthogonal hole into each chamber. A schematic drawing of the system is shown in Fig. 36. The sensing ports are located such that the pressure differences between chambers 1 and 2 are proportional to the product of the impact pressure times the $\cos^2\theta$, where θ is the angle between the velocity vector and the "x" direction. The output from 3 and 4 is proportional to the impact pressure times $\sin^2\theta$. Mathematical manipulation of these pressures results in the calibrated airspeed. With the known calibration constants and appropriate airspeed transducer a voltage output can be made proportional to the calibrated airspeed in orthogonal directions. An additional set of ports can be added to measure ambient or static pressure, which enables both orthogonal airspeeds and pressure altitude measurements to be obtained from a single sensor. The sensor incorporates a heater for in-flight de-icing and vaporization of surface and internal moisture. Calibration data is obtained in flight testing to convert local ds airspeed to true flight conditions.

The sensor was tested in the wind tunnel, in atmospheric wind, mounted on a ground vehicle, and in flight.

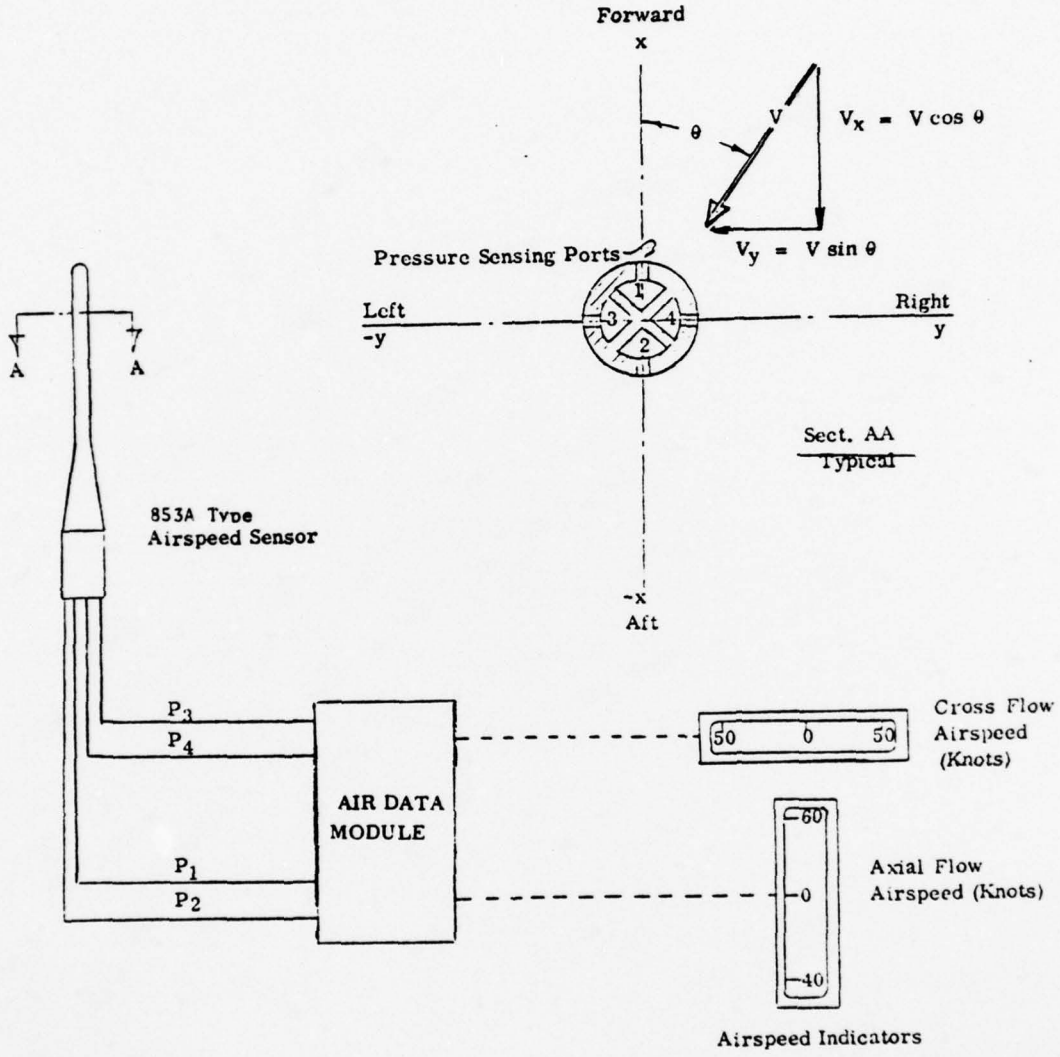


Figure 36 - ORTHOGONAL AIRSPEED SYSTEM

Flow direction in the wind tunnel covered a full 360°, and covered a speed range of 20.4 to 51.0 knots, while in the case of the ground vehicle test, speed ranged from 2.5 to 47.5 mph. In the latter test, varied from -20 to +20. The flight tests were conducted with a NUH-1M helicopter. Two locations for the sensor were investigated, above the rotor and above the cabin. The former proved superior. Comprehensive tests were conducted encompassing longitudinal and 1 lateral low speed flight, climbs, descents, sideslips to 30, and operations in ground effect (Ref. 17). With the above the rotor installation, all tests were within 5 knots.

The air data module suitable for orthogonal airspeed measurements consists of the following components:

1. Differential pressure transducer for fore-aft axis (ΔP_x)
2. Differential pressure transducer for side-to-side axis (ΔP_y)
3. Computation circuitry for airspeed in fore-aft axis
4. Computation circuitry for airspeed in side-to-side axis
5. Temperature compensation circuitry for correction of temperature induced errors.
6. Reference voltage source
7. 28 VDC to ±15 VDC converter, and EMI filter circuitry.

This module is in production.

DISCUSSION

This system, like the LORAS system, requires that the sensor be mounted above the rotor. The pressures at low airspeed are very low and although many manufacturers build transducers which are satisfactory in these ranges (.05 PSI at 40 knots), this is still a potential problem area. The scheme used is simple and straight forward. It may seem attractive to many proponents of the "old school" since it looks a lot like the conventional pitot-static probe. The system deserves more testing to evaluate its possible use on future Navy V/STOL aircraft.

3. Ultrasonic Wind Vector Sensor

The Ultrasonic Wind Vector Sensor (UWVS) developed by Honeywell, Inc. uses ultrasonic signal transmissions through the moving air mass, and has no moving parts. The sensor and the relationship between angle of attack, sideslip, and wind magnitude is shown in Fig. 37. The three unknowns (W_x, W_y, W_z) can be obtained from the three equations describing the measured transmission times from the three transmitters to the receivers. The UWVS geometry is shown in Fig. 38. The wave velocity in air as a function of temperature is computed from the temperature sensor on the probe.

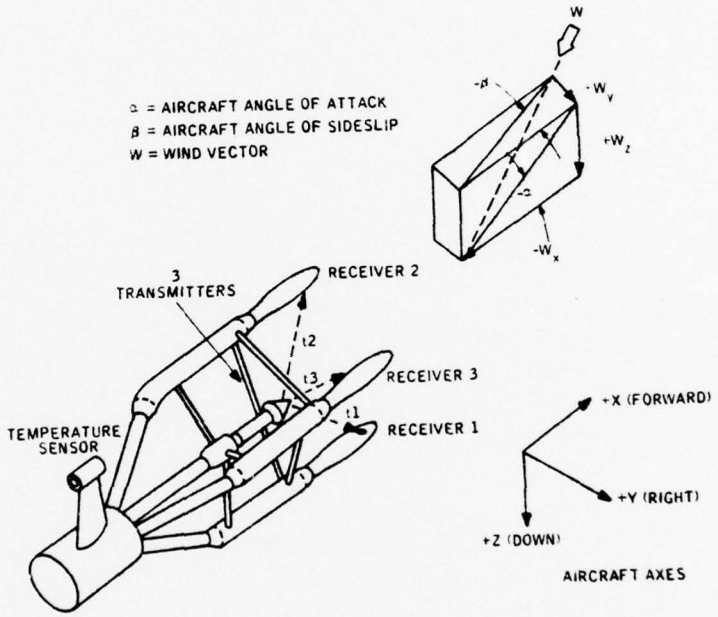


Figure 37 - WIND VECTOR DEFINITION

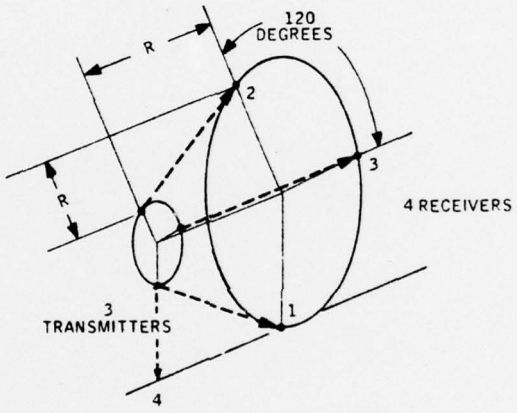


Figure 38 - UWVS GEOMETRY

Typically, the transmitters are simultaneously pulsed, and 200 to 300 microseconds later the wave reaches the receivers. An equation is written for each wave path containing the unknowns and the three transit times. The resulting equations are functions of W and therefore are solved by iterative feedback methods.

With zero relative wind, the three transit times are identical. When a relative wind exists and is parallel to the x-axis, all times are equal again. For a relative wind from an arbitrary direction, the three times assume different values.

The block diagram for the UWVS is shown in Fig. 39. The system uses piezoelectric transducers as transmitters, wide bandwidth ceramic microphones as receivers, and a platinum element as the temperature sensor. The temperature sensor amplifier and three receiver amplifiers are contained in the sensor unit, while the transmitter drive, timing logic, pulse detection circuitry, and the electronics used to solve the equations are contained in a separate unit. The present mechanization solves the equations by an analog multiply/divide technique. A digital processor approach, with approximately equal performance and cost, has been configured.

The factors affecting UWVS performance are:

Transmitter locations
Aerodynamic effects
Signal noise
Installation alignment
Environmental conditions
Electronic circuitry

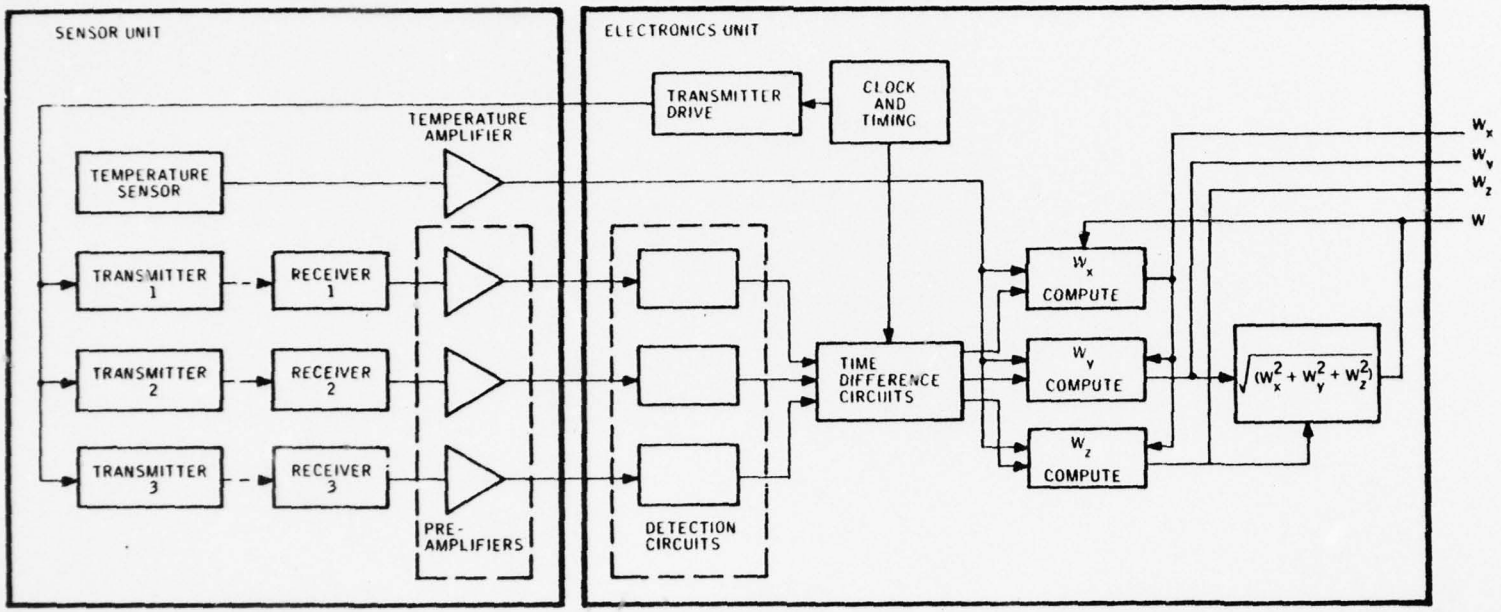


Figure 39 - UWVS BLOCK DIAGRAM

AD-A046 500 NAVAL POSTGRADUATE SCHOOL MONTEREY CALIF F/G 1/3
A STATE-OF-THE-ART ASSESSMENT OF AIR DATA SENSORS FOR NAVAL AIR--ETC(U)
SEP 77 R D NEIL

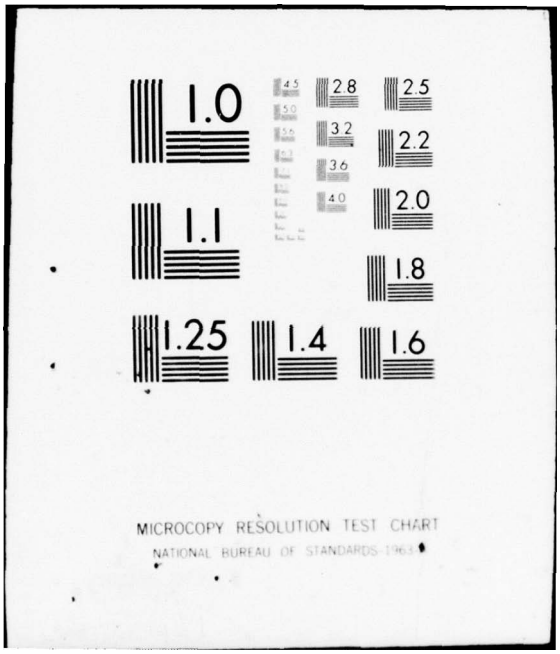
UNCLASSIFIED NL

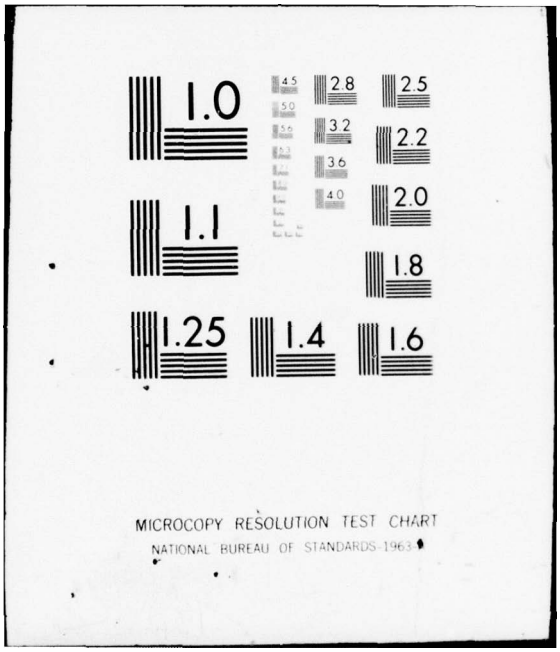
2 OF 2 AD A046500

2 OF 2 AD A046500



END
DATE FILMED
12-77
DDC


1.0
1.1
1.25
1.4
1.6
1.8
2.0
2.2
2.5
2.8
3.2
3.6
4.0
4.5
5.0
5.6
MICROCOPY RESOLUTION TEST CHART
NATIONAL BUREAU OF STANDARDS-1963-A


1.0
1.1
1.25
1.4
1.6
1.8
2.0
2.2
2.5
2.8
3.2
3.6
4.0
4.5
5.0
5.6
6.3
MICROCOPY RESOLUTION TEST CHART
NATIONAL BUREAU OF STANDARDS-1963-A

Of these, aerodynamic effects seem to be the most critical. These effects are similar to those of any other probe mounted on an airframe. Flow around the airframe changes the sensor measurements, and thus the location of the probe must be chosen with care.

The UWVS system has been tested in the wind tunnel and on board Army Cobra helicopters as part of a rocket firing control system from June to September, 1975 at Aberdeen Proving Ground, Fort Hood and at the Naval Weapons Center, China Lake. Additional testing was conducted at Edwards Air Force Base in which different mounting locations were evaluated. The optimum position was found to be above the rotor head. Data showed that with this position, the forward component was linear to within 3 knots out to 130 knots, and the lateral component generally linear to within 3 knots out to 25 knots. The structure allowed measurement of rearward and upward aircraft velocities, but performance at rearward velocities above 20 knots was not as good. The flight test results showed some scattered data points which may be due to electronic processing in the presence of missed timing pulses. Future work is aimed at improving pulse processing.

DISCUSSION

This system was designed for use in rocket firing and thus is not really suited for airspeed measurement. Its performance in the latter regime is not impressive especially in rearward flight and therefore should be considered only as an aid in weapons delivery. The LORAS system is simpler, and this system is affected by turbulence which will certainly be evident on V/STOL aircraft. Finally, the system is fairly complex and requires improvements in the electronic circuitry. The author has no

information concerning the performance in adverse weather conditions such as fog, rain, ice, etc. and hence this is an area which must be explored.

4. Optical Convolution Velocimeter

This system, which was developed by D. Kim and G. Dubro, was presented at the Project Squid Second International Workshop in 1974, and has been jointly developed by the Air Force Flight Dynamics Laboratory and Bolt, Beranek, and Newman, Inc. (Ref. 18). The system employs no moving parts and uses an infrared-emitting diode (LED) as the light source. The output is collimated by a lens and projected through turbulence onto a grating. The turbulence is generated by the wake of an object placed upstream of the sensor. A mirror positioned behind the grating returns the light to a silicon photodiode detector. The turbulence refracts the light passing through it and forms a "shadowgraph" pattern of bright and dark bands on the grating. Figure 40 shows the basic set up of the OCV.

The signal from the photodetector is the frequency at which the shadowgraph crosses the grating. A heater was placed in the stream to increase the sensitivity for use in the low speed regime. Figure 41 shows the actual layout of a single detector OCV. "Time-of-flight" velocity measurement techniques are used with the assumption that the observed property is being convected with the flow stream at the flow velocity. Knowing the frequency at which the output of the photodiode fluctuates and the pitch of the grating, the average flow velocity can be deduced.

The first prototype was tested on board a Cessna 172 aircraft over a range of 50 to 120 mph. The major difficulty observed was a poor signal to noise ratio. A test program from 5 January 1976 to 31 August 1976 was undertaken to identify possible solutions to this problem, with the additional goals of improving the original design,

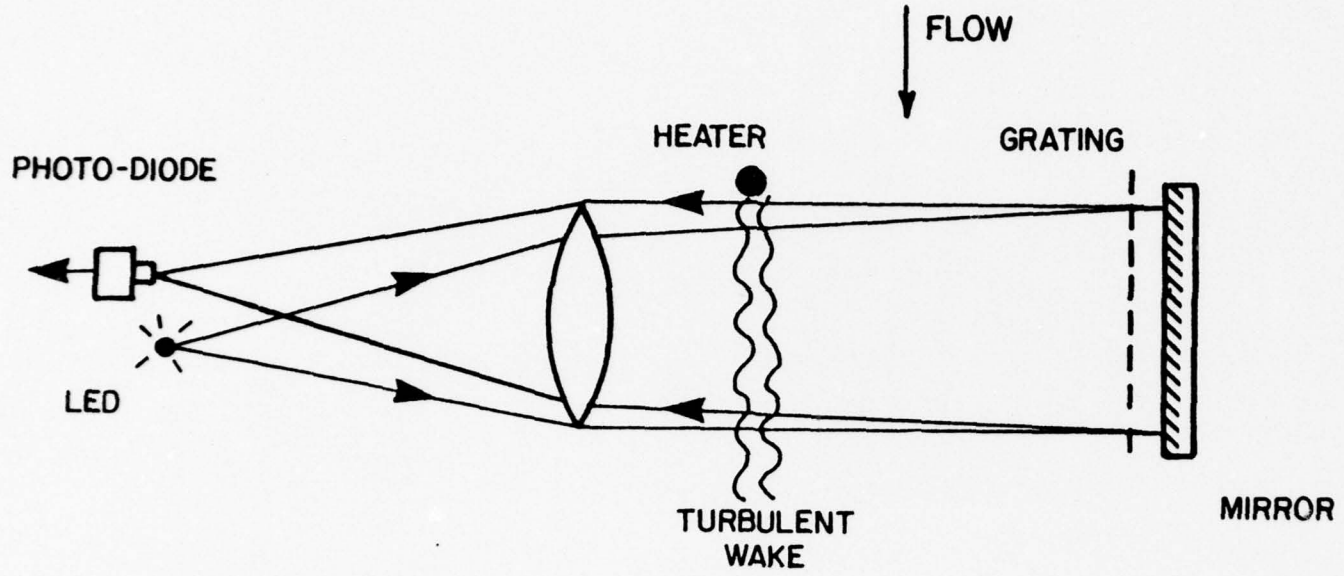
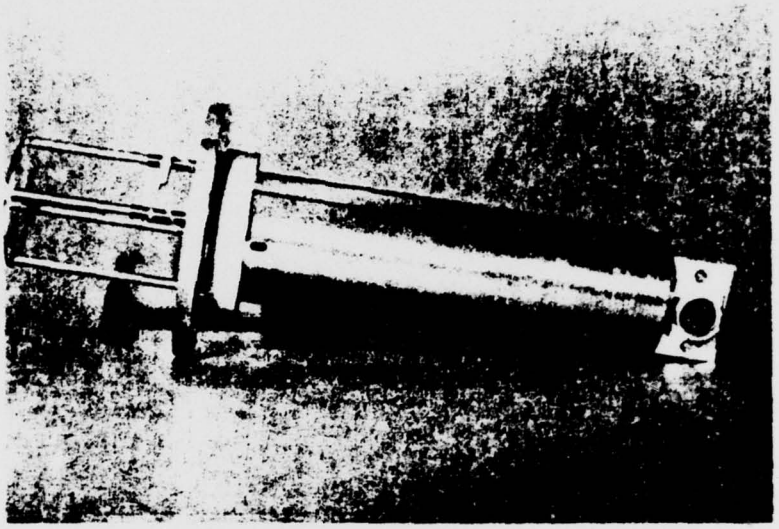


Figure 40 - PRINCIPLE OF THE OCV



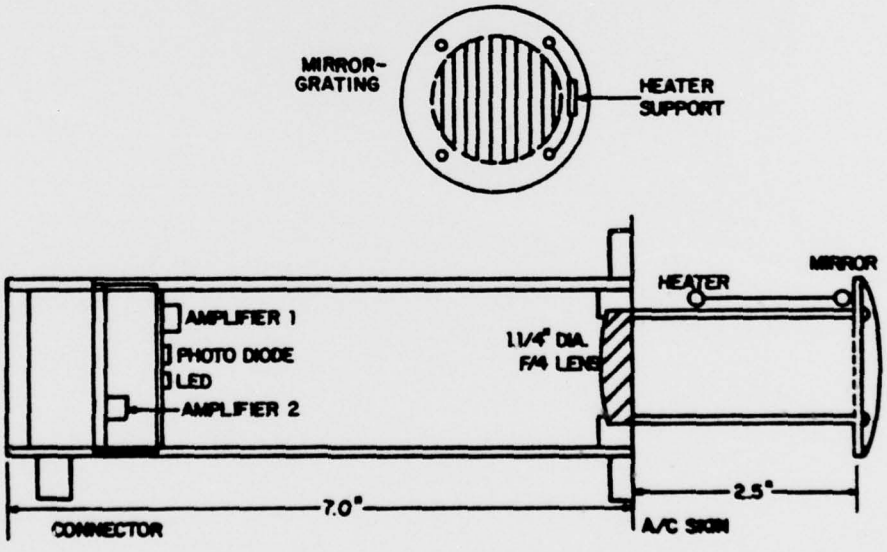


Figure 41 - SINGLE DETECTOR OCV

ascertaining the operational suitability of the system, and test and evaluation of the OCV II. Changes considered included increasing the number of LED's, alternate light sources, and improving optical efficiency.

An improved version of the OCV has been built and successfuly operated in the wind tunnel. Substantial improvements in the signal to noise ratio have been made, and a correlatien discriminator signal processing system capable of measuring the frequency of a signal buried in noise has been invented.

a major area which remains to be tested is the environmental effects on system performance. Consideration must be given to the following:

Low pressure
Vibratien
Acoustical noise
Rain
Salt fog
Dust
Humidity
High/lcw temperature
Electromagnetic interference (EMI)
De-icing and anti-icing

Low pressure has been shown to increase the sensitivity (Ref. 19), and the only potential problem occurs when the sensor returns to ground level. If moist air is allowed to enter the optics chamber, condensation may be produced, which would degrade the optical performance of the system. The problem can be overcome with a pressure-proof sensor head.

The OCV is somewhat sensitive to vibration of the mirror/grating which causes the return image to move about on the photodiode, which generates an output signal. Consequently, the mirror must be mounted sturdily in order to reduce this signal. The impact of vibration is reduced since vibrations tend to occur at lower frequencies than those used by the OCV. Acoustical noise presents a similar problem with higher frequencies. Again, a sturdy mount should solve the problem.

Rain can have both an adverse and favorable effect on OCV performance. The signal will be enhanced by raindrops passing through the t measurement volume, assuming the raindrops travel with the free stream velocity. However, signal degradation will result if raindrops build up on the mirror or lens of the OCV. This is avoided by flush mounting the lens and mirror in their supports. Even if the droplets form and move across the lens, they move at substantially lower velocities and the signal processor tends to filter out low frequencies and lock onto the high frequencies caused by the raindrops in the flow. Thus the manufacturer does not expect the system to "see" raindrops on the optical surface.

Salt fog presents a corrosion problem which can be overcome in the sensor body, but the mirror, which is coated with aluminum, and then coated with a layer of silicon monoxide, is susceptible to corrosion.

Dust presents another problem in the area of signal degradation, especially if it settles on the optical surfaces. As much as a 9 DB reduction in signal will occur for 50% coverage. As with the raindrops, dust moving with the free stream will enhance the signal.

High temperature limits are determined by the

electronic components, which with the present system is approximately 71 degrees Centigrade. Low temperatures can present problems with differential expansion, and brittle components. The present minimum temperature the system can withstand is -55 degrees C. This stems from photodiode limitations.

Electromagnetic Interference can produce spurious signals due to the sensitivity of the photodiode. Thus it is imperative that it be well shielded from all electronagnetic fields.

Icing is not as serious a problem as with pitot-static tubes since there aren't any small holes to clog with ice. Ice accumulation on the sensor of 1/4 inch will change the flow field which will result in erroneous readings. Hence there is still an icing/de-icing requirement.

The location of the sensor on the aircraft is of prime importance and a position with minimum airflow disturbance is desireable. Possible candidate locations are the nose or top of the vertical stabilizer.

DISCUSSION

The OCV is an interesting concept and one that has potential for some operational applications. At present, the system is not a viable approach due to the following factors:

(1) It has not been fully flight tested.

(2) Environmental effects have not been tested.

(3) Maximum temperature limits are too low and limit its use to low subsonic type aircraft.

(4) Problems remain with the heater design.

Final evaluation of the system must be reserved until the items noted above are corrected or thoroughly tested.

5. Laser Doppler Velocimeter

Grumman is in the initial stages of a research and development program which they hope will produce a Laser Doppler Velocimeter (LDV) which can be used aboard an airborne platform. Previous applications of this technology have been in the laboratory environment. The proposed program is divided into four stages, (1) proof of concept, (2) in-flight thrust measurement, (3) airspeed LDV tests, and (4) V/STOL flow field measurement.

Phase I is to be completed at the end of this year, and with a V/STOL prototype go-ahead at the end of 1979, the first flight would take place in 1984.

Phase II requires a Navy go-ahead in late 1977. This would be followed by the formulation of design criteria for the in-flight thrust measurement problem, flight hardware development, and flight tests in late 1979.

Phase III, airspeed measurement involves the same program of design criteria, hardware development, and flight

tests. Capabilities acquired in the previous stages is expected to reduce the design and development times and produce flight tests in the middle of 1980.

Phase IV, V/STOL flow field measurement, begins in 1980 and culminates in 1982 with flight tests.

This is an attempt to use Laser Doppler technology for the in-flight aerodynamic/propulsion interface and performance evaluation problem. The ability to measure velocities in complex flow fields without disturbing them makes the LDV particularly suited for non-contact fluid mechanic measurements. Possible applications include the fcllowing areas:

(1) Determination of thrust via the integral momentum equation, control volume technique.

(2) Quantification of thrust induced effects and additive drag components via the differential Navier Stokes equation, finite difference technique.

(3) The establishment of flow coefficients to relate design and wind tunnel data to flight test data.

(4) Identification of velocity profiles associated with
   a) Suckdown
   b) Fountains
   c) Hot gas reingestion
   d) Impingement.

(5) Establishment of a low speed measurement capability free of pcsition error.

(6) Angle of attack and sideslip measurement free of upwash

calibration.

The Laser Doppler Velocimeter offers substantial benefits over present systems. Design calculations may be verified through accurate 3-D vectored data. Correlation of wind tunnel and flight test data will reduce the scope of many programs, resulting in significantly lower costs. Accurate velocity profiles of the flow fields associated with V/STOL aircraft will be an invaluable aid to the designer.

The basic measurement scheme is shown in Fig. 42. The proof-of -concept setup which is currently being tested at Grummans' Calverton, Long Island test facility, is shown in Fig. 43. Once this system is fully tested, it will be used to verify installed thrust using an F-14 aircraft.

The ultimate goal is to produce a system to be used aboard a V/STOL aircraft. Ideally, the test engineer would be able to measure airspeed, angle of attack, sideslip, suckdown, recirculation, engine thrust, etc. without relocating the laser. Thus, Grumman plans to have one centrally located instrumentation package with remote sensing stations linked by fiber optics.

DISCUSSION

Since this program is still in the infancy stage, it is not possible to predict its success or failure with any certainty. The possibilities offered by such a system are sufficient to warrant a comprehensive RDT and E effort. Recent advances in fiber optics (to be discussed in a subsequent section of this paper) and the renewed interest shown by the Navy in laser technology, may make this

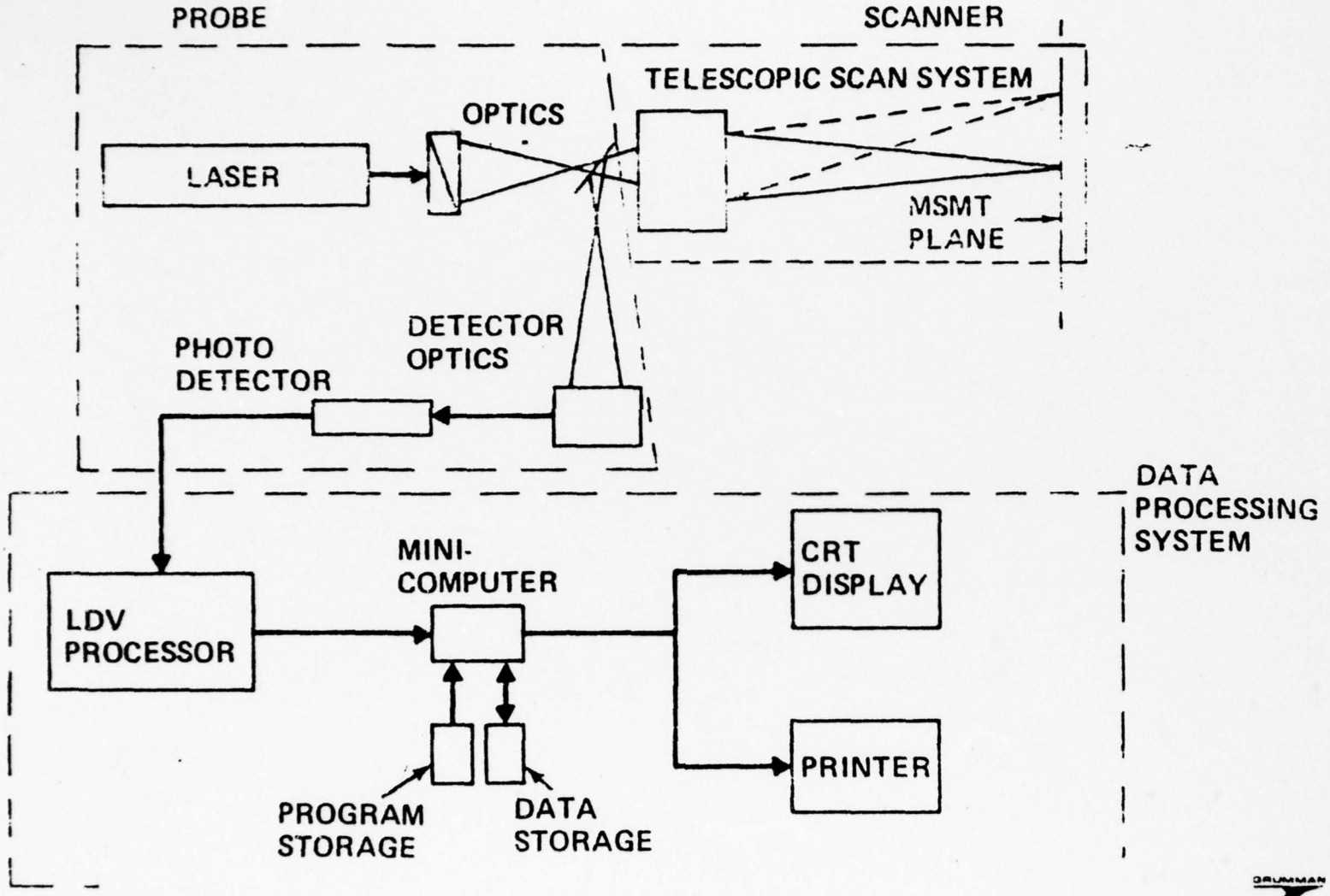


Figure 42 - LASER DOPPLER VELOCIMETER SCHEMATIC

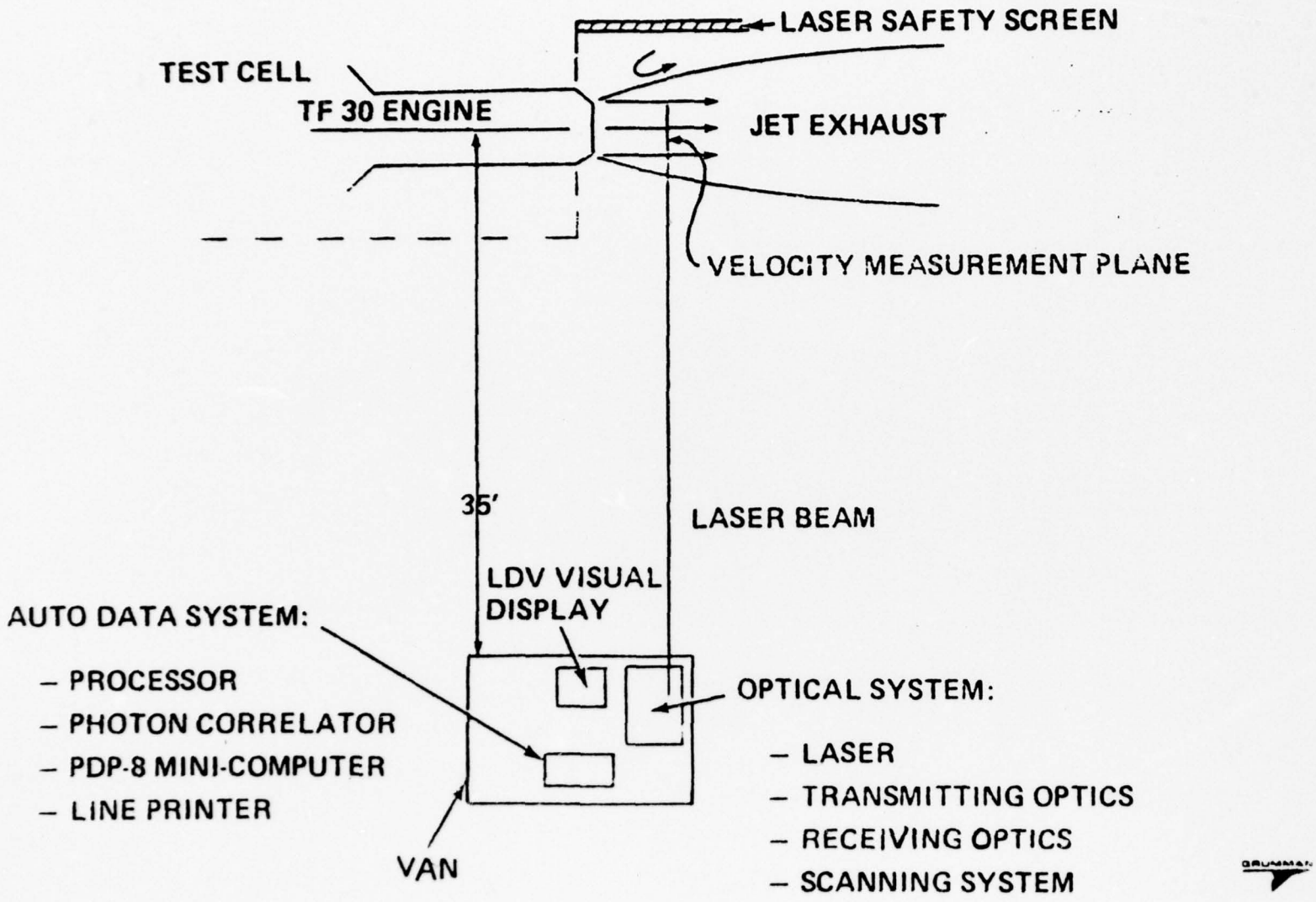


Figure 43 - PROOF-OF-CONCEPT SETUP

a practical system in the near future.

6. Airspeed By Vortex Detection

J-TEC Associates, Inc. has developed a system for measuring airspeed by vortices shed from a bluff body (Ref. 20). A characteristic vortex pattern is formed which is determined solely by the shape and size of the body and is independent of other fluid characteristics such as density or temperature. The vortices move at essentially the free stream velocity. Since vortices are no longer formed below a critical velocity, the system has the advantage of a zero point which is determined by the true velocity zero. In addition, the slope of the vortex frequency versus velocity is determined only by the characteristics of the vortex rod. These features free the system from the problem of zero drift which is present in pressure systems.

A typical vortex pattern is shown in Fig. 44. Votices are counted by passing an ultrasonic beam through the vortex trail. The rotational velocity of the fluid in the vortices tends to scatter the beam which reduces the energy impinging on the receiving transducer. The result is an amplitude modulation on the received ultrasonic carrier, from which velocity is determined. An example of ultrasonic modulation is shown in Fig. 45. The increase in modulation depth is approximately proportional to the fluid velocity.

Ultrasonic beam and transducer size are chosen such that 100% modulation is achieved at the upper velocity limit. A velocity range of 100 to 1 can be attained. The modulation frequency of the energy received at the transducer is passed through a zero crossing detector with hysteresis which produces a square wave at the vortex frequency, which is the primary output of the sensor.

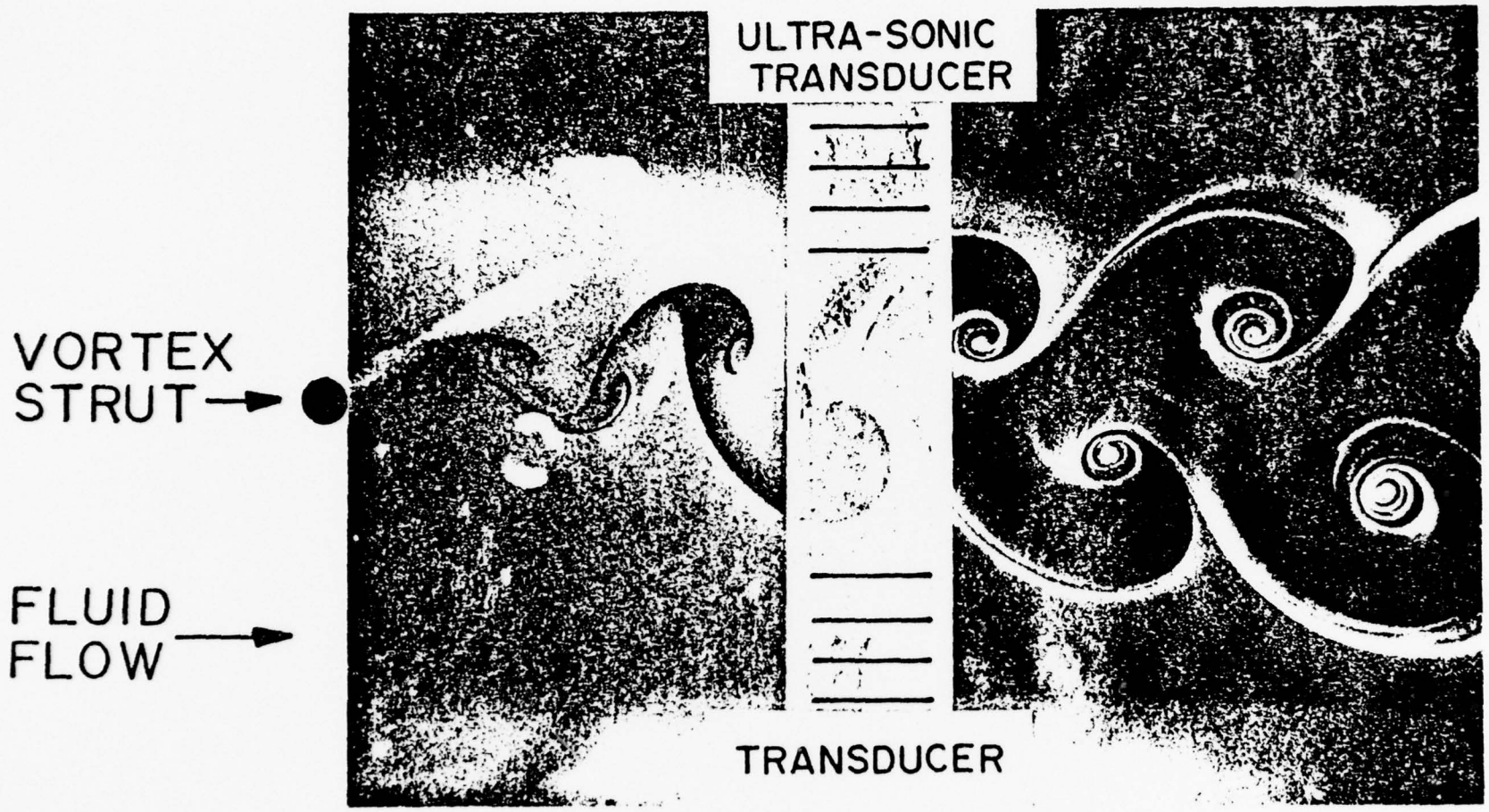


Figure 44 - BLUFF BODY VORTEX PATTERN

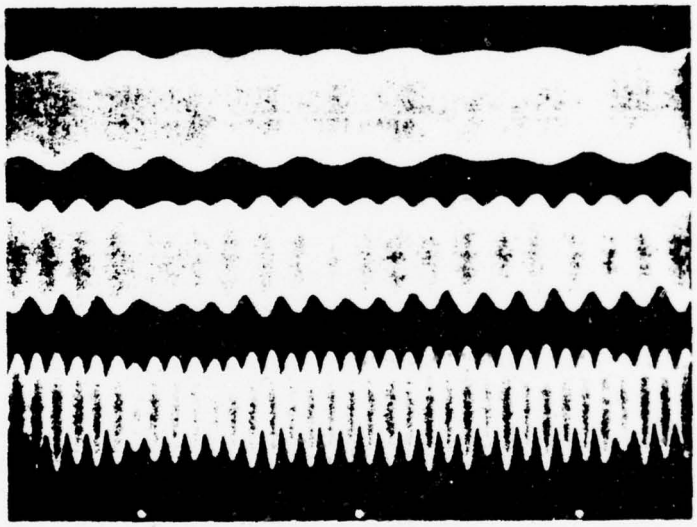


Figure 45 - ULTRASONIC BEAM MODULATION

The relationship between the vortex frequency and the velocity is:

$$f=SV/D$$

where S= the Strouhal constant
V= velocity
D= the cross section diameter of the vortex rod.

Typical vortex rod diameters are on the order of 0.1 inches which results in a frequency to velocity ratio of 50 Hz per knot. The threshold of these sensors is extremely low, approximately 1.5 knots, which suggested the application to rotary wing aircraft. The model VA-220 will operate up to 250 knots and has a linear calibration curve. The sensor has been tested to .85 mach and several units are in operation on subsonic aircraft. Various models and installation locations have been tested on H-500, CH-3, OH-58, and UH-1 helicopters.

In one of the tests, a bidirectional sensor having vortex struts located both fore and aft of the sonic beam was tested. The sensor could read either forward or rearward velocity, but could not distinguish between them. Typical results of tests conducted by the Army Flight Test Center at Edwards Air Force Base are shown in Fig. 46.

FIGURE 6
AIRSPEED CALIBRATION IN FORWARD AND REARWARD FLIGHT
J-TEC SENSOR VA 210 S/N L-72-18 NUH-1C USA S/N 63-8684

ROTOR MAST LOCATION-POST VERTICAL

SYMBOL	GROSS WEIGHT ∿LB	CENTER OF GRAVITY LONG FS	LATERAL BL	ROTOR SPEED ∿RPM	DENSITY ALTITUDE ∿FT	AMBIENT TEMP ∿°C	SKID HEIGHT ∿FT	FLIGHT CONDITION
□	6790	132.1	-.6	326.	2670	11.4	50	OGE LEVEL FLIGHT
○	6560	132.0	-.7	325.	2960	13.0	50	OGE LEVEL FLIGHT
△	6310	131.8	-.7	324.	3020	14.1	5	IGE LEVEL FLIGHT
◇	7000	131.8	-.7	324.	4970	6.9	>50	OGE LEVEL FLIGHT

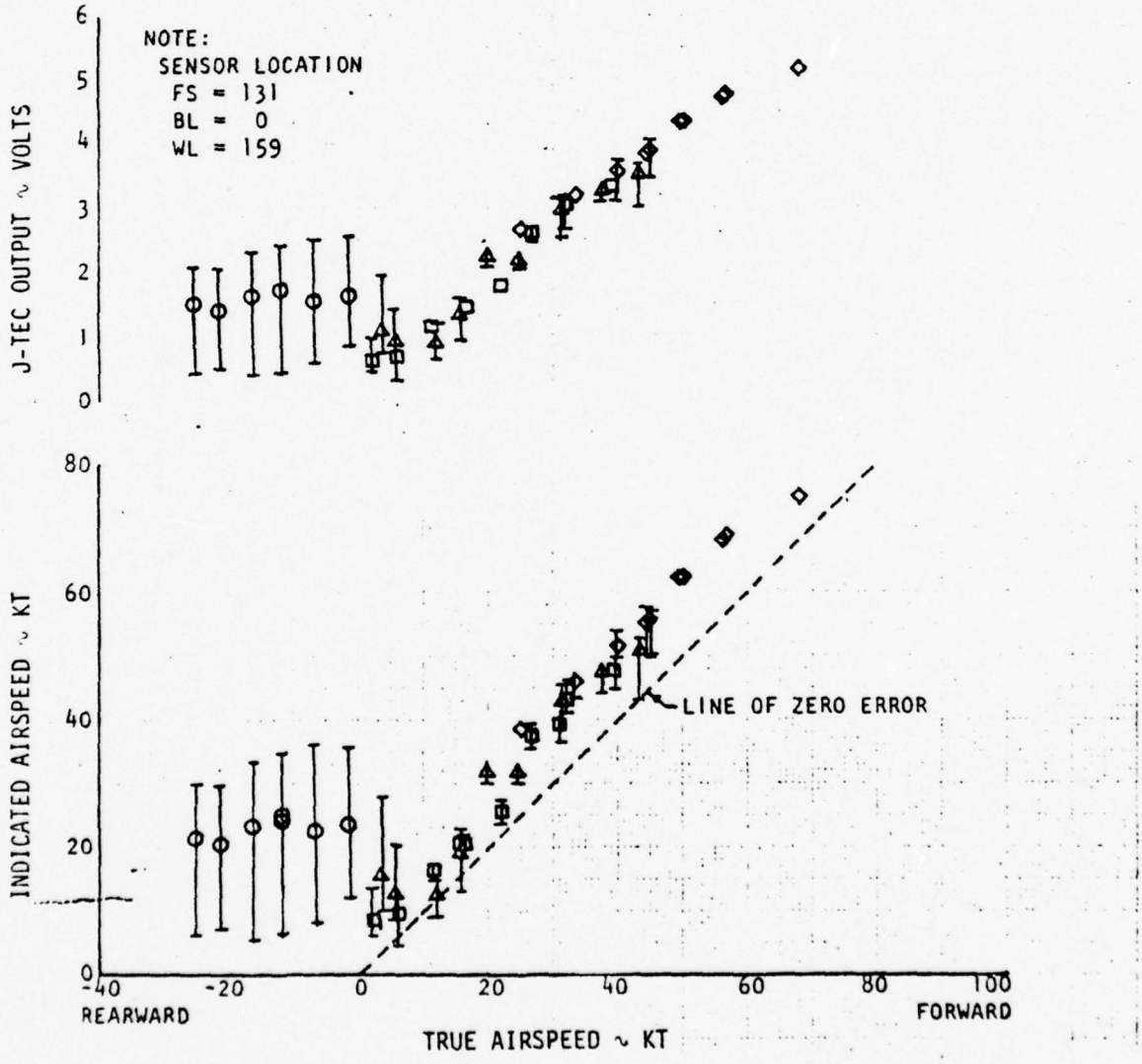


Figure 46 - ARMY FLIGHT TEST CENTER RESULTS

DISCUSSION

Although a capability has been shown, the system remains unattractive for the following reasons:

(1) It is a relatively complex means of measuring airspeed.

(2) Other systems offer savings in weight and complexity.

(3) The sensor should be mounted above the rotor to obtain the best results and preclude its use as a hand hold or step for maintenance personnel.

(4) Environmental effects have not been tested.

V. FIBER OPTICS

A. FIBER OPTICS FUNDAMENTALS

Fiber Optics deals with the transmission or guidance of light (rays or waveguide modes in the optical region of the spectrum) along transparent fibers of glass, plastic, or a similar medium. The phenomenon responsible for the fiber or light pipe performance is the law of internal reflection.

A ray of light, incident on the interface between two transparent optical materials having different indices of refraction, will be totally internally reflected (rather than refracted) if: (1) the ray is incident upon the interface from the direction of the more dense material; and (2) the angle made by the ray with the normal to the interface is greater than some critical angle, the latter being dependent only on the indices of refraction of the media (see Fig. 47).

An off-axis ray of light traversing a fiber 50 microns in diameter may be reflected 3000 times per foot of fiber length. This number increases in direct proportion to a decrease in diameter.

Total internal reflection between two transparent optical media results in a loss of less than 0.001% per reflection. Thus a useful quantity of illumination can be transported. This spectral reflectance differs from that of aluminum.

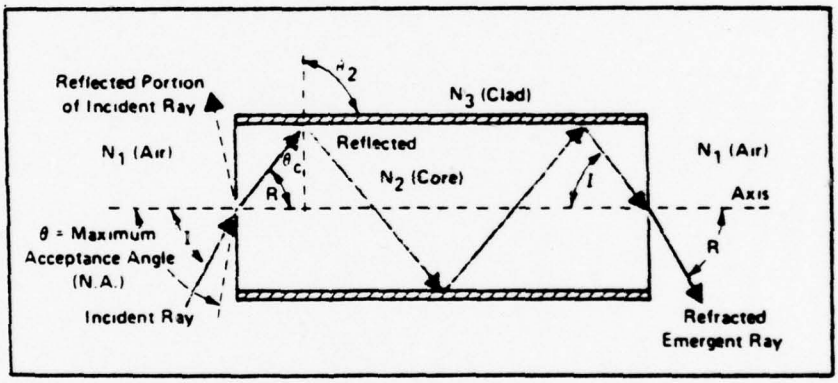


Figure 47 - SINGLE FIBER OPTIC STRAND

An aluminum mirror cladding on a glass fiber core would sustain a loss of about 10% per reflection.

Light is transmitted down the length of a fiber at a constant angle with the fiber axis. Scattering from the true geometric path can occur as a result of: (1) imperfection in the bulk of the fiber; (2) irregularities in the core/clad interface of the fiber; and (3) surface scattering upon entry. In the first two instances, light will be scattered in proportion to fiber length, depending o the angle of incidence. To be functional, long fibers mu t have an optical quality superior to that of short fibers. Surface scattering occurs readily if optical polishing has not produced a surface that is perpendicular to the axis of the fiber; pits, scratches, and scuffs diffuse light very rapidly.

The speed of light in matter is less than the speed of light in air, and the change in velocity that occurs when light passes from one medium to another results in refraction. A portion of the light incident on a boundary surface which is not transmitted, is totally reflected from the sides, assuming that the angle is less than the critical angle.

B. ADVANTAGES

Current Naval aircraft utilize twisted pair wire or coaxial cable for signal data transmission in avionics systems. This means of electromic signal transmission, which dates to post-World War II, exposes the system to degradation caused by EMI (electromagnetic interference), RFI (radio frequency interference), and nuclear generated EMP (electromagnetic pulse) , which are problems inherent to

metallic conductors of this type. Additional problems include crosstalk, ground looping, reflection, and short circuit loading.

The tremendous advances in fiber optics technology have led many engineers to consider glass fiber cables as a replacement for the twisted pair/coaxial cables. The advantages offered by fiber optics are:

(1) EMI/RFI/EMP immunity

(2) Electrical isolation

(3) Wide signal bandwidth

(4) Low crosstalk

(5) Weight and volume savings

(6) Elimination of sparks/fire hazards

(7) Elimination of short circuit/loading problems

(8) High thermal stability

(9) Low cost

(10) Fabrication from non-strategic materials

(11) Low attenuation

(12) Increased security against detection or interception.

The dielectric properties of optical fibers are

responsible for their immunity to EMI/RFI/EMP which greatly improves their elecrtomagnetic compatibility. The electrical isolation between sending and receiving terminals eliminates common ground connections and associated problems such as voltage offsets, ground currents, and noise. Fiber optic links present no fire hazards when damaged and in addition, no local secondary damage can occur because fiber cables neither produce sparks nor dissipate heat.

When a wire cable is damaged, it may in turn, harm the terminal circuits by shorting or grounding them, or by inducing dangerous voltages and currents in the wires which connect to them. With optical fibers, this problem is eliminated.

Conventional wiring is greatly affected by connector discontinuities because it needs solid physical and electrical contact at the connector interfaces for optimal signal transfer. No physical contact is required in an optical interface between the light source or detector and the fiber optic bundle, since light can pass through a small air gap between the end of each fiber in the interface.

Tests have shown that most liquid contaminants found in aircraft which may saturate the interface actually increase the signal coupling. However, bubbles, granular materials and opaque substances can degrade coupling efficiency and damage connector surfaces as well.

The signal attenuation of typical fibers ranges from 2 dB/km to 1,000 dB/km (Ref. 21). Figure 48 shows the properties of typical optical fibers (Ref. 22).

Fiber optic cables offer much greater bandwidth over twisted pair or coaxial cables. For example, the signal bandwidth of a 300-m fiber which has 50 dB/km attenuation

Fiber Type	Mfg.	Core	Cladding	NA	Loss (.85μ)	Profile	Cost
Coreguide	Corning	SiO_2-GeO_2	SiO_2	.18	3-10(db/km)	step or graded	$1-$5
GS-02-10	ITT	SiO_2-GeO_2	SiO_2	.25	4-12	step	$3
BTL-X1*	Bell Labs	SiO_2	SiO_2-B_2O_3	.15	1-5	step	---
BTL-X2*	Bell Labs	SiO_2-GeO_2	B_2O_3	.3	1-5	graded	---
S-10	FCI	SiO_2	SiO_2-B_2O_3	.25	10	step	$4
Quartzwire	FOC	SiO_2	plastic	.25	20	step	$1.65
Low-loss	VALTEC	SiO_2	plastic	.22	40	step	$2
PS-50H	ITT	SiO_2	silicone	.25	< 50	step	---
HYTRAN	Pilkington	Pb glass	borosilicate	.50	80	step	$3
(5010, K2K 101, LGM)	Numerous	Pb glass	borosilicate	.60	800	step	$.25
Crofon	Dupont	PMMA	EVA	.53	2000	step	$.05
PFX-0715†	Dupont	PMMA	EVA	.53	1000	step	$3

*These designations are the author's for experimental Bell Fibers.

†Plastic fibers have their lowest losses in the visible, this one being 470 db/km at .67 μ.

Figure 48 - PROPERTIES OF TYPICAL OPTICAL FIBERS

and the proper light transmission characteristics is 200MHz. The bandwidth of coaxial cable, independent of signal processing electronics, is limited to 20MHz for the equivalent diameter and length of fiber optic cable, while a twisted pair wire has a 1MHz bandwidth. The potential signal bandwidth of small diameter fibers extends beyond 1GHz.

Typical glass fibers currently available remain stable well beyond 300°C. Special glass cables can withstand temperatures up to 1000°C. The maximum operating temperature of fiber cables usually depends on their jacket material or on the epoxy used to secure them in connector ferrules.

Don Williams, program manager at the Naval Electronics Laboratory Center in San Diego, estimates that the 450 pounds of copper wire now used in fighter aircraft could be replaced with only 50 pounds of fiber cable. In the A-7 aircraft, 13 optical fiber cables supplanted 115 signal channels representing 302 separate conductors; replacing almost a mile of electric cable with 224 feet of fiber (Ref. 23).

Present day fiber materials include silicas, silicate glasses, and various polymers. These materials are abundant and are non-strategic.

Cost is an important consideration when evaluating the advisability of replacing proven systems with state-of-the-art technology. Currently, optical fiber cables cannot compete with twisted pair or coaxial cable. Twisted pair wire costs only a few cents per foot while graded-index-fiber cable in quantities up to 50 kilometers cost approximately $ .45 to $ .75/ft. What most people fail to consider is that materials for shielding the twisted pair

wire can cost $2 per foot. With sufficient demand, prices for fiber optic cables may drop to 7 cents per foot by 1978. Therefore, the Navy must weigh the tremendous advantages noted above against falling costs when deciding if the switch to optical fiber cables is warranted.

The number of manufacturers producing optical fibers is quite large and is growing at a rapid rate. Many experts in this field feel that with the emphasis fiber optics is receiving, there is little doubt that by the 1980's optical fibers will often be a practical alternative to copper wire.

C. DISADVANTAGES

Fiber optic's with all its advantages still possess a few disadvantages. The most important ones are:

(1) Production control

(2) Joints for individual fiber segments

(3) Limited lifetimes of light sources

(4) Fiber protection

(5) Radiation effects.

The extremely small fiber diameters require very precise control of production parameters. This is a difficult task, but one that must be overcome in order to obtain near-ideal fiber dimensions and index profiles.

Initial optical cables employed numerous fibers in order to relax the alignment problem and associated signal loss at connectors. The present trend is toward cables with a single optical fiber. Hence, there is more and more emphasis on developing low loss connectors for individual fiber segments. Several current techniques will be presented in section D-3.

A suitable light source is a prime consideration in a fiber optic system. Present light sources have limited lifetimes which impacts on system reliability. The various light sources will be compared in section D-1 of this paper.

Another perplexing problem is fiber protection. The optical cables for operational use must be rugged enough to withstand rough installation and maintenance. Cladding materials which are rugged and posses sufficient tensile strength may not be flexible enough to fulfill the minimum-bending-radius requirements and vice versa.

Dielectric glass or plastic cables are particularly well suited for nuclear environments because of their immunity to electromagnetic pulse (EMP) effects. However, as NRL scientists have pointed out, many existing fiber-optic cables suffer substantial losses in optical transmission when subjected to ionizing or nuclear radiation. The major problems that arise are associated with light-absorbing and light-emitting defect centers produced by the impinging radiation in the fiber waveguide itself.

NRL scientists have identified the damage mechanisms in the irradiated fibers, and a program to develop more radiation-resistent materials is underway. Special emphasis is being placed on the development of suitable fibers for near-term Navy systems such as the A-7 and P-3 aircraft. The lead silicate type fibers used in the ALOFT

demonstration cannot tolerate more than a few rads of irradiation without sustaining damage. A Tri-Service Radiation Effects Working Group has been established to coordinate and address radiation hardening needs.

Most of the disadvantages discussed above can be overcome with sufficient research and development. Radiation effects present the most serious drawback to the operational use of fiber optic systems .

D. COMPONENTS

A typical fiber optic system contains a pulse signal source, current driver (transistor or wide-band amplifier), light source, fiber optic bundle, interfaces and connectors, photodiode, and signal processing equipment.

1. Light Sources

The light source converts the electrical signal into an optical signal, and is either an incoherent LED (light-emitting diode), a semi-coherent semiconductor laser, or a coherent Nd:YAG laser. An acceptable light source should possess the following characteristics: faithful reproduction of the electrical signal, monomode excitation, high optical output at low current density, small emitting area, high frequency response, and long lifetime.

Light-emitting diodes are the most widely used light source today. This is primarily due to their availability, compatibility with available photodetectors, power requirements, and long life. The intensity of light output from LED's is proportional to the current through it, and

since LED's operate at much lower current densities than semiconductor lasers, they do not suffer inslovable degradation and reliability problems. The amount of information an LED can transmit is limited by its frequency response, which presently is up to a few hundred megahertz for the best LED's. Typical laser diodes, on the other hand, can be modulated at speeds up to 1 gigahertz.

High-radiance LED's for optical communications are either surface emitters ("Burrus" type developed at Bell Laboratories) or edge emitters. The edge emitter is inherently capable of better coupling efficiency than the surface emitter, but the latter more than compensates for this by its higher total radiated power. The most promicing LED's use a double-heterojunction design, fabricated by sandwiching a thin layer of gallium between two layers of GaA1As that absorb no energy and act as light guides (in the case of the edge-emitter). Extrapolation from accelerated aging tests indicate that high-radiance Burrus-type LED's should provide greater than 100,000 hours of operation.

The desire to use optical cables with single fibers as opposed to bundles of fibers requires the efficient coupling of source power into the fibers. The smaller optical aperture of the single fiber requires the higher source power of the laser diode. Laser diodes are also used in high-speed, high-power systems using fiber bundles.

There are two types available today: gallium-arsenide and gallium-aluminum-arsenide laser diodes in single and double-heterojunction structures. The most important difference is the much higher data-rate capability of the double-heterojunction type (greater than 100 megahertz versus 100 kilohertz). Single-heterojunction laser diodes are low cost, off-the-shelf items used in low-duty-cycle applications requiring high output power.

The double-heterojunction laser diode requires relatively low drive current and voltage (less than 400 milliamperes at 2 volts).

Laser diodes have not been widely used due to several problems. First, relatively small changes in temperature can change the output significantly. If high enough temperatures are reached (without increasing applied current), the threshold current of the drive may increase sufficiently to prevent lasing.

Second, laser lifetime remains a problem. Although actual laser-lifetime data is not yet available, data interpolated from selected samples translates into a mean time between failure of only 10 hours for some lasers with a heat sink temperature of 22C.

The third big problem area is achieving an efficient coupling of laser to fiber. This should be alleviated with construction techniques that attach a short length of fiber directly to the laser pellet.

2. Fiber Optic Cables

Most early fiber optic systems employed bundles of fibers packaged together in a single link, all carrying the same signal. This redundancy was necessary largely because of the high probability of breakage in long length cables and the off-the-shelf nature of components which could couple to the fiber bundles. However, as reliability increases and the cost of ultra low loss glasses remains high, the trend is towards single multimode fiber cable configurations, each with its own discrete light source and detector, with perhaps 4 to 6 single fibers incorporated into an actual cable design.

As previously mentioned, present day fibers are made from high purity silicas, doped silicas, silicate glasses and various polymers. Fiber core-cladding geometries fall into three categories: (1) step-index multimode, (2) graded index, in which the index of refraction decreases continuously with increasing distance from the fiber axis, and (3) single-mode step-index, in which core diameters are reduced to a few microns so that only one mode will propagate. The difference in index of the core and cladding materials determines the angle of light acceptance of a fiber, its numerical aperture (NA). Cladding thickness and the NA of a fiber also effect the minimum radius to which a fiber can be bent before light is ejected and lost from the waveguide and are therefore important for both microbending and cross-talk problems.

Plastic fibers in use today are normally fabricated from polymethyl-methacrylate (PMMA) and polystyrene. As can be seen from Fig. 48, the losses are quite high, but there is a good possibility of reducing attenuations perhaps to the 100 dB/km level at certain selected wavelengths. These losses result from very high scattering losses due to both unwanted suspended particles and high interface losses. Plastic fibers offer excellent mechanical properties near room temperature and do not suffer the brittle fracture problems of the glasses. The good radiation resistance, light weight, mechanical flexibility and breakage resistance of plastics makes them attractive for short run applications.

3. Connectors

Splices for joining lengths of optical-communications cable must provide low-loss, quick but permanent connections, and also be small, lightweight,

and rugged. Single-fiber splicing losses of less than 0.1 decibel have been reported in the lab but have yet to be demonstrated in the field.

The most critical parameter, axial or lateral alignment, is also the most difficult to control. Slight offset between the two fiber ends dramatically increases optical loss. Alignment accuracy in the order of micrometers is needed, thus requiring similar machining tolerances of the associated hardware. Three currently used techniques will now be presented.

One splicing technique in widespread use is the precision sleeve or tube, which by conforming precisely to the outer diameter of the fiber, guides it into position and then holds it there. This method is most suitable for single fibers or small cables. Bell Northern Research has developed a splice using this technique in which a stainless steel preform tube is crimped into the fiber's plastic coating. With a silicon fluid pre-injected into the splicing element, insertion losses average 0.3 decibel from a LED source.

Another technique used by Bell Telephone Laboratories is the loose tube splice which exploits the self-aligning tendency of fibers in a "V" groove as shown in the top of Fig. 49. Prepared fiber ends are inserted into a rectangular tube already filled with index-matching epoxy. Losses average about 0.1 dB when a laser source is used.

Another single fiber connector, a variation of the precision sleeve splicing element, has been developed by Bell Northern Research for use with plastic-coated multimode fibers. The system uses a plug and jack arrangement shown in the lower portion of Fig. 49. The plug and its mating

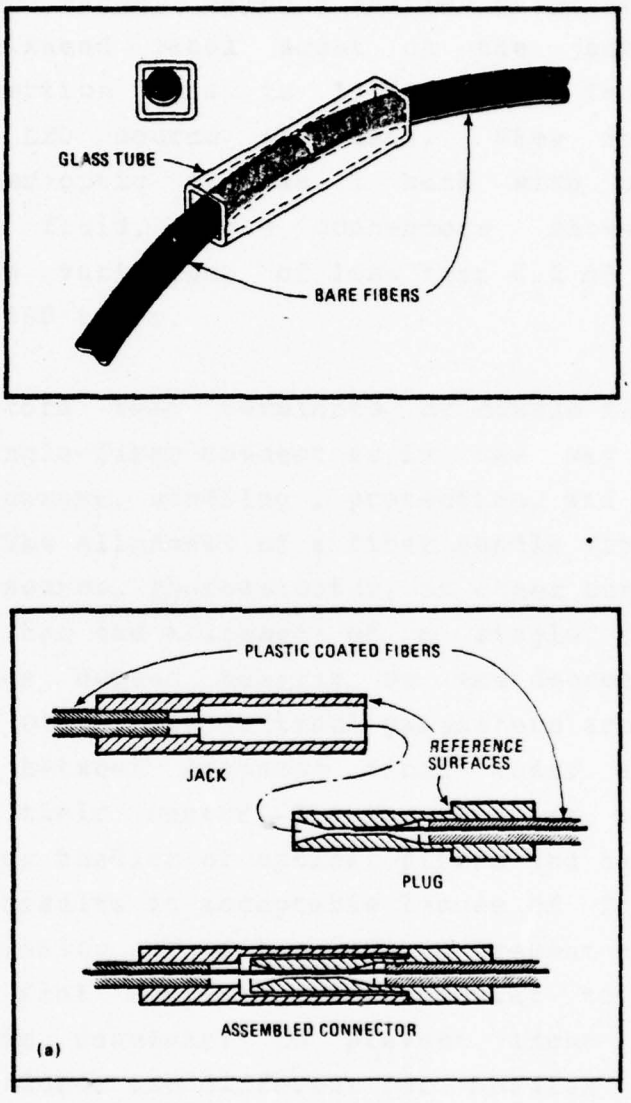


Figure 49 - TOP: LOOSE-TUBE SPLICE; BOTTOM: PLUG AND JACK

jack are mounted separately on a fixture, prepared fiber ends are inserted into each connector half until they butt against the fixture's stops, and the stainless-steel tubing is crimped into the fiber's plastic coating. The plug and jack are then mated, using a knurled coupling nut on the plug and a bulkhead panel mount on the jack. Typical rematable insertion loss is 1 dB when an index-matching fluid and a LED source are used. When installed in prototype fiber-optic systems , both with and without index-matching fluid, these connectors showed typical insertion loss variations of less than 0.2 dB after being remated up to 100 times.

Connectors that terminate or couple fiber bundles differ from single-fiber connectors in the way they deal with fiber alignment, handling , protection, and optical end preparation. The alignment of a fiber bundle with a LED or laser diode source, photodetector, or other bundles is far less critical than the alignment of a single fiber. The coupling losses depend heavily on the degree of lateral misalignment. Other less critical parameters are the size of the gap between prepared fiber ends, and angular alignment of their center lines. Angular misalignment within $\pm 1^{\circ}$ for bundles of optical fibers and half that for single fibers results in acceptable losses of from 0.1 to 0.2 dB. Polishing of fiber ends to present a chip-free, scratch-free, flat surface, perpendicular to the fiber centerline, is necessary to prevent light scattering. Polishing procedures are different for bundles and single fibers and a quick, efficient process is of prime importance for operational use. Coupling losses depend on the size and number of fibers in the bundle, the core-to-cladding ratio of each fiber, and the numerical aperture of the fiber bundle. Losses from fiber bundle to fiber fall between 2.5 to 3.5 dB.

Source-to-fiber and fiber-to-detector coupling efficiency varies not only with the connector but with the device characteristics and how well the fiber is matched to either detector or source. Source-to-fiber bundle coupling loss can vary from 3 to 14 dB with off-the-shelf devices while fiber-to-bundle-to-photodetector coupling loss can vary from 0.5 to 8.5 dB. ITT Electric has recently marketed a single-fiber-per-channel connector which can be used to join two single fibers or to couple a photo or LED or laser diode to the fiber.

Another recent arrival is the molded thermoplastic connector, which is inexpensive, fast, and reliable. This connector is lighter than the metal connectors and interferes less with the optical polishing of the bundle ends. It can be installed in the field by people without special skills or training. Insertion loss is about 3 dB, but can be reduced to 2 dB by using an index-matching fluid.

4. Detectors

The receiver portion of any fiber system requires a photodetector that responds strongly to both the peak output wavelength of the sources and the low-loss spectral portion of the fiber cable used. P-i-n diodes best fulfill these requirements. High performance p-i-n type silicon photodiodes have been in production for many years and cost less than $1 each. They exhibit nanosecond response times and can have a dynamic light-level range of 8 to 10 orders of magnitude at rleatively low bias voltages. Their peak response between 850 and 950 nanometers matches well with the peak emissions of light-emitting diodes and the low-loss spectral regions of optical fibers.

5. Couplings

In a multiterminal fiber-optics communication system, light signals have to be tapped at intermediate points along the data bus. Currently, two fiber-coupling configurations are used, one employing access or "tee" couplers and the other using a radial-arm or "star" coupler. Figure 50 shows the two methods and the equations to measure their performance in terms of the loss introduced between pairs of remote terminals by the distribution system itself. In a serial system with access couplers having a constant tap ratio, the optical power decreases as the signal travels through more couplers, while a parallel system using a star coupler, the optical power is independent of the pairs of system terminals being considered. As the number of terminals in a system increases, the distribution losses of the serial format grows rapidly while those of the parallel format increase gradually. With low-loss connectors and couplers for single fibers, serial distribution systems should be able to handle at least 20 terminals without consuming an unreasonable proportion of the available power budget.

Since the parallel system needs only a single mixing point, it doesn't suffer signal-level or dynamic-range problems. The more constant signal level available with parallel systems minimizes the complexity of both transmitter and receiver design. But the cost of this uniformity is offset by the additional amount of fiber cable needed. A star coupler was used in a fiber-optic multiterminal aircraft data link for carrying flight control signals in a successful test aboard an Air Force C-131 aircraft.

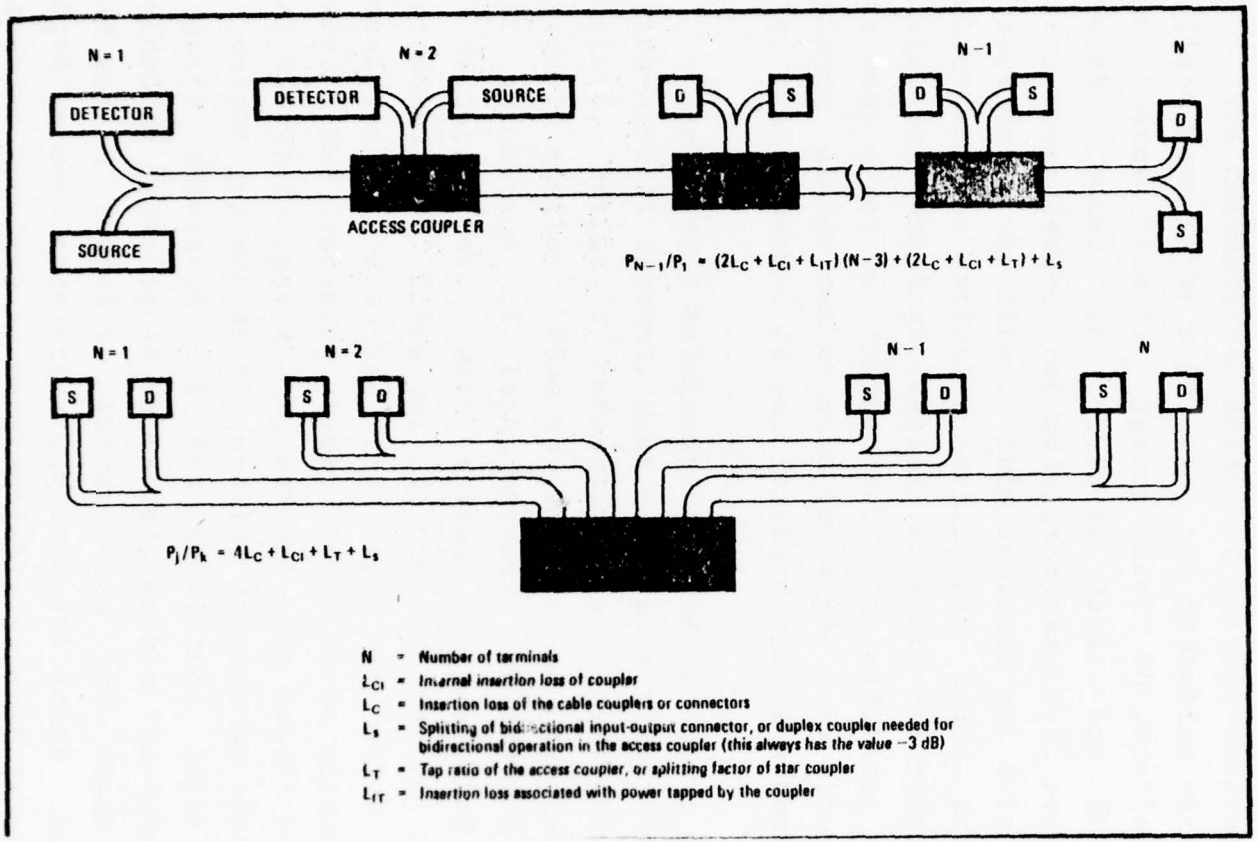


Figure 50 - COUPLING COMPARISONS

6. Modulation

The conventional method of loading information onto the light beam is by modulating the injection current of the light source itself. Sperry Rand Corporation's Sperry Research Center in Sudbury, Mass. has developed an electro-optic device that modulates the light beam after is is already in the fiber. This approach not only eliminates an electronic-to-optical interface,but could prove to be usefull at very high frequencies where the response of the light source may be inadequate. In addition, the basic modulator design can be used to switch data along different paths, a requirement of multiplexers and data buses.

The Sperry modulator is based on a thin wafer of an electro-optical crystal, such as lithium niobate or lithium tantalate, having a refractive index that changes when a voltage is applied. When no voltage is applied, only a small percentage of light entering the crystal will reach the output fiber. When voltage is applied to the electrodes, the index of refraction in that part of the crystal varies, changing the angle at which the light enters. The incoming light tends to be guided along the metal-electrode path to the output. The amount of light at the output depends on the applied voltage so that output is intensity modulated. A 50% modulation depth could be obtained by applying 14 volts rms, with a throughput loss of 18 dB and a bandwidth larger than 600 megahertz. One hundred percent modulation requires 900 volts. However, the throughput loss may be substantially reduced (with a slight increase in required voltage) by butting the fiber up against the crystal so that the axis of the fiber is not perpendicular to it. For 50% modulation, throughput loss drops to 10 dB at 23 volts, and the voltage required for

100% modulation can be reduced to 225 volts.

E. APPLICATIONS

In addition to the impressive credentials already noted, fiber optic technology is extremely versatile. Unlike many other air data sensors that may be utilized to measure only one specific parameter, fiber optics can handle a variety of tasks, and new applications are being found every day. Specifically, fiber optic digital status-monitoring devices can be used to measure:

(1) Linear displacement

(2) Rotational displacement

(3) Strain

(4) Temperature

(5) Pressure

(6) Fuel level

(7) Event counting

(8) Flow rate.

Some of the major applications will now be presented, starting with the ALOFT project.

1. A-7 Aloft Demonstration

The ALOFT (Airborne Light Optical Fiber Technology) demonstration was a two year program sponsored by the Naval Air Systems Command. The program was designed to satisfy five specific objectives:

(1) Verify that fiber optics is a pratical, mature technology for use in internal aircraft data signal transmission.

(2) Demonstrate the feasibility of a full system application.

(3) Provide an operational demonstration to compare the performance of fiber optics with the perfcrmance of existing wire systems.

(4) Acccmplish a meaningful, low-risk step toward the development of a full multiplex data bus avionics system.

(5) Predict its future worth through estimates of life-cycle costs and expected benefits.

Initial project funding was received by NELC (Naval Electronics Laboratory Center) from NAVAIR in March 1974. The Navigation and Weapons Delivery System (NWDS) in a Navy A-7 aircraft served as the primary demonstration vehicle in which selected wiring was replaced with multiplexed optical data links. In August 1975 an industrial contract was awarded to design, develop, and fabricate a multiplexed subsystem that would provide the optical communications

links between the aircraft's tactical computer and peripheral avionics units. A number of Governmemt and industrial activities contributed to the overall program effort:

(1) NAVAIRSYSCOM-program sponsor

(2) NELC-program management

(3) Naval Weapons Center-software development/flight testing

(4) IBM-prime contractor for hardware development

(5) ITT-computer interface connector

(6) LTV-ground test simulation/aircraft installation plan

(7) VALTEC-fiber optic cables

(8) Sealectro-bulkhead connector fabrication

(9) Spectronics/Hewlett-packard-LEDs/photodetectors

The original A-7 data communication system in the NWDS is a pcint-to-point system which uses twisted pair and coaxial cable interfaces. One hundred and fifteen (115) signals, normally transmitted over individual wire channels, were multiplexed into thirteen (13) optical channels (cables) converging at one optical connector at the computer interface. The fiber optics configuration reduces cable weight by 21 times without increasing susceptibility to EMI. A comparison of the two systems is shown below.

	Original Wire	F.O. (mult.)
Number of wires/cables	302	13
Length	1890 ft	224 ft
Cables/connectors, wt	31.9 lb	2.7 lb
Cables/connectors, $	0.35k	0.24k
Termination/test, $	1.28k	0.24k
TOTAL COST $	1.63k	1.03k

The system underwent flight tests in the spring of 1976 at Naval Weapons Test Center, China Lake, climaxing in a bombing and rocket firing demonstration in May. The optical system matched the performance of the existing fleet configuration, and the pilots could not detect any difference.

ANALYSIS

The ALOFT project has demonstrated that substantial reductions is weight and size are possible. The freedom from ground loops, the low cross talk and the much greater bandwidth make multiplexing possible with optical fibers and difficult or impossible with the wire system. The major payoff for avionics systems using fiber optics comes from electromagnetic compatibility. This should result in substantial cost savings in the design and test phase of advanced aircraft. In addition, the increased use of composite materials in aircraft makes RFI and EMI immunity crucial to performance. Fiber bandwidths permit the use of

serial rather than parallel transmission techniques.

The major stumbling block, which is being addressed by the Tri-Service FO Committee, is the lack of military-qualified components for optics systems. NELC and NAFI have joined together to draw up a Manufacturing and Technology program for avionics applications. Standardization of cables and connectors is being encouraged, and cost, reliability, and failure analysis studies of all components are underway. Radiation effects must be eliminated before fiber optic systems can be employed in operaticnal applications.

2. P-3C Aircraft

An advanced Navy P-3 aircraft weapons system (PROTEUS) with a fiber optic interface is a candidate for the first actually deployed fiber optic avionics system. Possible application areas include a 10 MHz intercomputer channel, a 10 Hz to 30 MHz video channel and a 8 Hz to 40 kHz acoustical channel with a 48 dB dynamic range. Lockheed, California of Burbank has designed the system. A fiber optic transfer link has been configured and evaluated in the P-3C integration test facility at Burbank with totally satisfactory performance.

The P-3 fiber optic system is expected to reduce weight by a factor of 10 and volume by a factor of 3 compared to the copper wire system. Electromagnetic compatability is again the greatest payoff with electromagnetic crosstalk, interference, ground loops, impedence matching, and security problems greatly reduced or eliminated.

Lockheed has successfully developed a fiber optic

interface for the P-3 which included the design of external serial to parallel and parallel to serial converters for the 30 bit parallel information links. Galileo fiber optic bundles of lead silicate glasses with losses of 700 dB/km were used, similar to the Valtec fibers employed in the ALOFT project. Both of these fibers have been shown by NRL to be unacceptable in operational systems because of high sensitivity to radiation. The P-3 system is being contemplated for FY 1979.

VI. LASER GYROS

Although the laser gyro has been around for 14 years, it is getting renewed attention for some specific applications. These include short-range tactical missiles, aircraft inertial navigation and attitude/heading reference systems, shipboard stabilized platforms and possibly some space and strategic applications. Boeing is considering a Honeywell laser inertial navigation system as one of three strapped-down systems for its 7x7 transport.

The intrinsic characteristics of the laser gyro that make it attractive are:

(1) Performance that is unaffected by a high-g environment.

(2) An absence of rotating parts which suggests high reliability and minimal maintenance.

(3) Accuracy is largely independent of cost.

(4) Extended warm-up is not required.

Two manufacturers, Honeywell and Sperry Flight Systems (who developed the first laser gyro in 1963), have competitive designs that will be presented in the following pages. The Honeywell design has achieved the lowest errors, while Sperry Gyroscope's device has yielded the smallest overall size and weight, with sufficient accuracy for

tactical missile applications.

A basic difference between the Sperry and Honeywell design approaches is the method used to minimize interference between the gyro's two contrarotating laser beams that occurs when the unit is at rest or is experiencing low angular rates. Honeywell utilizes mechanical oscillation, called "dither", while Sperry selected an cptical means to solve this problem which is known as "mode-locking."

The other major difference in the two designs is the fabrication of the laser cavity. Honeywell employs an integral design in which the entire path length of the gyro functions also as a laser cavity. Sperry, on the other hand, builds its laser as a separate unit, sealed in a glass enclosure.

The Naval Air Systems Command has funded a program at Honeywell whose objective is to find a means of mass producing the laser gyros at low cost. In addition, the Navy has budgeted nearly $10 million over the next few years to develop the knowledge and manufacturing techniques that can reduce the cost of building laser gyros. One of the major stumbling blocks is the interaction of the laser beam and the mirrors used in Sperry's design. Factors such as random drift, lock-in threshold, lasing threshold, and null stability must be considered.

The USAF Office of Scientific Research is sponsoring work at Stanford University on mercury lasers for possible use in laser gyros and other applications. The improved stability of a mercury laser could significantly improve gyro perfcrmance.

In the first production application laser gyros will

provide pitch and roll axis stabilization of a Mark-68 fire control system for shipboard anti-aircraft guns. But the largest potential market for laser gyros is expected to be in tactical missiles and long-range glide-bomb weapons.

A. HONEYWELL LASER GYRO

Honeywell has taken the laser concept and developed it to its most accurate implementation to date. This was borne out by extremely successful tests in 1975 of a Honeywell laser inertial navigation system (LINS) which caused the U.S. Air Force to propose a major effort in Fiscal 1978.

The Honeywell system was operated for 1,300 hours, including 65 hours in flight onboard a USAF Lockheed C-141. In the flight tests it exhibited an overall error of only 0.65 nautical mile/flight hour circular error probability (CEP). Honeywell reported that during the 1,300 hour test, the system did not experience any failures and did not require any system recalibration.

Honeywell's approach to the "mode-locking" problem, which yields higher accuracy, is to use a high-frequency, small amplitude mechanical oscillation ("dither") of the entire laser gyro about its sensitive axis. Each gyro must be oscillated about its own sensitive axis which precludes the possibility of combining the three laser gyros into a small cluster.

Another part of the cost-reduction program mentioned earlier calls for Honeywell to deliver a prototype aircraft inertial navigation system with no more than a 1-naut. mi./hr. error performance that can be packed into a 3/4 ATR-size case (the previous system occupied a full ATR

case).

The GG-1342 was developed to meet this requirement, and employs a path length of only 12.6 inches compared to a length of 17.1 inches in the GG-1300. The new gyro still provides comparable accuracy, however.

In addition to the GG-1342, Honeywell is using company funds to build a laser inertial system designed to be aligned on an aircraft carrier, for flight tests on a Grumman F-14 and McDonnell Douglas F-4 in mid 1978. With this system, Honeywell hopes to exploit its present advantage in being able to produce laser inertial systems with better than 1 naut. mi./hr. performance.

B. SPERRY FLIGHT SYSTEMS LASER GYRO

Sperry has chosen a design that yielded the smallest laser gyro in overall size and weight, with accuracy sufficient for tactical missile applications. This design permits three laser gyros, with their sensitive axes orthogonally oriented, to be fabricated in a single cluster that measures only 4.5 inches in diameter and 4.5 inches long, excluding gyro control circuitry. SLIC-7 (Sperry Laser Inertial Cluster, 7 inch laser path length) is the name given to this miniaturized design. When combined with accelerometers and digital computer to form a complete inertial guidance system, it can be housed in a cylindrical container measuring only 6 inches in diameter by 9 inches long that weighs 14 lb. Sperry plans to use a SLIC-7 to explore the use of strapped-down laser gyros for military attitude-heading reference system applications. Sperry has operated some of its laser tubes, used in the gyro, for more than 6 years and 55,000 hours without a single failure, and

complete laser gyros have operated for more than 20,000 hours without failure or need of maintenance.

The long-term stability and "shelf-life" of the current laser gyro is borne out by the performance of a gyro used at the Naval Weapons Center. The device was tested for 6 months, stored for 2 years, tested , stored another 2 years, and tested a third time. At the end of the 4 year 6 month period, its performance was still within original specifications.

In a redundant six-gyro cluster (using older SLIC-15's) which is being developed for NASA's Marshall Center, each gyro can detect motion about 2 of an aircraft's three axes of motion. This feature improves accuracy (all six gyros operating) and enables the system to detect malfunctions automatically in any 2 gyros and disregard their erroneous data.

Sperry's solution of the "mode-locking" problem is an optical approach which eliminates all moving elements from the laser gyro. This optical technique employs the Kerr Transverse Magnetoptic Effect which is sometimes referred to as "magnetic mirrors." These mirrors are placed transverse to the plane of incidence of the laser beam. When a field is applied to the mirror, it causes the phase of one beam to be advanced while that of the contrarotating beam is retarded.

One disadvantage of the magnetic mirror technique is that it introduces considerable path loss within the optical cavity, which in turn degrades performance. As a result, Sperry is investigating the possible use of magnetic garnet crystals to reduce optical path losses.

Sperry's fabrication of the laser cavity differs

significantly from Honeywell's. The laser is built as a separate device, sealed in a glass enclosure. Independently, the optical paths for the laser are machined into a Cervit block, after which the mirrors and laser tube are simply installed without the need for vacuum sealing. The entire cluster is placed in a metal enclosure and then evacuated. Sperry estimates that its three-gyro cluster can be built for little more than the cost of a single-axis Honeywell gyro. Furthermore, Sperry believes that a full SLIC-7 inertial guidance system could be built today in quantity for approximately $18,500, possibly dropping to $10,000 in time.

Another advantage of the Sperry design is that the laser gas itself has no opportunity to interact with the mirrors, which eliminates the problems (random drift, etc.) mentioned earlier.

ANALYSIS

There have been tremendous advances in the laser gyro concept, but present laser gyro technology is far from achieving the extremely high-accuracy/low-drift rates of more conventional precision gyros. However, these gyros remain desireable for military applications due to their ability to operate in high-g environments with no degradaticn in performance. The lack of moving parts could possibly pay large dividends in reliability.

The concept deserves further testing and development, which it is getting through Navy and Air Force programs. The progress made in these programs should be monitored closely, and another evaluation made when more data is available.

VII. TEMPERATURE

At the present time, the thermocouple is the most common device for temperature measurement. resistance temperature detectors (RTDs) are rapidly gaining acceptance in the U.S. This trend toward greater usage of resistive devices can be attributed to decreasing sensor and associated instrument costs. There are five basic sensors, both active and passive. The classification of the five basic temperature sensors and their operating ranges are shown below.

SENSOR CLASSIFICATION	OPERATING RANGE, °C
Active sensors (no excitation)	
Thermocouples	-273 to +3,000
Radiaticn pyrometers	+1,000 to +4,000
Passive sensors (excitation required)	
RTDs	-273 to +1,000
Thermistors	-273 to +250
Semiconductor junctions	-273 to +150

The wide temperature range of the thermocouple makes it particularly well suited for use in hostile environments in today's aircraft applications. Radiation pyrometers offer the highest temperature range and have been used to measure turbine blade temperatures (this application will be presented in subsequent pages). Each of the sensors listed above have limitations, some of which can be alleviated by proper interfacing of the sensor and its readout device and

appropriate selection of signal circuitry.

Thermocouples operate on the Seebeck principle: when the junctions of two dissimilar metals forming a closed circuit are exposed to different temperatures, a net electromotive force is generated which induces a continuous electrical current. The thermocouple measures only the temperature difference between its reference junction and the measuring junction. Therefore, system accuracy depends on reference junction temperature compensation.

Resistive temperature detectors (RTDs) utilize the temperature coefficient of resistance as the basis for measuring temperature. Various circuits can generate an output signal for readout as a function of resistance change, including classical bridge configurations. Most metals used to form RTDs exhibit a positive temperature coefficient of resistance, a relatively stable function as compared to the output of thermocouples.

One of the main disadvantages of RTD measurements has historically been the high cost of sensors, but less expensive ones are becoming available. In addition, the lead wires for RTDs cost much less than the extension wires normally required for TCs (thermocouples). Improved platinum sensors and other materials such as nickel are becoming more widely used. Platinum or nickel RTDs are relatively insensitive to parasitic thermal emf's , and can operate quite satisfactorily with standard copper-plated extension wires.

Of all usable metals platinum best meets the requirements of thermometry. It can be highly refined. It resists contamination. It is mechanically and electrically stable. The relationship between temperature and resistance is quite linear. Production units can be made closely

interchangeable in calibration. Drift and error with age and use are negligible.

The output level of a typical RTD is higher than the output of a thermocouple. Measurement is based on the increase in resistance with temperature, and hence excitation current must be applied to the sensor so that a measureable voltage output can be generated.

Radiation pyrometry, an indirect noncontact technique, permits a target's temperature to be inferred by measuring its radiated energy. This technique possesses a number of advantages: (1) it can measure temperatures above 3,000 °F; (2) it neither damages the measured object nor is itself harmed by the object; and (3) it can monitor moving targets and large surfaces. Either spectrally selective techniques or total radiation can be used for temperature measurement. Brightness or optical pyrometry is the most common form of the latter technique.

Two examples of state-of-the-art temperature measurement techniques will be presented in the next section. The first uses radiation pyrometry and imaging methods (like photography and photoelectric scanning) to make accurate temperature measurements on turbine airfoils. The second, employs electronic circuitry and an LED matrix to detect and graphically display engine over-temperature incidents.

A. TURBINE BLADE TEMPERATURE MEASUREMENTS

The desire to operate with higher turbine inlet gas temperatures (and thereby obtaining higher efficiency) has led to engines with cooled turbine blades. The upper limit in the turbine inlet gas temperature is strongly determined

by the required turbine life which is a function of airfoil temperature and stress levels. The goal of the turbine cooling design is to maintain the airfoils at the design temperature without producing any severe thermal gradients on the airfoil surface.

Surface temperature distributions are used at NASA-Lewis Research Center to experimently evaluate the performance of cooled turbine blades and vanes in ground based turbine test facilities (Ref. 31). The temperature distribution measurement techniques which will be described are invaluable in heat transfer, thermal stress, and blade life studies and provide correlation with analytical prediction methods. An infrared (IR) photographic method was selected for temperature measurement of stationary vanes using conventional photographic equipment along with a densitometer and a computer for film data reduction.

A photoelectric scanning system was developed for obtaining temperature distribution measurements on rotating turbine blades having blade tip speeds up to about 400 meters/second. This turbine blade pyrometer combines fiber optics with high speed electronics plus a computer for data reduction.

NASA-Lewis refers to their customized photoelectric system for temperature measurement on rotating blades as a turbine blade pyrometer (TBP). The optics together with the high speed electronics of the TBP are capable of resolving a spot diameter of 0.05 cm on a blade moving with speeds up to 300 to 400 meters/second. Near real time displays of temperature profile are generated for a single blade or for small groups of blades at steady state conditions.

A block diagram of the TBP is shown in Fig. 51. The protected fiber-optic probe (1) is positioned in the engine

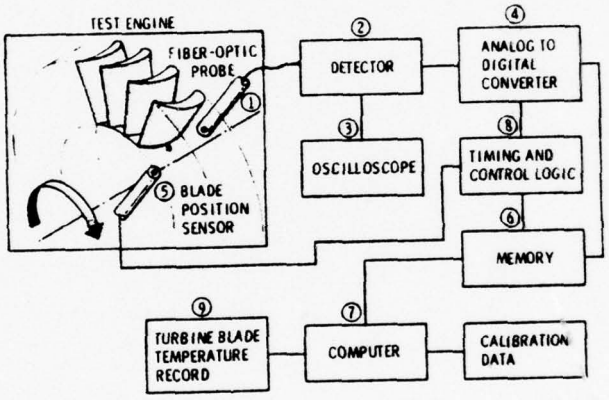


Figure 51 - TBP BLOCK DIAGRAM

by an actuator, and the fiber is focused in the plane of the turbine blades. As the heated blades rotate, the emitted radiation from the spot location (0.05 cm diameter instantaneous field of view of the fiber) is transferred optically to a fast response silicon avalanche detector (2), thereby generating a continuous high resolution intensity profile which is monitored on an oscilloscope (3) during the test. The amplified detector output is digitized by an analog to digital (A/D) converter (4) at ranges up to 2 MHz rate. A blade position sensor (5) supplies a trigger signal when the 1st test blade enters the field of view. This causes a 200 point sample of the digitized detector output to be stored in a high speed memory (6). Random noise may be averaged out by repeating the process a number of times. The 200 data points are transferred from memory at a slower rate to the computer (7) where each point is converted into temperature from a "look-up" table.

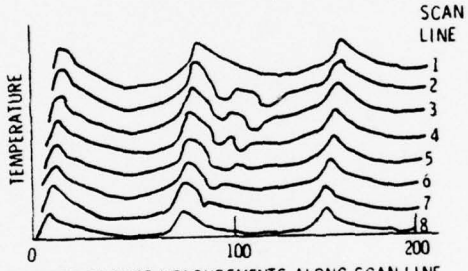
The timing and control logic circuit (8) provides interchange of control between the computer, the memory, and the A/D converter. The system performs all the required operations and presents data on a CRT display in the form of a temperature profile and a listing of the 200 points making up the profile. A hard copy of the turbine blade temperature record (9) is made in the test cell in about 3 seconds.

The system can also obtain a series of scans over a range of radial locations, using the probe actuator, and present them in an isometric view, or alternately as a two-dimensional contour map of temperature distribution with additional computer processing.

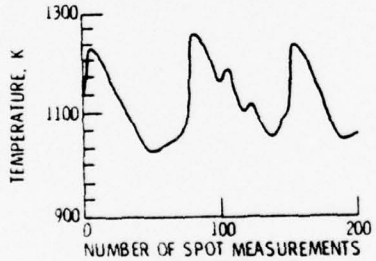
An example of data obtained with the TBP system is illustrated in Fig. 52. A group of conventionally cooled turbine test blades shown in the figure were instrumented



CONVECTION COOLED
TURBINE BLADES



NUMBER OF SPOT MEASUREMENTS ALONG SCAN LINE
ISOMETRIC DISPLAY OF SCAN LINES 1 - 8



NUMBER OF SPOT MEASUREMENTS
ALONG SCAN LINE
TEMPERATURE PROFILE ALONG SCAN LINE 3

Figure 52 - TYPICAL TEST DATA

with surface thermocouples. Comparison of TBP and thermocouple measured temperatures agreed to within 2% of temperature (expressed in degrees C).

B. TURBINE ENGINE HOT SECTION DISPLAY CONCEPT

The required frequency of inspection, servicing and overhauling of gas turbine engines is to a large extent determined by the history of excessive or over-temp conditions of each engine. ELDEC Corporation has developed a device to monitor and record each such over-temp condition (Ref. 32). The system employs electronic circuitry for processing a temperature signal from the engine in conjunction with an LED matrix to graphically display each over-temp condition. when the engine temperature exceeds a threshold over-temp point, this occurrence is sensed and the circuitry within the cockpit indicator functions to automatically store and visually display the engine temperature as a function of time for the succeeding several seconds after the over-temp condition has commenced.

All the diodes of the matrix lying under the temperature versus time profile that lie above the over-temp reference point are energized so as to present a histogram display of the severity of the condition, where the severity is a function of the magnitude and duration of the over-temp . Another version of the concept senses, graphically displays, and stores for later retrieval a succession of over-temp events. Maintenance personnel may subsequently interrogate the indicator which will sequentially display each recorded or electrically stored over-temp event.

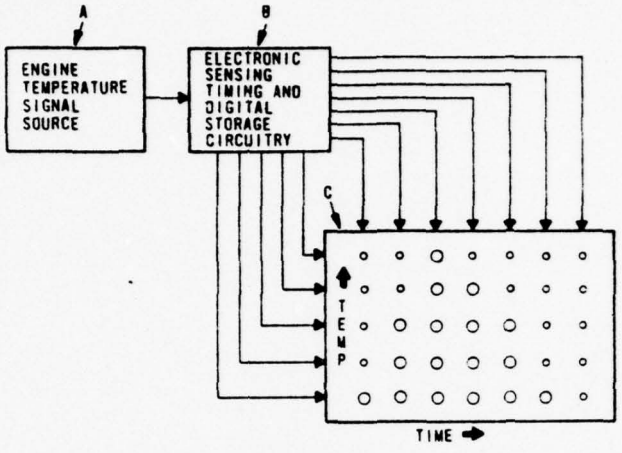
In operation, the HSD (hot section display) senses an electrical signal representing the magnitude of a salient

engine temperature, such as the turbine inlet (TIT) or exhaust gas (EGT) temperature, and processes it. The commencement of an over-temp condition is sensed and the circuitry begins to digitally store the instantaneous temperature magnitude at each of a plurality of succeeding time intervals.

The temperature versus time information is then graphically presented by selectively energizing the appropriate rows and columns of the LED matrix. Temperature is displayed on the vertical axis, while time is represented on the horizontal axis.

The intensity of the histogram -type graph (the number of diodes energized) is a function of the severity of the temperature versus time characteristics of the engine's over-temp condition. This type of display is quickly and easily interpreted by the aircrew, resulting in the timely execution of corrective procedures. Closer inspection of the stored information by maintainence personnel can reveal the maximum temperatures reached and the time duration over which the excessive temperatures occurred.

The top of Fig. 53 is a functional block diagram of the Hot Section Display concept showing the LED graphical display matrix. The bottom of the figure shows a graph of a typical engine over-temp event as a function of time illustrating a brief over-temp excursion of the type monitored by the instrument. Figure 54 shows ELDEC's Model 9-311. This instrument combines TIT vertical scales (analog) with 7 segment (digital) displays and includes a HSD above each engine channel.



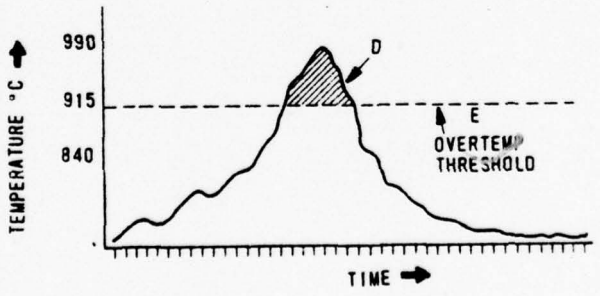


Figure 53 - TOP: FUNCTIONAL HSD BLOCK DIAGRAM, BOTTOM: TYPICAL OVER-TEMP EVENT

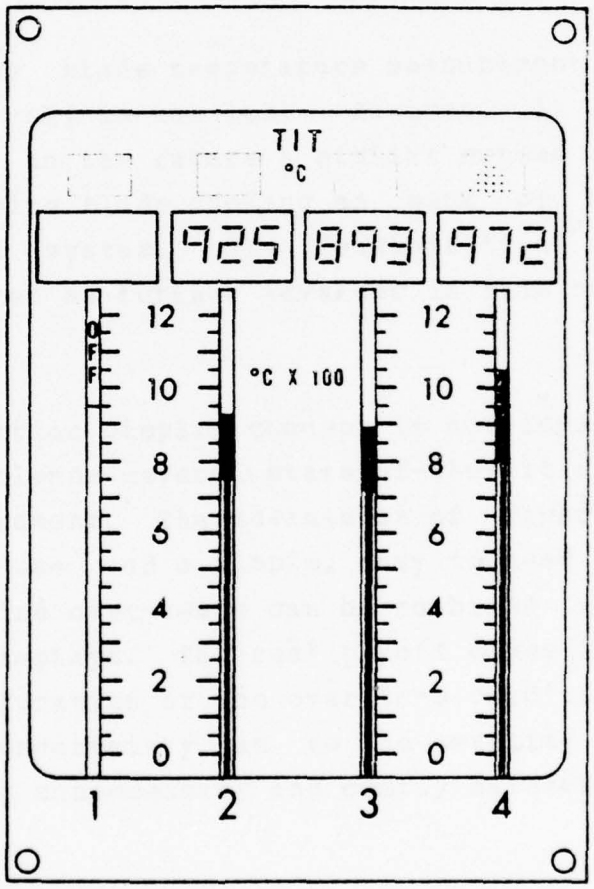


Figure 54 - ELDEC MODEL 9-311

ANALYSIS

Thermocouples offer the capability to measure extremely high temperatures, but have inherent problems concerning reference points, accuracy, and drift. The advances in RTDs should result in their use instead of TCs in applications not requiring high temperatures.

The turbine blade temperature measurement technique is presently used only in the lab. However, it is entirely possible that in the future a similar scheme could be used to monitor turbine blade cooling as part of an automatic engine control system. The feasibility of such a system must be evaluated as further advances in this technique are made.

The Hot Section Display concept is developed and ready for use. It blends several state-of-the-art trends into an efficient instrument. The advantages of fiber optics are put to good use and a simple, easy to read and interpret display of engine over-temps can be combined with vertical and digital displays. The real payoff comes in storing the magnitude and duration of the over-temp condition which will dispell any uncertainty as to the severity of the event, thus preventing unneccessary and costly maintenance.

VIII. FUEL QUANTITY

Fuel quantity systems have been notoriously inaccurate and unreliable in military and commercial aircraft. Capacitive systems in use today exhibit continuously increasing errors as aircraft fuel is consumed especially when fuel quantity approaches the critical value. It has been observed that the present state-of-the-art capacitor type fuel guaging systems are prone to various errors due to small signal variations resulting from weather changes, wiring and connectors as well as other component malfunctions. Such systems have been found to have errors exceeding 1% of tank capacity plus 2% of reading, which means an aircraft carrying 100,000 lbs fuel may actually be carrying only 97,000 lbs. As the fuel quantity decreases, the error increases, and may go as high as 12% in some systems.

These errors are due to a combination of the following factors:

(1) Fuel chemistry variations

(2) Thermal effects

(3) Instrument inaccuracy

(4) Inaccurate height vs volume data

(5) Changes in aircraft attitude

(6) Wing twist and deflection

(7) Manufacturing tolerances

(8) Fuel contamination.

In addition, system malfunctions can be attributed to one or more of the following:

(1) Electromagnetic interference

(2) Stray capacitance

(3) Line leakage

(4) Poor workmanship

(5) Electrical component failure

(6) Humid environment.

Grumman Aerospace Corporation's Advanced Design Group initiated an internally funded program in November of 1973 whose objectives were (1) to minimize fuel quantity system errors, and (2) reduce aircraft maintainability requirements. The program resulted in a patented fuel quantity probe (U.S. Patent #3,995,168) which will be presented in the following pages.

A. ELECTRO OPTICAL FLUID MEASUREMENT SYSTEM

The Electro Optical Fluid Measurement System was invented by Frederick Neuscheler and John J. Connelly (assignee: Grumman Aerospace Corporation). The patented design (see Ref. 33) is a fuel probe with a digital detection interface which includes the following: a light source and photodetectors to sense fuel level; and an optical desimeter to sense fuel density.

The system utilizes Snell's Law in reflecting light from an air/liquid-probe interface. Figure 55 shows the fluid level probe (26') which is a housing containing a group of light transmitting fiber-optic bundles (22') and a group of light conducting fiber-optic bundles (24'). The fiber-optic bundles are supported by a plate (38) on one face of the housing and emerge in paired groups at a multiplicity of locations (windows or optical-interfaces) (40), (42), (44), (46), (48), (50), (52). The sensitivity can be increased as fuel is exhausted by decreasing the spacing between the fiber-optic bundles. Irregular spacing can also be used to handle irregular tank shapes (see Fig. 56).

Figure 57 shows a frontal view and side view of the plate support, which is a thin elongated rectangular structure. A typical window is shown in the top of Fig. 58 in which fiber-optic elements (68) and (70) have been inserted into the triangular cavity whose surfaces (60) and (62) make a 45° angle with the plate face. The optical interface (72) is a glass or clear plastic prism-like structure which fills the cavity and may serve to align and space the fibers.

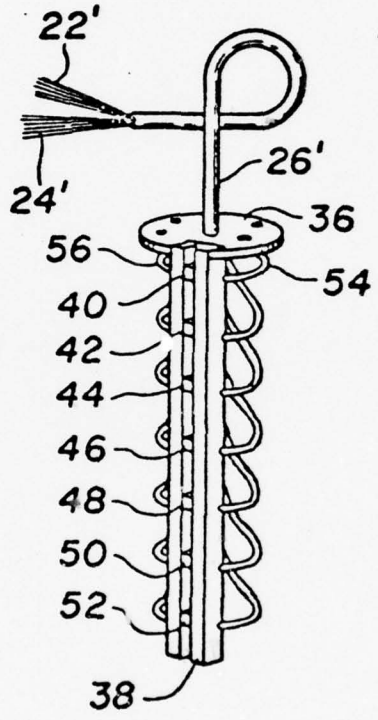


Figure 55 - ELECTRO OPTICAL FLUID LEVEL PROBE

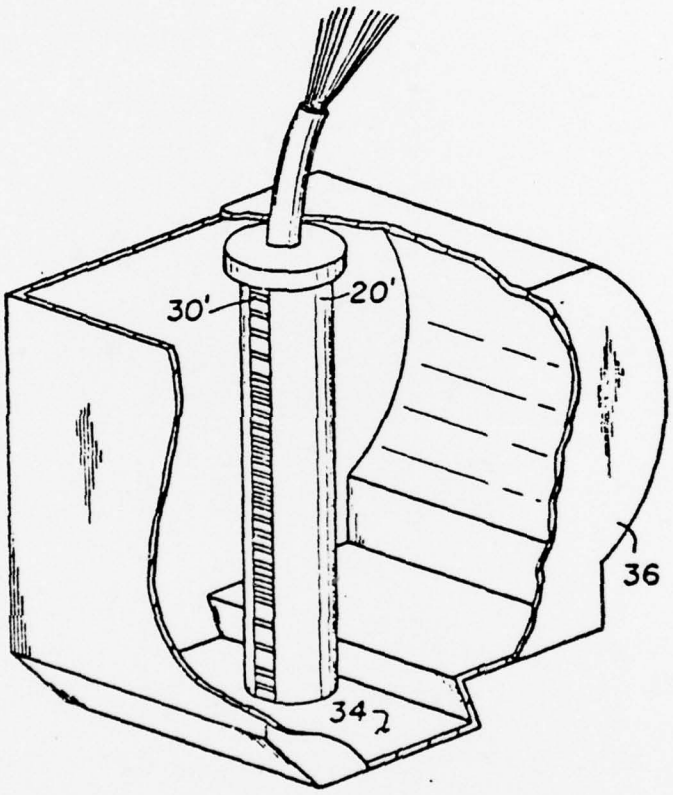


Figure 56 - MECHANIZATION FOR IRREGULAR TANK SHAPE

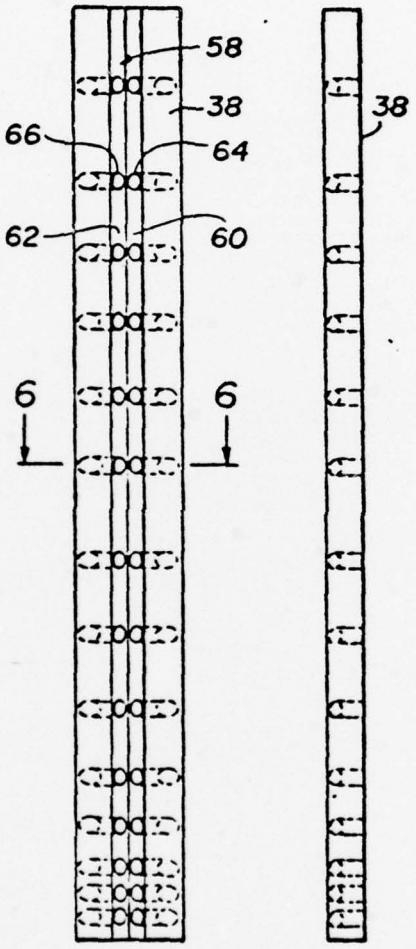
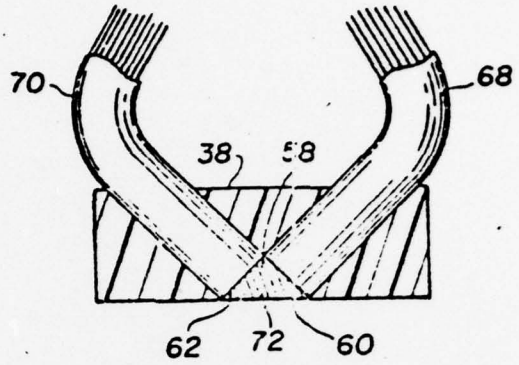


Figure 57 - PLATE SUPPORT

When the fuel level is below (72), the light carried by (70) is reflected into its counterpart (68) and this light is conducted to the photodetectors. The associated electronics takes the signal from the photodetectors and the signal from the density/contaminant probe and converts it to pounds of fuel remaining.

The electro-optical densimeter/contaminant probe is shown in the lower portion of Fig. 58. This detector also employs Snell's Law of reflection/refraction of light at an inclined optical interface (164) of a clear elongated lens (166) which has an aspherical end (168). A separate liquid chamber (172) fed by fluid from the bottom of the tank, is formed by the lens, its aspherical end, and the housing walls (170). Light enters the air chamber (174) via a fiber-optic bundle (178). The light transmitted by the fiber-optic bundle will enter the air chamber in a spherical pattern. The aspherical end (168) has one radius of curvature in the plane of the figure and another in the plane of surface (164). Therefore, light striking (168) will be directed to a focal point along surface (164) and/or to a focal point adjacent to the end of lens (166). This light will be either reflected and/or refracted at surface (164) so as to illuminate bundles (188), (190), (192), or bundles (196), (198), (200), or (202). The light received at bundles (188), (190), (192), (196), (198), (200) , and (202) will be indicative of density at one end and contamination at the other end. Appropriate summing circuitry will enable the proper electrical signal to show density, or warn of contamination such as too much water in the fuel.

Since the operation of the densimeter/contaminant probe does not require light to be passed through the fuel, fuel color does not affect the system. Discrimination between



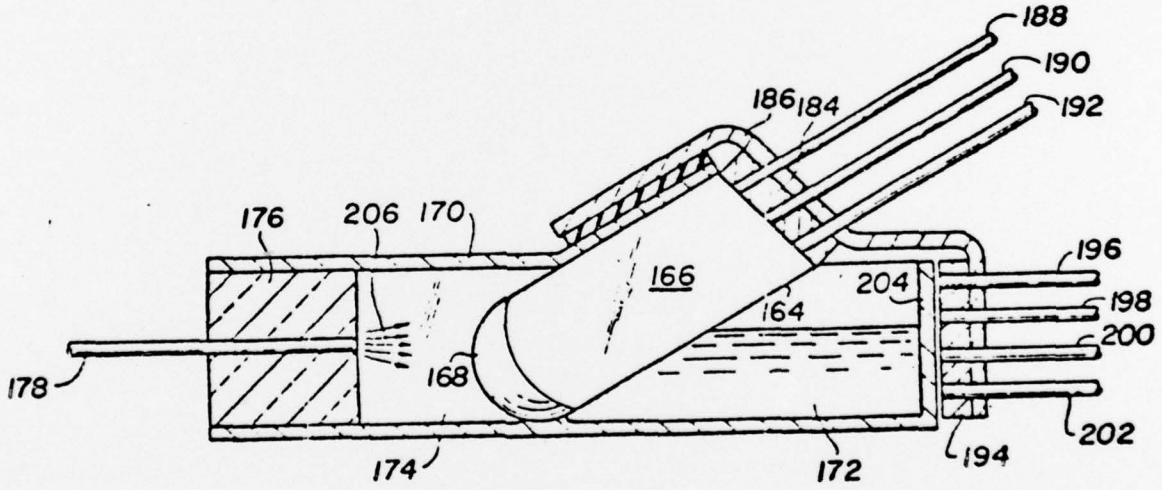


Figure 58 - TOP: OPTICAL INTERFACE, BOTTOM: DENSIMETER/CONTAMINANT PROBE

contaminants is a function of the optical fiber receiving the reflected/refracted light since different fibers will be illuminated as the contaminant level or density varies. Figure 59 shows a typical mechanization of the system utilizing two probes per tank, (90) and (92), one densimeter/contaminant probe per tank, (101), an electrical multiplying circuit, (106), summing circuit, (134), individual displays, (130) and (132), total display, (138), density indicator, (142), contaminant display, (144), and calibration controls, (146) and (148).

The system described above possesses significant advantages over current capacitive systems. These are:

(1) Probe and electronics provide manageable signal levels to minimize cabling and connector problems, thus increasing reliability.

(2) The system is not an EMI source and is not susceptable to EMI generated by adjacent equipment.

(3) The probe is completely passive in the tank, minimizing active hardware.

(4) The system is less susceptable to line leakage and stray capacitance.

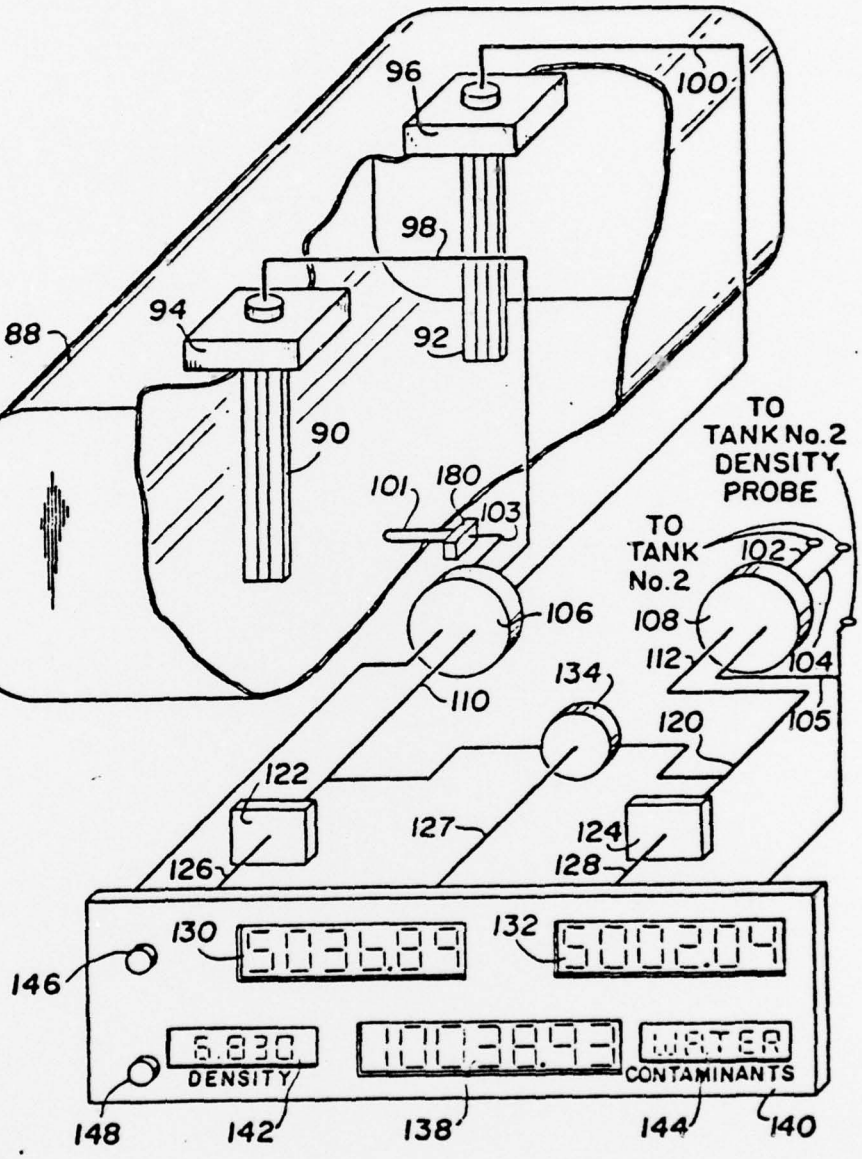


Figure 59 - MULTI-TANK SYSTEM

ANALYSIS

This system offers significant advantages over present fuel quantity systems. With the advances being made in fiber optics, there is no reason to doubt that this system will be cost competitive with current systems. Grumman has fabricated a lab version of the system, but has not tested it on an aircraft. Therefore, it should be flight tested before a meaningful evaluation can be made. There are questions still to be considered: (1) long-term fuel probe contamination, (2) flight worthy densimeters are not presently available, (3) a redundant low-power light source must be designed, and (4) the optical properties of fuels must be acquired.

IX. CONCLUSIONS

Today's rapidly advancing technology makes it extremely difficult to predict what the status of prototype systems will be in the years to come. In many cases, systems that look promising today were proposed years ago but were shelved until technology could make them feasible. Hence, the conclusions given are based on the current status of development and the trends in appropriate technologies.

(1) Fly-By-Wire aircraft will eventually replace conventional aircraft and will require redundant air data systems, posing difficult problems for the designer.

(2) Conventional aircraft should be equipped with gust load alleviation systems, multi-mode controls, and in-flight engine monitoring systems to realize their full potential.

(3) V/STOL aircraft must be equipped with an operational airspeed system capable of giving accurate, reliable longitudinal and lateral velocities in the takeoff/landing, hover, and transition regimes.

(4) An automatic carrier landing system for V/STOL aircraft must be developed if these aircraft are intended for all-weather operation from "sea control" type ships.

(5) Of the pressure transducers presented, the Solid State Silicon pressure sensor is the most attractive and is well suited for low cost high output moderate accuracy pressure transducers and accelerometers.

(6) LORAS is the most promising low range airspeed system and should be installed on helicopters and considered for future V/STOL aircraft.

(7) Laser Doppler Velocimeter technology should be monitored closely: if it becomes feasible, it would be invaluable in V/STOL applications.

(8) Fiber Optic cable will be competitive with twisted pair or coaxial cable in the very near future.

(9) The ALOFT project has verified the feasibility of a fiber-optic interface in operational aircraft; such an interface should be installed in future aircraft.

(10) RTDs offer significant advantages over thermocouples and should be utilized wherever possible.

(11) In-flight turbine blade temperature measurement and control should be possible using radiation pyrometry.

(12) The Hot Section Display concept is an example of what will be possible when state-of-the-art techniques are combined; designers should consider these systems for future Naval aircraft.

LIST OF REFERENCES

1. Abrams, C.R., Gertz, D., and Grobert, K., " Present and Future Naval Aircraft Air Data Systems", Air Data Symposium Proceedings, v. 1, p. 209 to 231, June 22-24, 1976.

2. Sheets, Charles J., " Air Data Sensors Or Air Data Computers; The Systems Integration Question", Air Data Sympcsium Proceedings, v. 1, p. 177 to 188, June 22-24, 1976.

3. Gaston, Dave, " Air Data Systems For Fly-By-Wire Aircraft", Air Data Symposium Proceedings, v. 1, p. 233 to 246, June 22-24, 1976.

4. Green, D.L., " Omnidirectional Low Range Airspeed, Display and System Requirements", Air Data Symposium Proceedings, v. 1, p. 357 to 404, June 22-24, 1976.

5. Lusk, Walter T. Capt., "Operational Test and Evaluation Of An Omnidirectional Low Range Airspeed System, LORAS", 1HS-AS-1101-76-9, 1st Helicopter Squadron (MAC) Andrews AFB, Md., December 1976

6. Mackenzie, D.M. and Kehret, W.E., " Review Of Temperature Measurement Techniques", Instrumentation Technolcgy, v. 23, #9, p. 43 to 48, September 1976.

7. Berger, Roger L., et. al., "The Compatibility Of Maneuver Load Control and Relaxed Static Stability Applied To Military Aircraft", McDonnell Douglas Aircraft Co. Technical Report, AFFDL-TR-73-33,April 1973

8. Oehman, Walter I., "Optimum Design Considerations Of A Gust Alleviator For Aircraft", NASA Technical Report TN-D-8152, NASA Langley Research Center, March 1976

9. Paros, Jerome M., " Digital Pressure Transducers", Measurements and Data, v. 10, #2, issue 56, p. 74 to 79, March-April 1976.

10. Lampard, G.W.N., and Carlin, C., IPCS Program (Integrated Propulsion Control System)", AF Systems Command, Wright Patterson AFB, Ohio, March 1976

11. Frische, Richard H., " The Sperry Vibrating Diaphram Pressure Transducer and Its Several Applications", Air Data Symposium Proceedings, v. 1, p. A-1 to A-33, June 22-24, 1976.

12. Raetz, R.C., " A Solid-State Silicon Pressure Sensor For Air Data Applications", Air Data Symposium Proceedings, v. 1, p. 273 to 294, June 22-24, 1976.

13. Chodes, M., Kahn, E.H., and Micali, J.A., " A Resonant Capsule Pressure Transducer", Air Data Symposium Proceedings, v. 1, p. 325 to 340, June 22-24, 1976.

14. "Flight Evaluation: Pacer Systems, Inc. LORAS II Airspeed System, Low Airspeed Sensor, Final Report III, U.S. Army Aviation Systems Test Activity, Edwards AFB, Ca., March 1974

15. Green, D.L., " Omnidirectional Low Range Airspeed, Display and Systems Requirements For Helicopters and V/STOL A/C", Air Data Symposium Proceedings, v. 1, p. 357 to 404, June 22-24, 1976.

16. DeLeo, Richard V. and Jensen, David P., " Low Range Orthogonal Airspeed System", Air Data Proceedings, v. 1, p. 405 to 446, June 22-24, 1976.

17. O'Connor, James C., Bullock, Jerry R., and Jeffries,

Robert P., "Flight Evaluation, Rosemount Orthogonal Low Airspeed System", Low Airspeed Sensor Final Report V, USAAEFA Project No. 71-30-5, November 1974

18. Rudd, M.J., "Development Of A Prototype Optical Convolution Airspeed Sensor", Technical Report AFFDL-TR-76-132, January 1977

19. Joy, Rcbert D., " Airspeed and Direction By Vortex Detection", Air Data Symposium Proceedings, v. 1, p. 505 to 537, June 22-24, 1976.

20. Williams, D. N., " Fiber Optics For Data Transmission", Instrumentation Technology, v. 39,#9, p. 61 to 66, September 1976.

21. Sigel, G.H. Jr., "Fiber Optics For Naval Applications: An Assessment Of Present and Near-Term Capabilities", Technical Report, Naval Research Laboratory, Wash., September 24, 1976

22. Gundlach, Richard, " Fiber-optic Developments Spark Worldwide Interest", Electronics, v. 49, #16, p. 81 to 104b August 5, 1976,

23. Klass, Philip J., " Laser Gyros Find Increased Applications", Aviation Week and Space Technology, v. 107, #4, p. 44 to 47, July 25, 1977.

24. Hickey, Jack, " Some Fiber Optics Basics", Instruments and Control Sysyems, v. 49, #10, p. 59 to 61, October 1976.

25. Montgomery, Jeff D., Wolf, Helmut F. and Socolovsky, Alberto, " Fiber Optics-The Data Highway Of The Future", Instruments and Control Systems, v. 49, #10, p. 53 to 57, October 1976.

26. Gundlach, Richard, " One-Fiber Optical Cable Is Rugged", Electronics, v. 49, #7, p. 118, April 1,

1976.

27. Andriev, Nikita, " Industrial Fiber Optics: Hanging By A Thread?", Control Engineering, v. 24, #3, p. 36 to 37, March 1977.

28. Editor, " Voltage-Responsive Crystal Allows Direct Modulation Of Light Beam", Electronics, v. 49, #11, p. 32, November 11, 1976.

29. McGrath, John Michael, and Michna, Kenneth Ralph, An Approach To The Estimation Of Life Cycle Costs Of A Fiber-Optic Application In Military Aircraft, Thesis , Naval Postgraduate School, Monterey, Ca., September 1975

30. Pollack, Frank G., " Advances In Turbine Blade Temperature Measurements", Proceedings Of The 2nd International Instrumentation Symposium, v. 22 Instrumentation In The Aerospace Industry, vol. 13 Advances In Test Measurement, p. 393 to 397, May 25-27, 1976.

31. Thorson, Eric and Codomo, Joe, " Turbine Engine Hot Section Display Concept", Proceedings Of The 22nd International Instrumentation Symposium, v. 22 Instrumentation In The Aerospace Industry, vol. 13 Advances In Test Measurement, p. 403 to 408, May 25-27, 1976.

32. Neuscheler, Frederick and Connelly, John J., "Electro Optical Fluid Measurement System", U.S. Patent #3,995,168, November 30, 1976

INITIAL DISTRIBUTION LIST

		No. Copies
1.	Defense Documentation Center Cameron Station Alexandria, Virginia 22314	2
2.	Library, Code 0142 Naval Postgraduate School Monterey, California 93940	2
3.	Department Chairman, Code 67Be Department of Aeronautics Naval Postgraduate School Monterey, California 93940	1
4.	Associate Professor Donald M. Layton, Code 67Ln Department of Aeronautics Naval Postgraduate School Monterey, California 93940	5
5.	LT Robert D. Neil Training Department NAS Dallas, Texas 75211	1
6.	Naval Air Systems Command (Attn: Mr. Glista, AIR-3022D) Washington, DC 20361	9